Advanced Signal Processing Laboratory

2024 IEEE Sensor Array and Multichannel Signal Processing Workshop Tutorial

Do More with Less: Revolutionize Direction Finding with Sparse Arrays

Yimin D. Zhang
Department of Electrical and Computer Engineering
Temple University

AIR FORCE OFFICE OF SCIENTIFIC RESEARCH

Outline

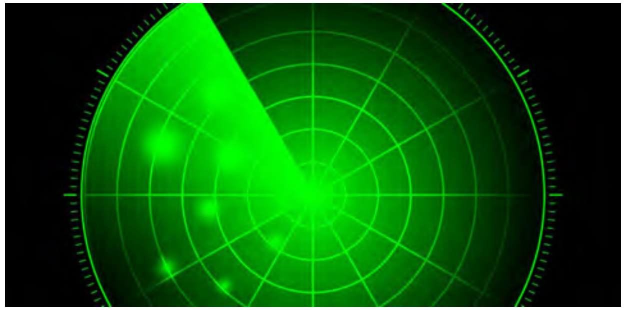

Do More with Less: Revolutionize Direction Finding with Sparse Arrays

Section I. Introduction

Section II. More consecutive lags and lower coupling

Section III. Sparsity-based processing and array design

- **A. Sparsity-based DOA estimation**
- **B. Structured matrix completion for DOA estimation**
- **C. Group sparsity-based DOA estimation**

Section IV. Additional topics

Section V. Concluding Remarks

A S P Lab

Part I: Introduction

- Direction-of-arrival (DOA) estimation and applications
- Narrowband array signal model
- Beamforming-based DOA estimation
- Subspace-based DOA estimation

Applications of array processing

- Array processing uses multiple sensors (antennas, microphones, transducers) and plays a fundamental role in wireless communications, radar and sonar sensing, autonomous driving, speech separation, and medical imaging
- **Beamforming**
  - Signal enhancement
  - Interference cancellation
  - Multi-user detection
  - Multiple-input multiple-output (MIMO) systems
  - Increased channel capacity
- **Sensing: Localization/imaging**
  - Ground-to-air radar
  - Automotive radar
  - Sonar
  - Ultrasonic imaging

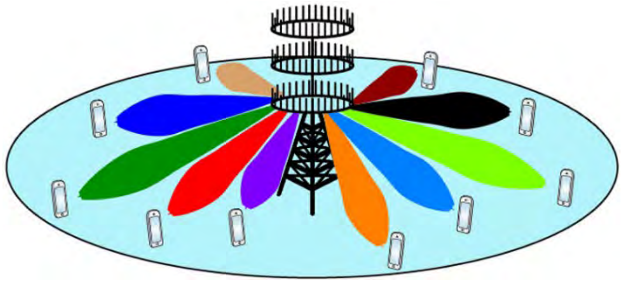

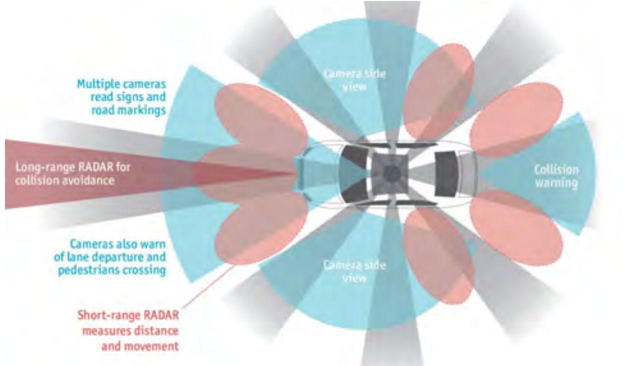

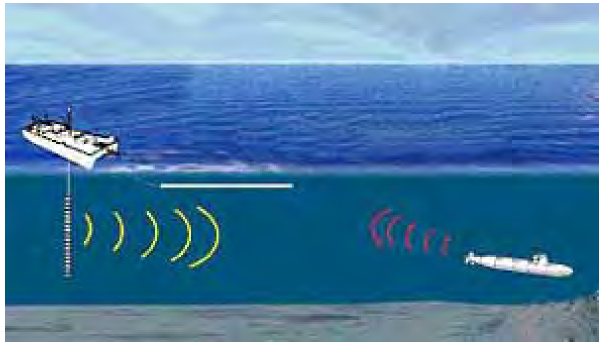

Four-dimensional sensing

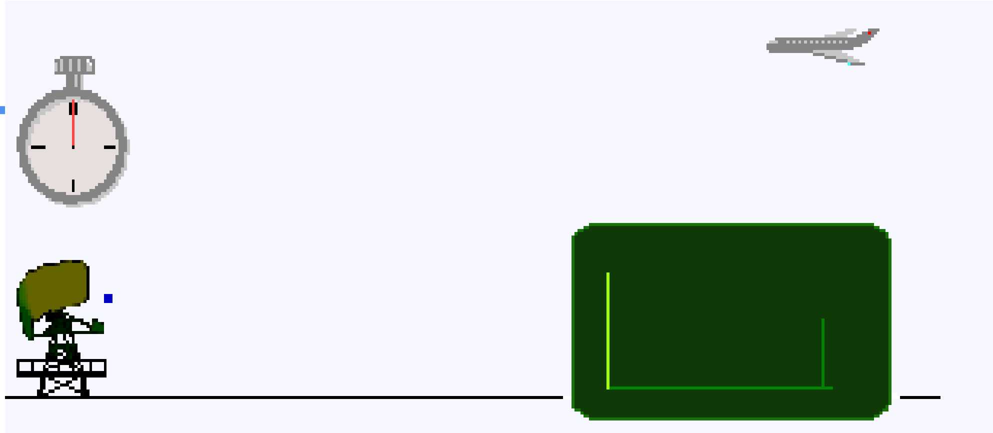

Radar sensing often requires high-resolution results in four dimensions (**4-D imaging**):

- **Range:** range resolution and accuracy are determined by signal bandwidth
- **Doppler frequency:** corresponding to radial velocity with its resolution determined by pulse repetition frequency
- **Azimuth angle**
- **Elevation angle**

This talk focuses on the angle estimation problem:

Estimating the directions-of-arrival (DOAs)

- more signals
- higher resolution
- few sensors

We mainly consider 1-D DOA estimation using linear arrays, but 2-D DOA estimation using 2-D arrays is also addressed.

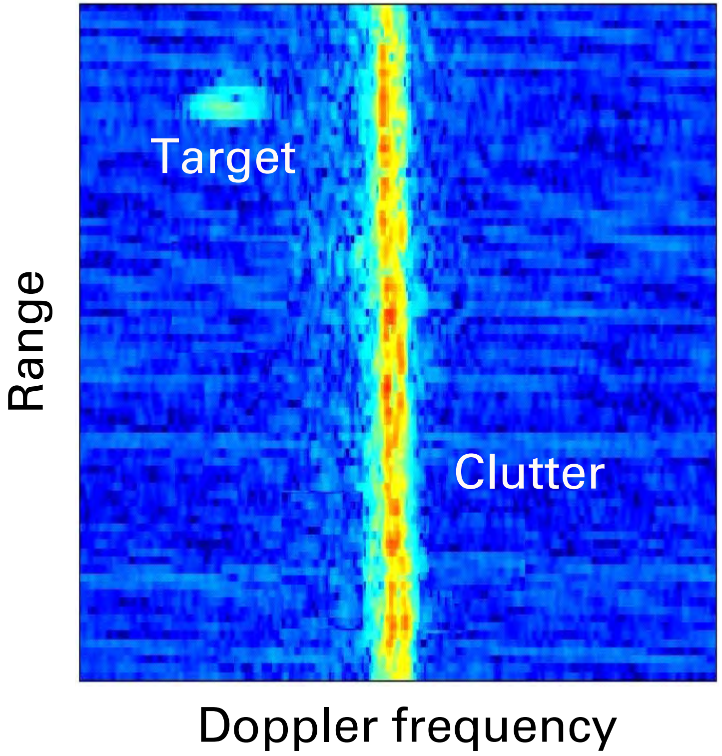

Signal model for ULA

Consider an N-element uniform linear array (ULA) with inter-element spacing d.

- **Time delay** for far-field signals: $\tau = (d \sin\theta)/c$

  c: speed of propagation

- **Phase delay:** $\phi = 2\pi f_c \tau = 2\pi(d/\lambda)\sin\theta$

  f_c: carrier frequency ($\omega = 2\pi f_c$)

  $\lambda = c/f_c$: wavelength

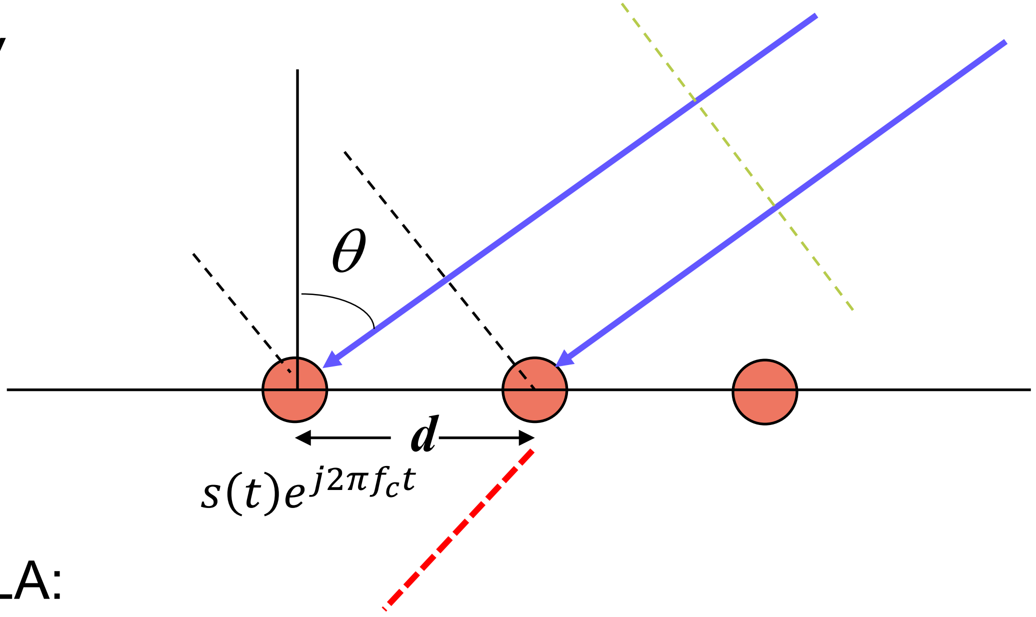

$$s(t+\tau)e^{j\omega(t+\tau)} \approx s(t)e^{j\omega(t+\tau)} = s(t)e^{j\omega t}e^{j\phi}$$

- Radio frequency (RF) model for an N-element ULA:

$$\tilde{\boldsymbol{x}}(t) = \begin{bmatrix} \tilde{x}_1(t) \\ \tilde{x}_2(t) \\ \vdots \\ \tilde{x}_N(t) \end{bmatrix} = s(t)e^{j\omega t}\begin{bmatrix} 1 \\ e^{j\phi} \\ \vdots \\ e^{j(N-1)\phi} \end{bmatrix}$$

- Baseband model:

$$\boldsymbol{x}(t) = \tilde{\boldsymbol{x}}(t)e^{-j\omega t} = \begin{bmatrix} x_1(t) \\ x_2(t) \\ \vdots \\ x_N(t) \end{bmatrix} = s(t)\begin{bmatrix} 1 \\ e^{j\phi} \\ \vdots \\ e^{j(N-1)\phi} \end{bmatrix} = s(t)\boldsymbol{a}(\theta)$$

Steering vector:

$$\boldsymbol{a}(\theta) = \begin{bmatrix} 1 \\ e^{j\phi} \\ \vdots \\ e^{j(N-1)\phi} \end{bmatrix} = \begin{bmatrix} 1 \\ e^{j2\pi(d/\lambda)\sin(\theta)} \\ \vdots \\ e^{j2\pi(N-1)(d/\lambda)\sin(\theta)} \end{bmatrix}$$

Signal model for ULA

Array signal model in the presence of K signals

$$\boldsymbol{x}(t) = \sum_{k=1}^{K} s_k(t)\boldsymbol{a}(\theta_k) + \boldsymbol{n}(t) = \boldsymbol{A}\boldsymbol{s}(t) + \boldsymbol{n}(t)$$

where

$\boldsymbol{a}(\theta_k) = \left[1, \mathrm{e}^{j\phi_k}, \mathrm{e}^{j2\phi_k}, \cdots, \mathrm{e}^{j\,(N-1)\phi_k}\right]^{\mathrm{T}}$: steering vector

$\phi_k = 2\pi(d/\lambda)\sin\theta_k$: phase delay between adjacent sensors

$\mathbf{A} = [\boldsymbol{a}(\theta_1), \boldsymbol{a}(\theta_K), \cdots, \boldsymbol{a}(\theta_K)]$: array manifold matrix

$\boldsymbol{s}(t) = [s_1(t), \cdots, s_K(t)]^{\mathrm{T}}$: signal vector

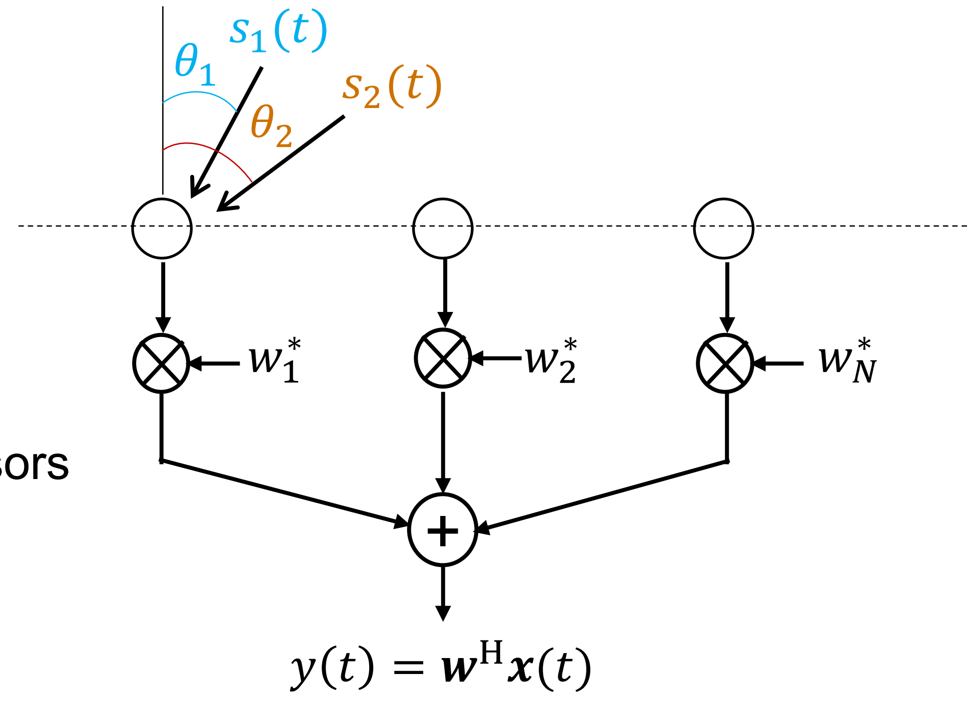

Beamforming for signal enhancement / interference cancellation: apply a weight vector $\boldsymbol{w}$ to $\boldsymbol{x}(t)$ such that $|\boldsymbol{w}^{\mathrm{H}}\boldsymbol{a}(\theta_d)|$ for some desired signal takes a high value and $|\boldsymbol{w}^{\mathrm{H}}\boldsymbol{a}(\theta_i)|$ for some interference signals takes a small value

DOA estimation: determine the directions of signal arrivals, $\theta_1, \cdots, \theta_K$, from the received signal vector $\boldsymbol{x}(t)$ over (typically) multiple samples $t = 1, \cdots, T$.

Beamforming-based DOA estimation

Traditional DOA estimation approach through beamforming (Fourier-based)**:**

- For $\mathbf{x}(t) = s(t)\mathbf{a}(\theta_0)$, by assuming $\boldsymbol{w} = \boldsymbol{a}(\theta)$ with different θ, the magnitude of $y(t,\theta) = \boldsymbol{a}^{\mathrm{H}}(\theta)\boldsymbol{x}(t) = s(t)\boldsymbol{a}^{\mathrm{H}}(\theta)\boldsymbol{a}(\theta_0)$ is peaked at θ_0.
- This approach has a low resolution because the beamwidth is wide.
- Note that the resolution is determined by the array aperture.

Beamforming-based DOA estimation has a low resolution (Example of 6-element ULA)

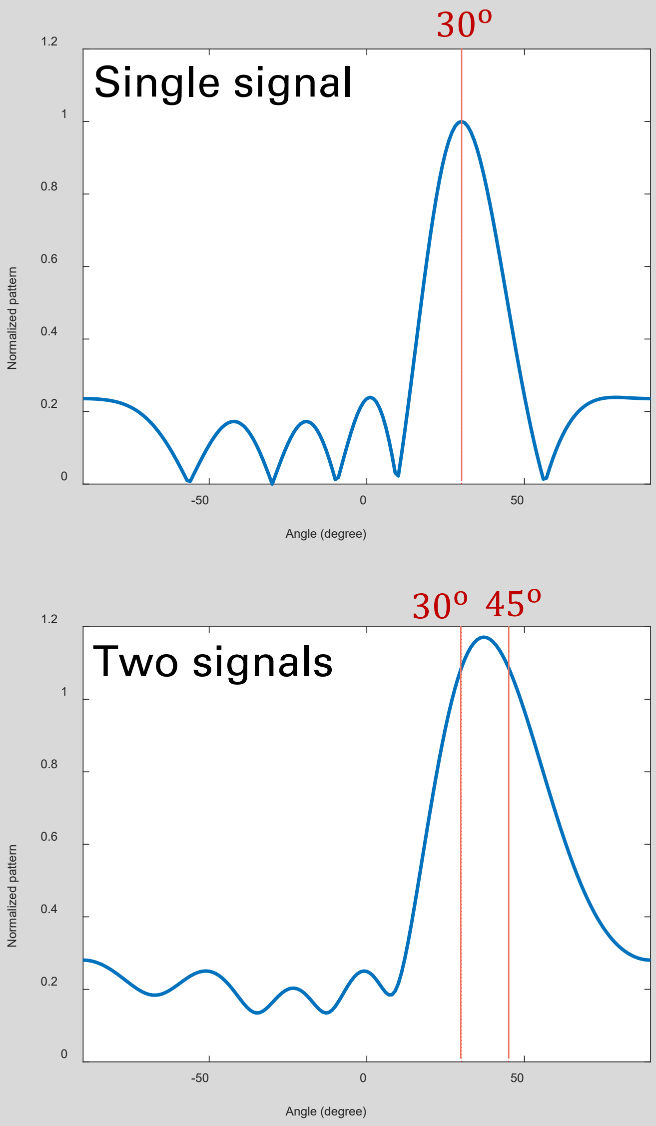

Beamforming-based DOA estimation

Achieving high resolution:

- Larger array aperture
  - More sensors: High cost
  - Large spacing (uniform): Alias
  - **Sparse arrays (irregular)**: To be discussed further

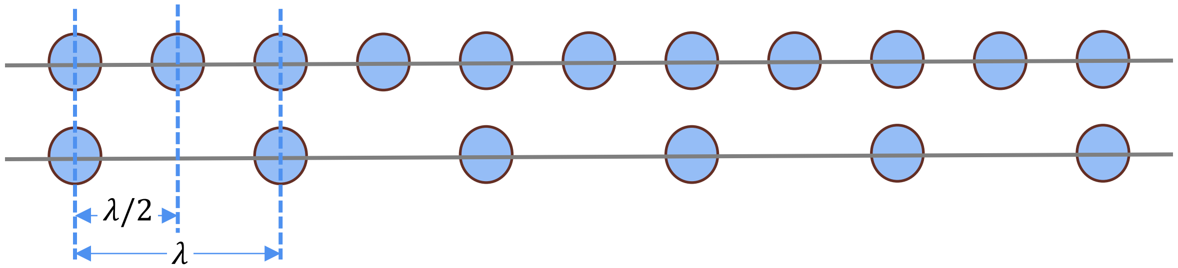

- High-resolution DOA estimation methods
  - Adaptive beamforming (e.g., Capon)
  - Maximum likelihood estimation
  - Subspace-based methods
    - **MUSIC**
    - ESPRIT
  - **Compressive sensing (sparse reconstruction)**

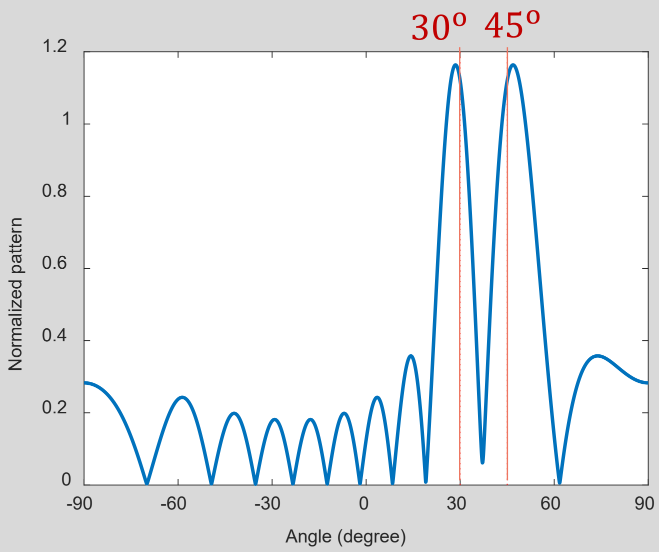

11 sensors, $d = \lambda/2$

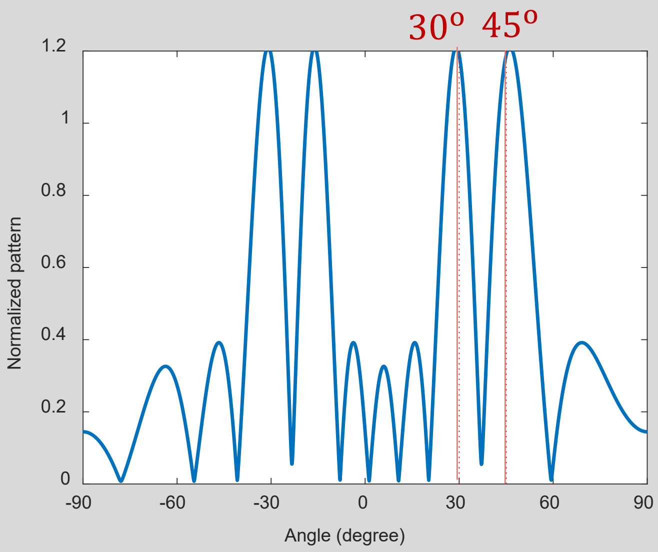

6 sensors, $d = \lambda$

DOA estimation

Subspace-based DOA estimation techniques based on the subspace analysis of the covariance matrix are commonly used to achieve a high resolution.

Covariance matrix:

$$\boldsymbol{R}_{\boldsymbol{xx}} = \mathrm{E}[\boldsymbol{x}(t)\boldsymbol{x}^{\mathrm{H}}(t)] = \begin{bmatrix} \mathrm{E}[x_1(t)x_1^*(t)] & \mathrm{E}[x_1(t)x_2^*(t)] & \mathrm{E}[x_1(t)x_3^*(t)] & \mathrm{E}[x_1(t)x_4^*(t)] \\ \mathrm{E}[x_2(t)x_1^*(t)] & \mathrm{E}[x_2(t)x_2^*(t)] & \mathrm{E}[x_2(t)x_3^*(t)] & \mathrm{E}[x_2(t)x_4^*(t)] \\ \mathrm{E}[x_3(t)x_1^*(t)] & \mathrm{E}[x_3(t)x_2^*(t)] & \mathrm{E}[x_3(t)x_3^*(t)] & \mathrm{E}[x_3(t)x_4^*(t)] \\ \mathrm{E}[x_4(t)x_1^*(t)] & \mathrm{E}[x_4(t)x_2^*(t)] & \mathrm{E}[x_4(t)x_3^*(t)] & \mathrm{E}[x_4(t)x_4^*(t)] \end{bmatrix}$$

Estimated covariance matrix using T snapshots:

$$\widehat{\boldsymbol{R}}_{\boldsymbol{xx}} = \frac{1}{T}\sum_{t=1}^{T} \boldsymbol{x}(t)\boldsymbol{x}^{\mathrm{H}}(t)$$

Eigen-decomposition of the covariance matrix

$$\boldsymbol{R}_{\boldsymbol{xx}} = \sum_{i=1}^{K} \lambda_i \boldsymbol{v}_{\boldsymbol{i}} \boldsymbol{v}_{\boldsymbol{i}}^{\mathrm{H}} + \sum_{i=K+1}^{N} \sigma_n^2 \boldsymbol{v}_{\boldsymbol{i}} \boldsymbol{v}_{\boldsymbol{i}}^{\mathrm{H}} = \boldsymbol{U}_{\boldsymbol{s}} \boldsymbol{\Sigma}_{\boldsymbol{s}} \boldsymbol{U}_{\boldsymbol{s}}^{\mathrm{H}} + \boldsymbol{U}_{\boldsymbol{n}} \boldsymbol{\Sigma}_{\boldsymbol{n}} \boldsymbol{U}_{\boldsymbol{n}}^{\mathrm{H}}$$

Signal subspace　　Noise subspace

Subspace-based DOA estimation

Eigen-decomposition of the covariance matrix

$$\boldsymbol{R_{xx}} = \underbrace{\sum_{i=1}^{K} \lambda_i \boldsymbol{v_i} \boldsymbol{v_i}^{\mathrm{H}}}_{\text{Signal subspace}} + \underbrace{\sum_{i=K+1}^{N} \sigma_n^2 \boldsymbol{v_i} \boldsymbol{v_i}^{\mathrm{H}}}_{\text{Noise subspace}} = \boldsymbol{U_s \Sigma_s U_s^{\mathrm{H}}} + \boldsymbol{U_n \Sigma_n U_n^{\mathrm{H}}}$$

Signal subspace   Noise subspace

Observations:

- The signal subspace and the noise subspace are orthogonal: $\boldsymbol{U_s^{\mathrm{H}} U_n} = \boldsymbol{0}$.
- Valid signal steering vectors are orthogonal to the noise subspace: $\boldsymbol{A}^{\mathrm{H}} \boldsymbol{U_n} = \boldsymbol{0}$.

Pseudo spatial spectrum of **MUSIC** (MUltiple SIgnal Classification):

$$P(\theta) = \frac{1}{\boldsymbol{a}^{\mathrm{H}}(\theta) \boldsymbol{U}_n \boldsymbol{U}_n^{\mathrm{H}} \boldsymbol{a}(\theta)} = \left\| \boldsymbol{U}_n^{\mathrm{H}} \boldsymbol{a}(\theta) \right\|_2^{-2}$$

- MUSIC is popular because only 1-D search is needed for multiple signals.
- An N-element ULA can detect $N-1$ signals.
- Knowledge of the number of signals K is required.

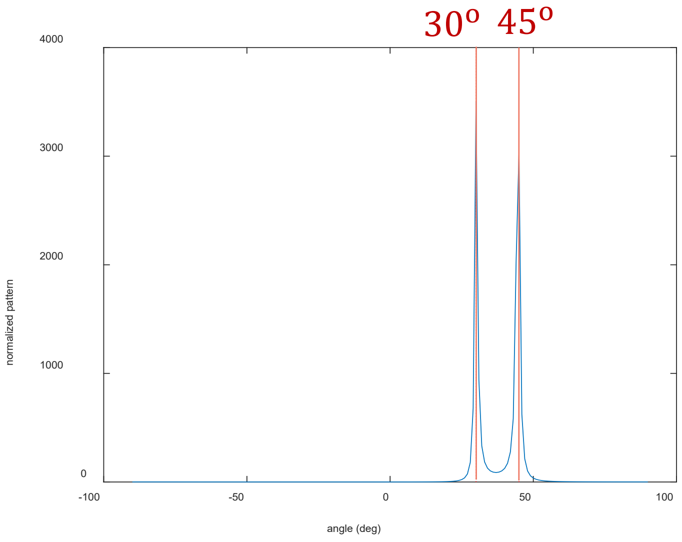

R. O. Schmidt, "Multiple emitter location and signal parameter estimation," *IEEE Trans. Antennas and Propagation*, 1986.

Sparse array design and processing

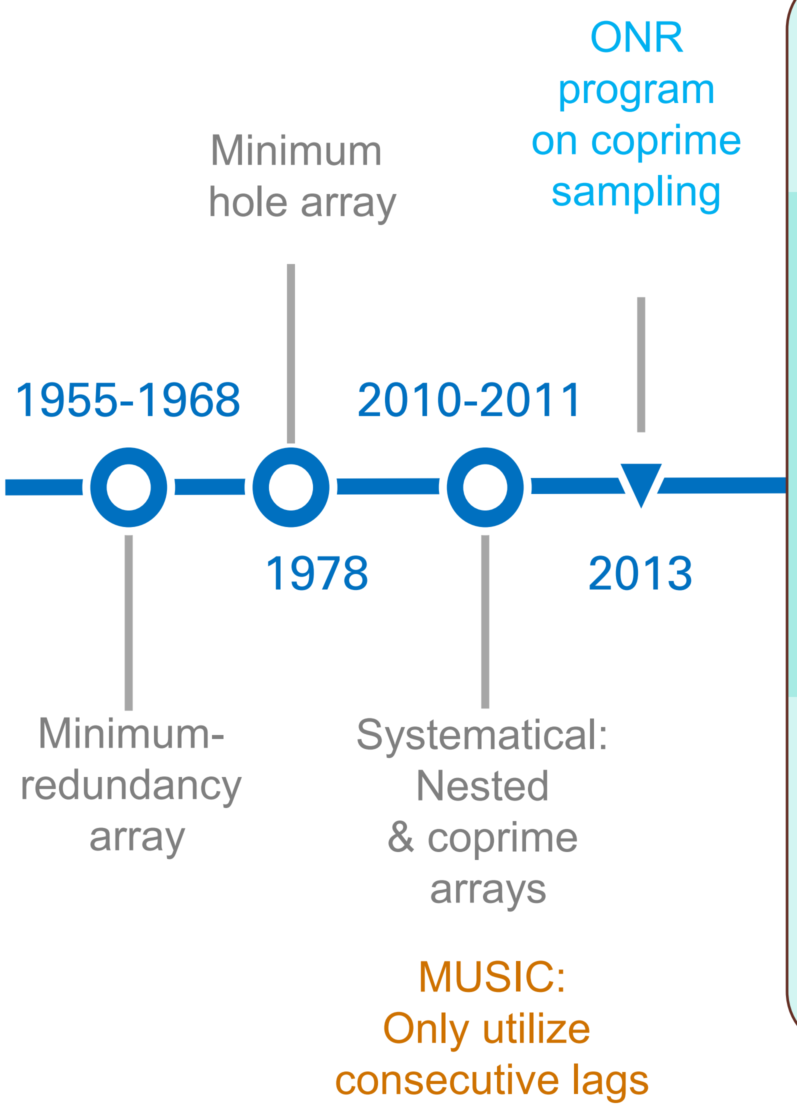

Section II. More consecutive lags and lower coupling

- Coprime array with compressed inter-element spacing (CACIS)
- Maximum inter-element spacing constraint (MISC) array

Section III. Sparsity-based processing and array design

III-A. Sparsity-based DOA estimation

- Coprime array with displaced subarrays (CADiS)

III-B. Structured matrix completion for DOA estimation

- Non-redundant sparse arrays
- 4D automotive radar sensing

III-C. Group sparsity-based DOA estimation

- Multi-frequency array
- Frequency-switching array

Section IV. Additional topics

- DOA estimation exploiting high-order statistics
- Distributed array with mixed-precision covariance matrices
- 2-D sparse arrays
- Signal coherency consideration
- Machine learning for DOA estimation

ASP Lab

Part II: More consecutive lags and lower coupling

- Difference coarrays
- Nested and coprime arrays
- More consecutive lags and less mutual coupling
- Design examples: CACIS, nested family, MISC family

Uniform and sparse sampling

Nyquist theorem: Sampling interval for periodic sampling should satisfy $T_s \leq T_{\min}/2$.

For periodic components, their parameters and waveforms may be estimated from sparse samples.

Similarly, conventional arrays use uniform linear arrays (ULAs) with inter-element spacing of $d = \lambda/2$.

Sparse arrays:

- **Direct DOA estimation**, we may sparsely place the array sensors with $N > K$ satisfied.
  - Larger aperture; same degrees-of-freedom (DOFs)
  - High sidelobe effects
- **DOA estimation exploiting difference lags:** A more popular approach based on second-order statistics
  - It increases both the array aperture and the number of DOFs, estimating more signals than sensors
  - May achieve consecutive lags to effectively suppress sidelobe issues

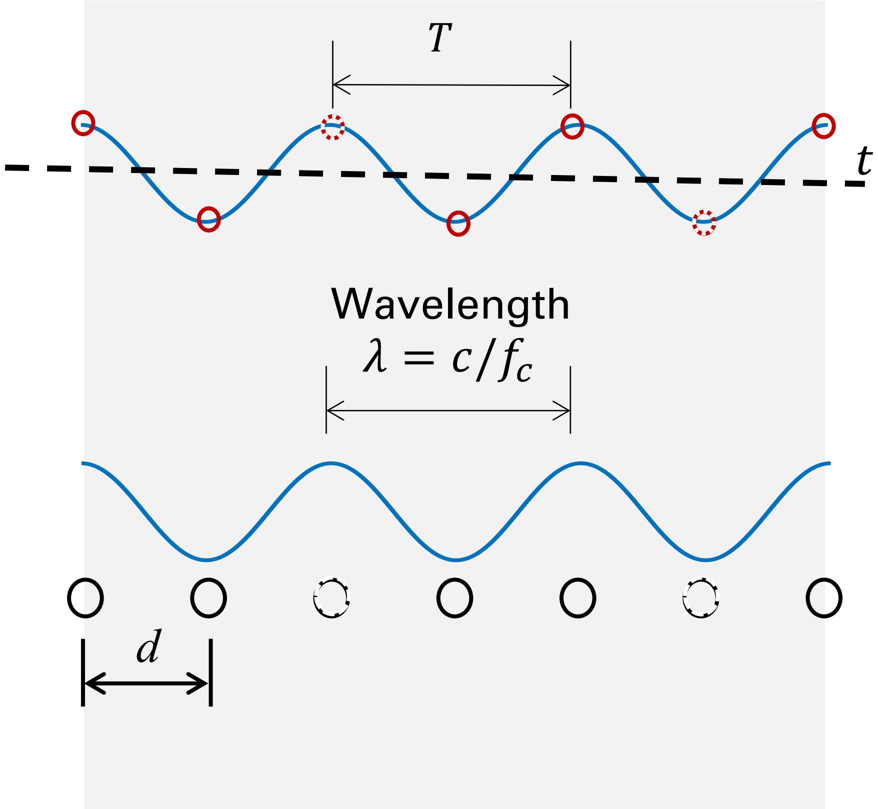

$$\boldsymbol{x}(t) = \sum_{k=1}^{K} s_k(t)\boldsymbol{a}(\theta_k) + \boldsymbol{n}(t)$$

$$\boldsymbol{a}(\theta_k) = \left[1, \mathrm{e}^{j\phi_k}, \mathrm{e}^{j2\phi_k}, \cdots, \mathrm{e}^{j(N-1)\phi_k}\right]^{\mathrm{T}}$$

$$\phi_k = 2\pi(d/\lambda)\sin\theta_k$$

Difference coarray

Subspace-based DOA estimation exploits the data covariance matrix $\boldsymbol{R}_{xx}$.

For a ULA with uncorrected signals:

- $\boldsymbol{R}_{xx}$ is Toeplitz (diagonal-constant) and Hermitian
- $\boldsymbol{R}_{xx}$ is highly redundant: Only N elements are unique in the $N \times N$ covariance matrix
- We may not need N sensors to estimate the $N \times N$ covariance matrix

Consider removing the third sensor from a 4-element ULA:

- All the entries of the ULA covariance matrix can be recovered: e.g., $\mathrm{E}[x_2 x_3^*] \Rightarrow \mathrm{E}[x_1 x_2^*]$.
- The 4-element ULA and the 3-element sparse array are **different coarray equivalent** because they generate the same number of correlation lags.
- For physical array $\mathbb{G}$, the difference lags are given as: $\mathbb{C}_G = \{\boldsymbol{z} | \boldsymbol{z} = \boldsymbol{u} - \boldsymbol{v}, \boldsymbol{u}, \boldsymbol{v} \in \mathbb{G}\}$.

$$\boldsymbol{R}_{xx} = \begin{bmatrix} \mathrm{E}[x_1 x_1^*] & \mathrm{E}[x_1 x_2^*] & \mathrm{E}[x_1 x_3^*] & \mathrm{E}[x_1 x_4^*] \\ \mathrm{E}[x_2 x_1^*] & \mathrm{E}[x_2 x_2^*] & \mathrm{E}[x_2 x_3^*] & \mathrm{E}[x_2 x_4^*] \\ \mathrm{E}[x_3 x_1^*] & \mathrm{E}[x_3 x_2^*] & \mathrm{E}[x_3 x_3^*] & \mathrm{E}[x_3 x_4^*] \\ \mathrm{E}[x_4 x_1^*] & \mathrm{E}[x_4 x_2^*] & \mathrm{E}[x_4 x_3^*] & \mathrm{E}[x_4 x_4^*] \end{bmatrix}$$

Correlation lags (difference coarray)

Minimum redundancy array

Minimum redundancy array (MRA): For a given number of physical sensors, MRA maximizes the number of consecutive virtual sensors in the resulting difference coarray.

- **Restricted arrays:** All lags are consecutive
- **General arrays:** Not all lags are consecutive

The difference lags an N-element sparse array can achieve is in the order of $\frac{1}{2}N(N-1)$.

For an MRA, the redundancy is defined as $R = \frac{\frac{1}{2}N(N-1)}{N_{\max}}$, where $N_{\max}$ is the maximum number of consecutive lags.

- R is found to be $1.217 \lesssim R \lesssim 1.674$.

However, MRA cannot be systematically designed.

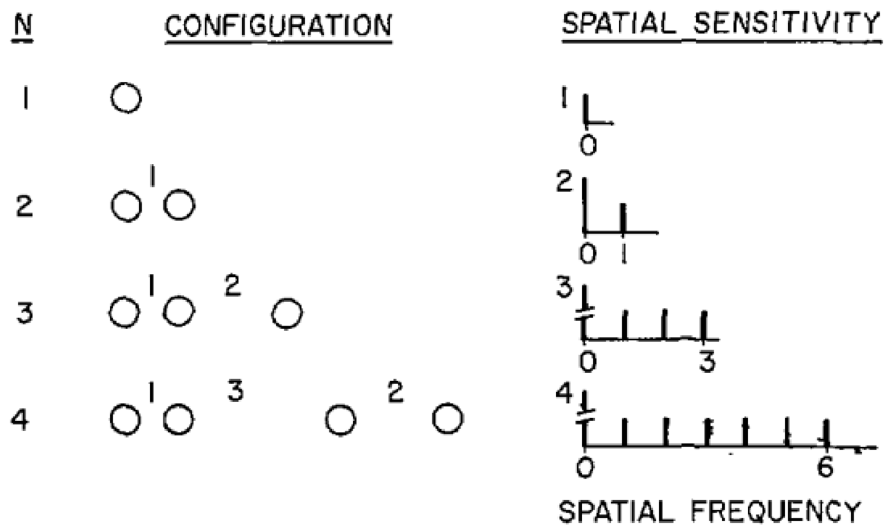

N	$N_{\max}$	R	Configuration
Restricted Arrays:			
5	9	1.11	·1·3·3·2·
6	13	1.16	·1·5·3·2·2
7	17	1.24	·1·3·6·2·3·2·
8	23	1.22	·1·3·6·6·2·3·2·
9	29	1.24	·1·3·6·6·6·2·3·2·
10	36	1.25	·1·2·3·7·7·7·4·4·1·
General Arrays:			
5	9	1.11	·4·1·2·6·
6	13	1.16	·6·1·2·2·8·
7	18	1.17	·14·1·3·6·2·5·
8	24	1.17	·8·10·1·3·2·7·8·
10	37	1.22	·16·1·11·8·6·4·3·2·22·

A. Moffet, “Minimum-redundancy linear arrays,” *IEEE Trans. Antennas and Propagation*, 1968.
M. Ishiguro, "Minimum redundancy linear arrays for a large number of antennas," *Radio Science*, 1980.

Systematical sparse array design: Nested array

Systematical design: **Nested array** is a simple sparse array configuration which consists of two uniform linear subarrays, one of which has a unit spacing.

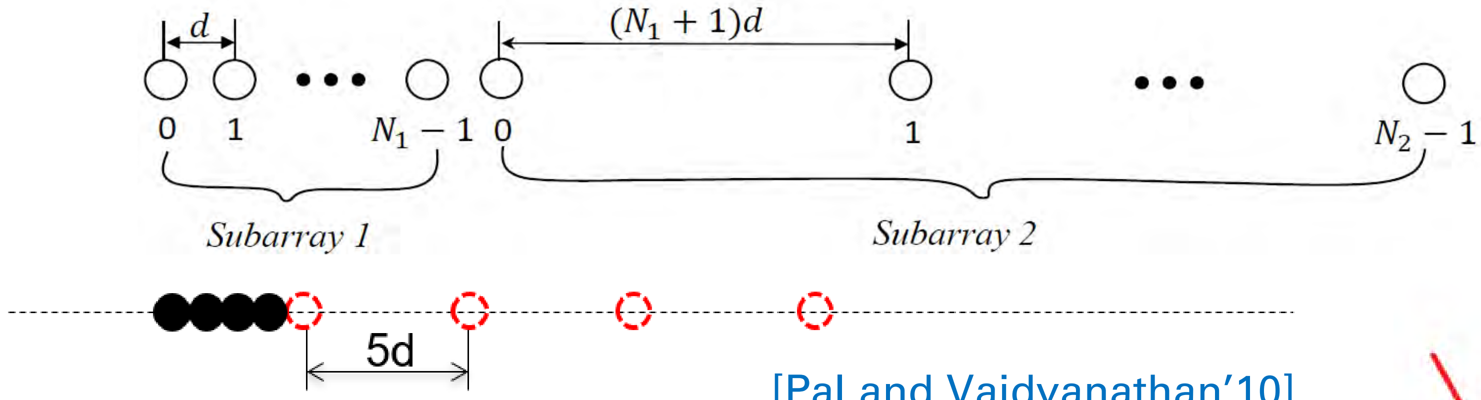

[Pal and Vaidyanathan’10]

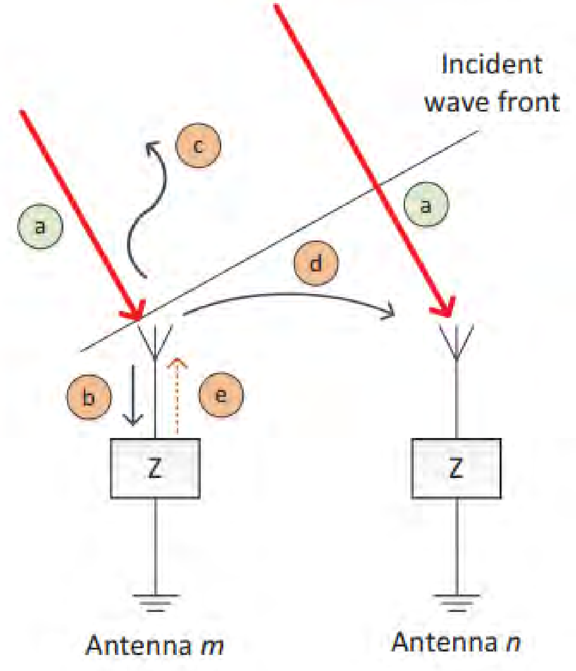

- For nested arrays, all lags are consecutive.
- Depending on the applications, the high number of consecutive physical sensors may cause high **mutual coupling effect**, degrading DOA estimation performance.
- Mutual coupling brings higher impact when the interelement spacing is small (e.g., half-wavelength spacing or less).
- The coprime array is proposed as an alternative to nested array.

P. Pal and P. P. Vaidyanathan, “Nested arrays: A novel approach to array processing with enhanced degrees of freedom,” *IEEE Trans. Signal Processing*, 2010.

Systematical sparse array design: Coprime array

Coprime array: utilizes a pair of uniform linear subarrays with M and N being coprime integers (greatest common divisor $\gcd(M,N) = 1$).

Example: $M = 3$ and $N = 5$ (6 elements)

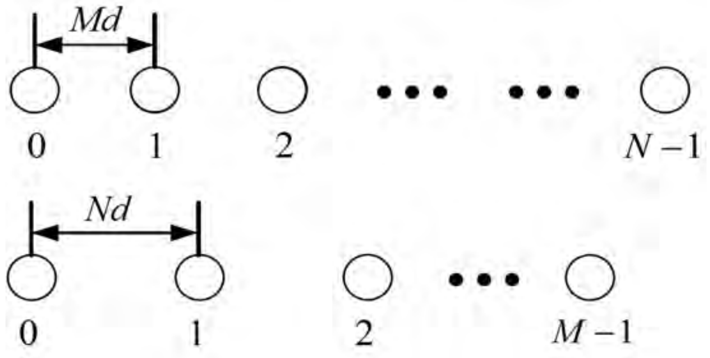

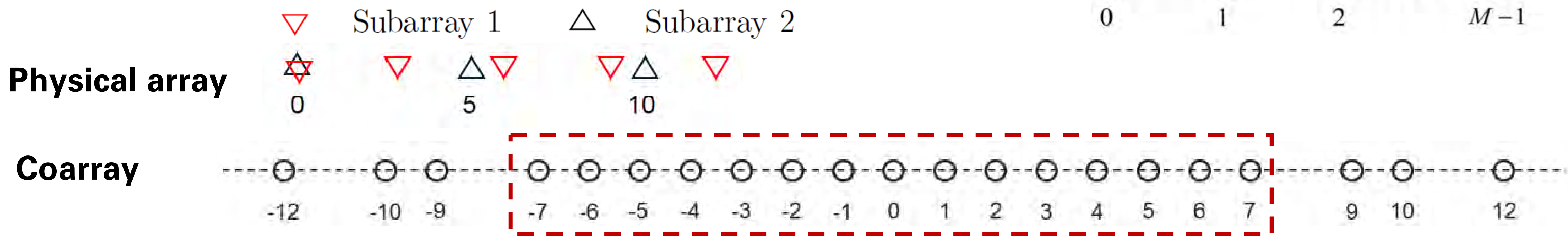

- Unlike nested arrays, coprime arrays generally have holes in the resulting lags.

P. P. Vaidyanathan and P. Pal, "Sparse sensing with co-prime sampler and arrays," *IEEE Trans. Signal Processing,* 2011

Direct MUSIC-based DOA estimation

Vectorizing $\boldsymbol{R}_{xx}$ yields

$$\boldsymbol{z} = \mathrm{vec}(\boldsymbol{R}_{xx}) = \widetilde{\boldsymbol{A}}\,\boldsymbol{b} + \sigma_n^2\,\tilde{\boldsymbol{\imath}} = \boldsymbol{A}^o\boldsymbol{b}^o$$

$\widetilde{\boldsymbol{A}} = [\boldsymbol{a}(\theta_1)\otimes\boldsymbol{a}^*(\theta_1), \ldots, \boldsymbol{a}(\theta_Q)\otimes\boldsymbol{a}^*(\theta_Q)]$: Manifold matrix for the difference coarray

$\boldsymbol{b} = [\sigma_1^2, \ldots, \sigma_Q^2]^{\mathrm{T}}$: Source power vector

$\tilde{\boldsymbol{\imath}} = \mathrm{vec}(\boldsymbol{I}_N)$

$\boldsymbol{A}^o = [\widetilde{\boldsymbol{A}}, \widetilde{\boldsymbol{I}}]$

$\boldsymbol{b}^o = [\boldsymbol{b}^{\mathrm{T}}, \sigma_{\mathrm{n}}^2]^{\mathrm{T}}$

$\boldsymbol{z}$ acts as received data of a virtual array (difference coarray)

- Manifold matrix corresponds to virtual sensors which are much more than physical antennas
- Only a single snapshot corresponding to vector $\boldsymbol{b}$
- Subspace-based DOA estimation cannot be directly applied because the single-snapshot covariance matrix $\boldsymbol{z}\boldsymbol{z}^H$ is rank-1

P. Pal and P. P. Vaidyanathan, "Coprime sampling and the MUSIC algorithm," *IEEE Digit. Signal Process. Workshop/ IEEE Signal Process. Educ. Workshop*, 2011.

Direct MUSIC-based DOA estimation

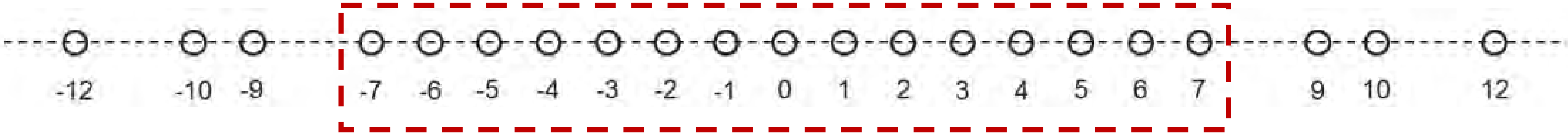

Spatial smoothing

Example: $N_z = 15, K = 8$

- By dividing the rank-1 matrix $\boldsymbol{R}$ into $K = (N_z + 1)/2$ subarrays $\boldsymbol{R}_k$, their average $\frac{1}{K}\sum_{k=1}^{K} \boldsymbol{R}_k$ becomes rank-K.
- It is equivalent to placing the elements of $\boldsymbol{z} = \left[z_{-(K-1)}, \cdots, z_{K-1}\right]^T$ in a Hermitian and Toeplitz manner.
- Only consecutive lags can be used for this purpose (e.g., lags of [−7:1:7]; detect up to 7 signals).
- In this context, **optimum design** of parse arrays is to
  - A high number of consecutive lags
  - Low mutual coupling (few lag-1 and lag-2 pairs)

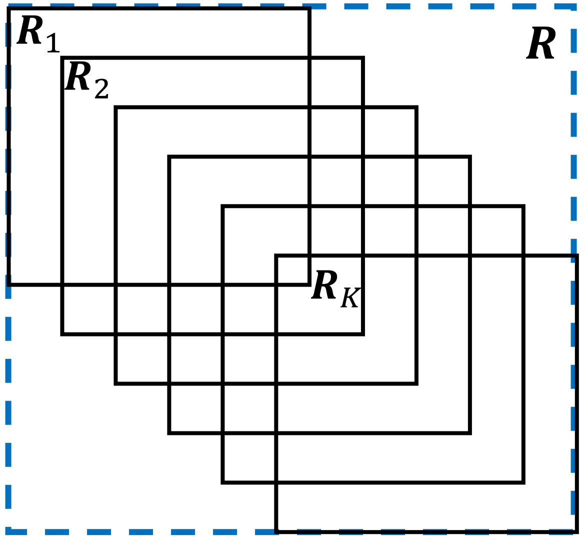

$$\tilde{\boldsymbol{R}}_{xx} = \begin{bmatrix} z_0 & z_1 & \cdots & z_{K-1} \\ z_{-1} & z_0 & \cdots & z_{K-2} \\ \vdots & \vdots & \ddots & \vdots \\ z_{-(K-1)} & z_{-(K-2)} & \cdots & z_0 \end{bmatrix}$$

P. Pal and P. P. Vaidyanathan, “Coprime sampling and the MUSIC algorithm,” *IEEE Digit. Signal Process. Workshop/ IEEE Signal Process. Educ. Workshop*, 2011.

C.-L. Liu and P. P. Vaidyanathan, "Remarks on the Spatial Smoothing Step in Coarray MUSIC," *IEEE Signal Processing Letters*, 2015.

Generalized coprime arrays: CACIS

Problems:

- Coprime array: have holes in the lags
- Nested array: high mutual coupling

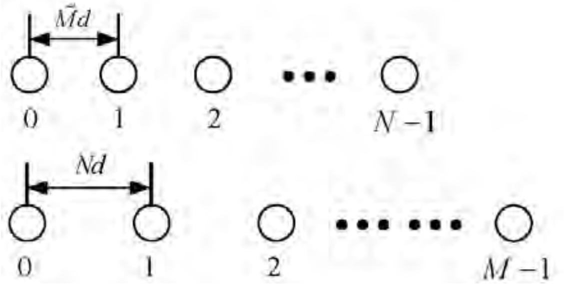

CACIS (Coprime array with compressed inter-element spacing):

Compresses the interelement spacing of one subarray $\breve{M} = M/p$ with $2 \leq p \leq M$ to increase the number of consecutive lags η_c

Example: $M = 6, N = 7$

(Only showing nonnegative lags)

$\breve{M} = 6, p = 1, N = 7, \eta_c = 25$ (prototype)

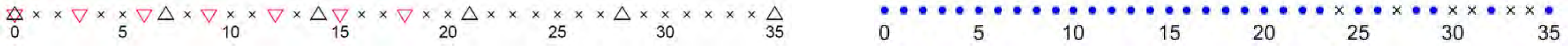

$\breve{M} = 3, p = 2, N = 7, \eta_c = 47$

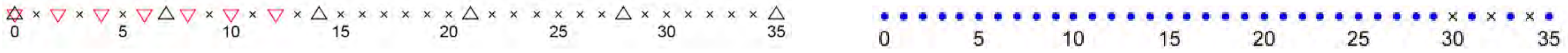

$\breve{M} = 2, p = 3, N = 7, \eta_c = 59$

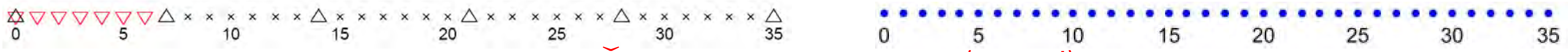

$\breve{M} = 1, p = 6, N = 7, \eta_c = 71$ (nested)

S. Qin, Y. D. Zhang, and M. G. Amin, "Generalized coprime array configurations for direction-of-arrival estimation," *IEEE Trans. Signal Processing*, 2015.

More consecutive lags and less mutual coupling

Many sparse arrays are proposed for (i) more consecutive lags and (ii) less mutual coupling.

- **Augmented nested array:** Split the densely located elements in inner subarray to reduce the mutual coupling. Several variations.
- **Thinned Coprime Array:** provides the same number of consecutive lags, unique lags, and aperture as the conventional coprime array but with fewer sensors.

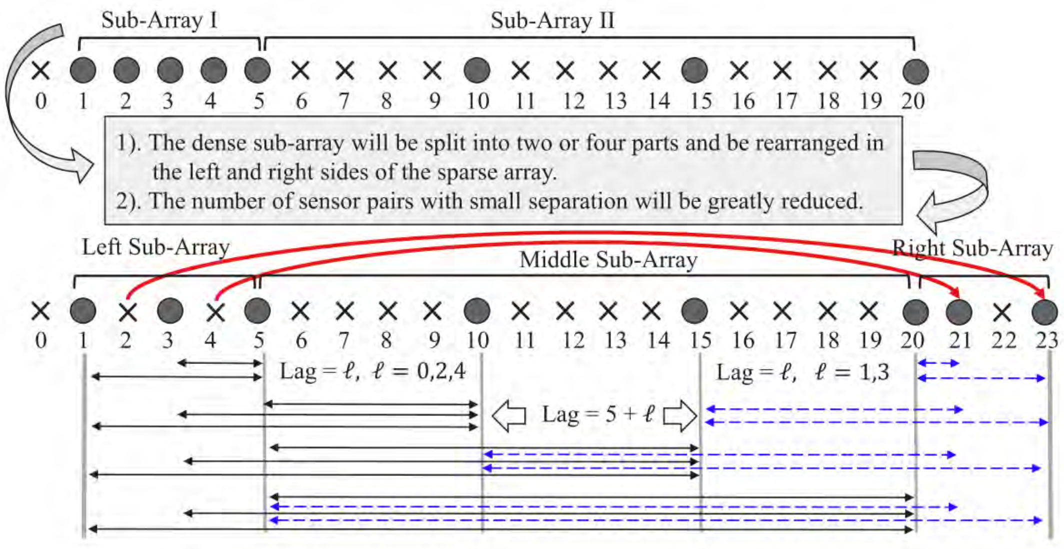

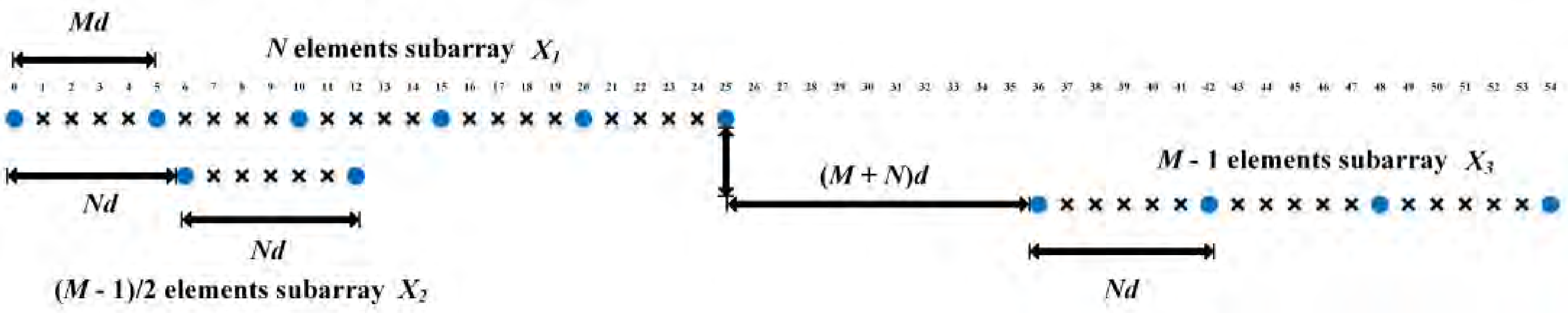

J. Liu, Y. Zhang, Y. Lu, S. Ren and S. Cao, "Augmented nested arrays with enhanced DOF and reduced mutual coupling," *IEEE Trans. Signal Processing*, 2017.

A. Raza, W. Liu and Q. Shen, "Thinned coprime array for second-order difference co-array generation with reduced mutual coupling," *IEEE Trans. Signal Processing*, 2019.

Sparse array: MISC family

MISC (maximum interelement spacing constraint): A four-segment configuration to achieve a high number of consecutive lags with low mutual coupling

$$\mathbb{A}_{\mathrm{MISC}} = \{1, P-3, \underbrace{P,\dots,P}_{N-P}, \underbrace{2,\dots,2}_{\frac{P-4}{2}}, 3, \underbrace{2,\dots,2}_{\frac{P-4}{2}}\} \quad \text{with } P = 2\lfloor N/4 \rfloor + 2 \ \ (N \geq 5)$$

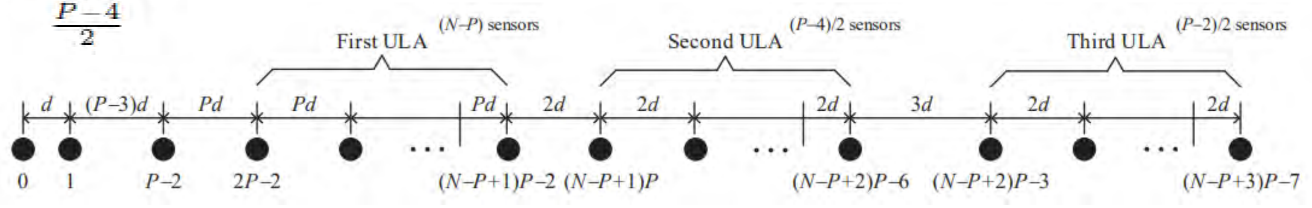

MISC (4 segments)

Modified versions: Use more segments to achieve higher freedom and better performance

- Improved MISC (I-MISC)
- Enhanced MISC (EMISC)
- Symmetry improved MISC (S-IMISC)
- Extended MISC (xMISC)

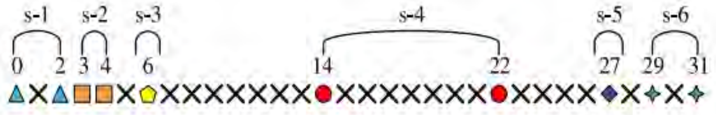

I-MISC (6 segments)

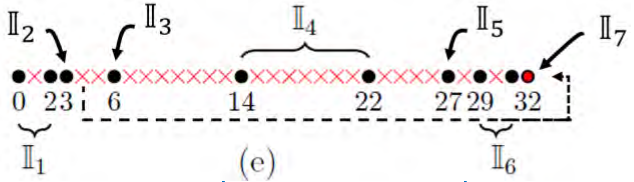

xMISC (7 segments)

Z. Zheng, W-Q. Wang, Y. Kong, and Y. D. Zhang, "MISC Array: A new sparse array design achieving increased degrees of freedom and reduced mutual coupling effect," *IEEE Trans. Signal Processing*, 2019.

W. Shi, Y. Li, and R. C. de Lamare, "Novel sparse array design based on the maximum inter-element spacing criterion," *IEEE Signal Processing Letters*, 2022.

X. Sheng, D. Lu, Y. Li, and R. C. de Lamare, "Enhanced MISC-based sparse array with high uDOFs and low mutual coupling," *IEEE Trans. Circuits and Systems II: Express Briefs*, in press.

X. Li, H. Yang, J. Han, and N. Dong, "A novel low-complexity method for near-field sources based on an S-IMISC array model," *Electronics*, 2023.

S. Wandale and K. Ichige, "xMISC: Improved sparse linear array via maximum inter-element spacing concept," *IEEE Signal Processing Letters*, 2023.

Sparse array: Performance evaluation

DOF ratio:

$$\gamma(N) = \frac{N^2}{\mathcal{S}_u}$$

$\mathcal{S}_u$: one-side uniform DOF (uDOF)

Coupling leakage:

$$\mathcal{L}(N) = \frac{\|\boldsymbol{H} - \text{diag}(\boldsymbol{H})\|_\text{F}}{\|\boldsymbol{H}\|_\text{F}}$$

$\boldsymbol{H}$: mutual coupling matrix whose elements depends on the distance between elements

Simulations assumed

$$\langle \boldsymbol{H} \rangle_{j,l} = \begin{cases} c_{|j-l|}, & \text{if } |j-k| \leq V \\ 0, & \text{otherwise} \end{cases}$$

with $c_0 = 1$, $c_1 = 0.2e^{j\pi/3}$, $\left|\frac{c_b}{c_l}\right| = \frac{l}{b}$

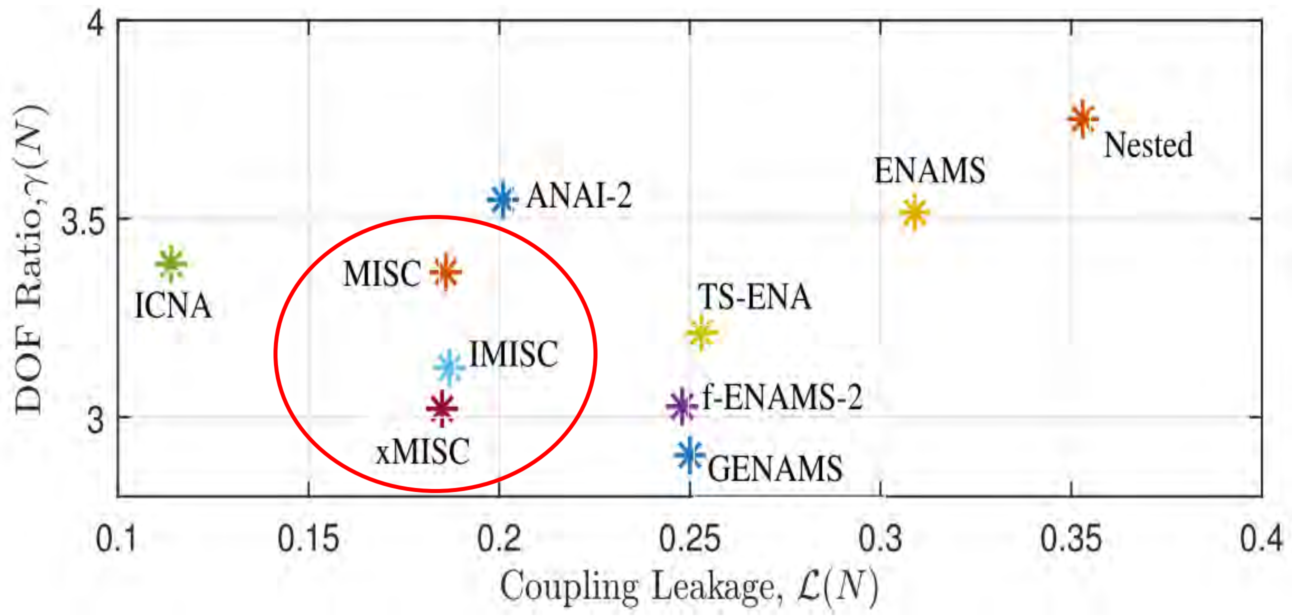

(N=30)

S. Wandale and K. Ichige, "xMISC: Improved sparse linear array via maximum inter-element spacing concept," *IEEE Signal Processing Letters*, 2023.

Part III: Sparsity-based processing and array design

III-A. Sparsity-based DOA estimation

- Compressive sensing
- Sparsity-based DOA estimation
- Coprime array with displaced subarrays (CADiS)

III-B. Structured matrix completion for DOA estimation

III-C. Group sparsity-based DOA estimation

Sparse signal reconstruction

Sparse signal reconstruction:

given linear model $\boldsymbol{y} = \boldsymbol{\Phi x}$

with observation $\boldsymbol{y}$ and dictionary matrix $\boldsymbol{\Phi}$

find $\boldsymbol{x}$

- When $M < N$, the linear model is underdetermined with infinite number of solutions.
- In order to obtain meaningful solutions, additional constraints are needed.
- Sparsity-based signal reconstruction assumes sparsity in x.
- For x with K nonzero entries, $\boldsymbol{x}$ may be solvable when $K < M \ll N$.

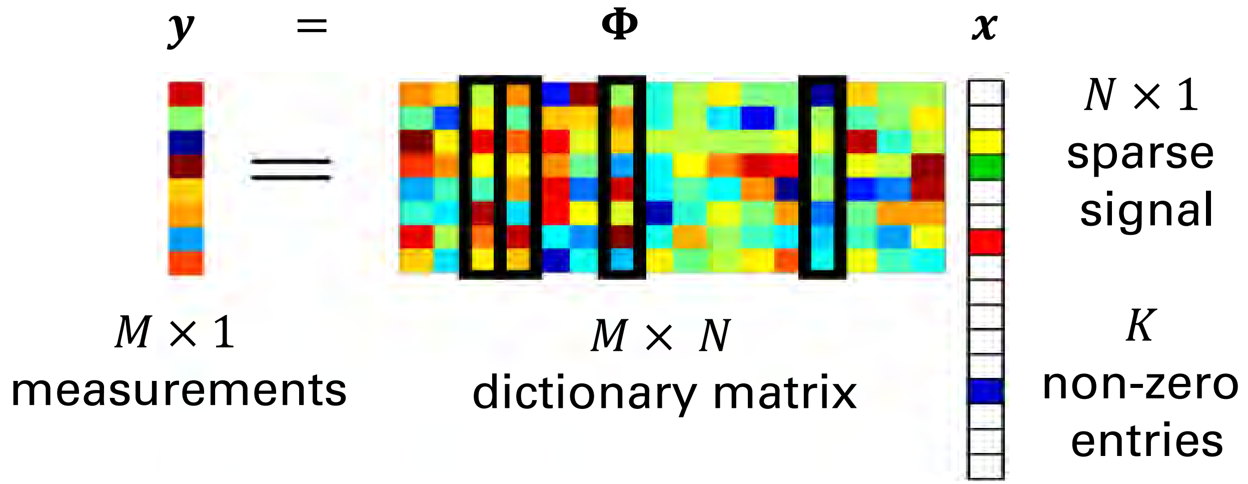

Sparse signal reconstruction

- Compressive sensing problems are expressed as

$$\min_{\boldsymbol{x}} \|\boldsymbol{x}\|_0 \quad \text{s.t. } \boldsymbol{y} = \boldsymbol{\Phi x}$$

- Considering noise, a more general expression is

$$\min_{\boldsymbol{x}} \|\boldsymbol{x}\|_0 \quad \text{s.t. } \|\boldsymbol{y} - \boldsymbol{\Phi x}\|_2 \leq \epsilon$$

  where $\epsilon > 0$ specifies the tolerable bound.
- Because of the l_0 norm operation, such problems are non-convex and NP-hard.

- **Greedy algorithms**

  Greedy construction of "support" (=column combination) by adding one-by-one/best choice at each iteration: Orthogonal matching pursuit (OMP), …
- **Convex relaxation**

  Approximation of the cost by convex functions (typically l_1-norm recovery): LASSO (least absolute shrinkage and selection operator), …
- **Probabilistic inference**

  (Approximate) employment of probabilistic inference: Bayesian compressive sensing (sparse Bayesian learning)

Sparse signal reconstruction: Greedy algorithms

- Basic idea – Sample vector $\boldsymbol{y}$ stands for a linear combination of columns ϕ_i of $\boldsymbol{\Phi}$.
- Construct an appropriate set of columns whose coefficients are non-zero, which is termed *support*, in a greedy manner.

Orthogonal matching pursuit (OMP)

Initialization: Initialize $k = 0$, and set $\boldsymbol{x}^0 = 0,\ \boldsymbol{r}^0 = \boldsymbol{y} - \boldsymbol{\Phi}\boldsymbol{x}^0 = \boldsymbol{y},\ \mathbb{S}^0 = \emptyset$

Main iteration: let $k = k + 1$, and perform the followings:

- **Rating of the columns:** $\varepsilon(i) = \min_{x_i} \left| x_i \boldsymbol{\phi}_i - r^{k-1} \right|^2$
- **Update support:** $i_0 = \arg \min_{i \notin \mathbb{S}^{k-1}} \{\varepsilon(i)\},\ \mathbb{S}^k = \mathbb{S}^{k-1} \cup \{i_0\}$
- **Update provisional solution:** $\widehat{\boldsymbol{x}}^k = \arg \min_{x_{\mathbb{S}^k}} \left| \mathbf{y} - \boldsymbol{\Phi}_{\mathbb{S}^k} \mathbf{x}_{\mathbb{S}^k} \right|^2$
- **Update residual:** $\boldsymbol{r}^k = \boldsymbol{y} - \boldsymbol{\Phi}_{\mathbb{S}^k} \widehat{\boldsymbol{x}}^k$
- **Stopping rule:** Stop if $\left|\boldsymbol{r}^k\right| < \varepsilon_0$ holds. Otherwise, apply another iteration

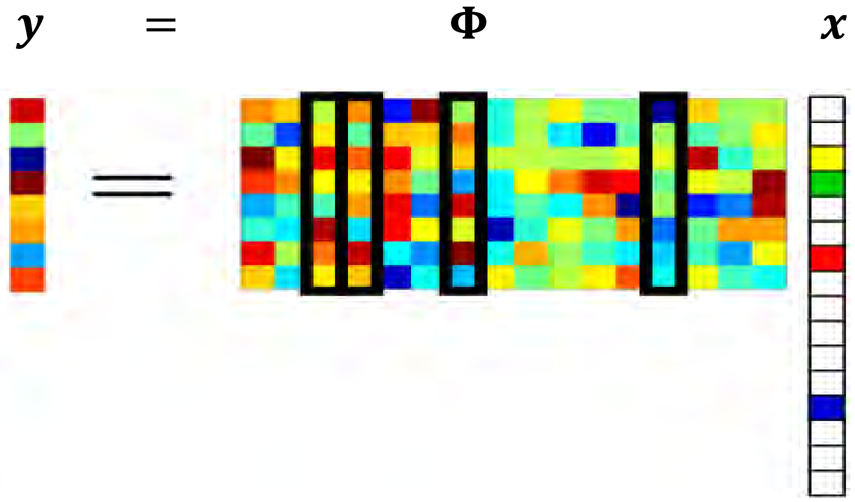

Sparse signal reconstruction: Convex relaxation

- Compressive sensing problem:

$$\min_{\boldsymbol{x}} \|\boldsymbol{x}\|_0 \quad \text{s.t.} \|\boldsymbol{y} - \boldsymbol{\Phi x}\|_2 \le \epsilon$$

- The non-convex l_0-norm problem is relaxed to l_1-norm one:

$$\min_{\boldsymbol{x}} \|\boldsymbol{x}\|_1 \quad \text{s.t.} \|\boldsymbol{y} - \boldsymbol{\Phi x}\|_2 \le \epsilon$$

- LASSO

$$\min_{\boldsymbol{x}} \ \|\boldsymbol{y} - \boldsymbol{\Phi x}\|_2 + \eta \, \|\boldsymbol{x}\|_1$$

  η: regularization parameter

- l_1-norm
  - is convex (easy to solve)
  - has corners (to provide sparse solutions)
  - Used in LASSO

l_p-norm:
$||\boldsymbol{x}||_p$

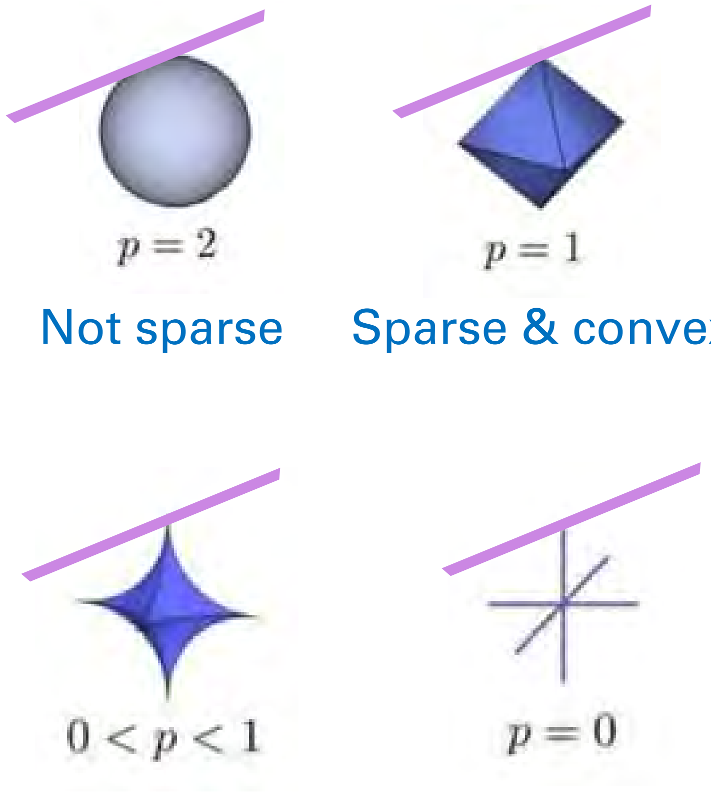

Not sparse

Sparse & convex

Not convex

A
S
P
Lab

Sparse signal reconstruction: Sparse Bayesian learning

- Obtain maximum *a posteriori* (MAP) solution of $\boldsymbol{x}$ from

$$\boldsymbol{y} = \boldsymbol{\Phi}\boldsymbol{x} + \boldsymbol{\varepsilon}, \quad \boldsymbol{\varepsilon} \sim \mathcal{N}(\boldsymbol{\varepsilon}|\boldsymbol{0}, \beta \boldsymbol{I})$$

- Sparse Bayesian learning based on relevance vector machine:

$$p(\boldsymbol{y}|\boldsymbol{\Phi}, \boldsymbol{x}) = \mathcal{N}(\boldsymbol{y}|\boldsymbol{\Phi}\boldsymbol{x}, \beta \mathrm{I})$$

Place Gaussian prior on $\boldsymbol{x}$

$$p(\boldsymbol{x}|\boldsymbol{\gamma}) = \prod_i \mathcal{N}(x_i|0, \gamma_i)$$

- Inverse Gamma priors are placed over hyperparameters β and $\boldsymbol{\gamma}$
- Key advantages of sparse Bayesian learning (Bayesian compressive sensing):
  - Close to l_0-norm sparse solution
  - Less sensitive to sensing matrix coherence
  - Convenient to consider signal structures through priors

M. E. Tipping, "Sparse Bayesian shrinkage and selection learning and the relevance vector machine," *Journal of Machine Learning Research*, 2001.

S. Ji, D. Dunson, and L. Carin, "Multi-task compressive sampling," *IEEE Trans. Signal Processing*, 2009. [MATLAB code available]

Z. Zhang and B. D. Rao, "Extension of SBL algorithms for the recovery of block sparse signals with intra-block correlation," *IEEE Trans. Signal Processing*, 2013 [MATLAB code available]

Mutual coherence of dictionary matrix

- Mutual coherence of a matrix: the largest absolute normalized inner products between different columns
- For dictionary matrix $\mathbf{\Phi} = [\boldsymbol{\phi}_1, \boldsymbol{\phi}_2, \dots, \boldsymbol{\phi}_m]$, its mutual coherence is

$$\mu(\mathbf{\Phi}) = \max_{1 \le i \ne j \le m} \frac{|\phi_i^H \phi_j|}{||\phi_i||_2 \cdot ||\phi_j||_2}$$

- It characterize the dependence between columns of $\mathbf{\Phi}$
- For unitary matrices, $\mu(\mathbf{\Phi}) = 0$
- For recovery problems, we desire a small $\mu(\mathbf{\Phi})$ as it is similar to unitary matrices
- In order to achieve high-resolution signal reconstruction, however, the mutual coherence could be high

A
S
P
Lab

Sparsity-based DOA estimation

Sparsity-based DOA estimation:

$$\boldsymbol{z} = \mathrm{vec}(\boldsymbol{R}_{xx}) = \widetilde{\boldsymbol{A}}\,\boldsymbol{b} + \sigma_n^2 \tilde{\boldsymbol{i}} = \boldsymbol{A}^o \boldsymbol{b}^o$$

- The linear coarray model well fits into the compressive sensing problem by defining dense dictionary matrix $\boldsymbol{A}^g$ over a grid, e.g., $[-90:1:90]$:

$$\min_{\boldsymbol{z}} \|\boldsymbol{b}^g\|_0 \ \mathrm{s.t.}\ \|\boldsymbol{z} - \boldsymbol{A}^g \boldsymbol{b}^g\|_2 \le \epsilon$$

- The positions of the nonzero solutions of $\boldsymbol{b}^g$ represent the signal DOA
- This approach does not require a specific array structure (e.g., consecutive coarray lags) and all difference lags can be utilized in sparsity-based DOA estimation: **Unique lags**

CADiS (Coprime array with displaced subarrays):

- Displaces two subarrays to increases unique lags
- Very low mutual coupling
- In general, the resulting lags are disconnected in the center region

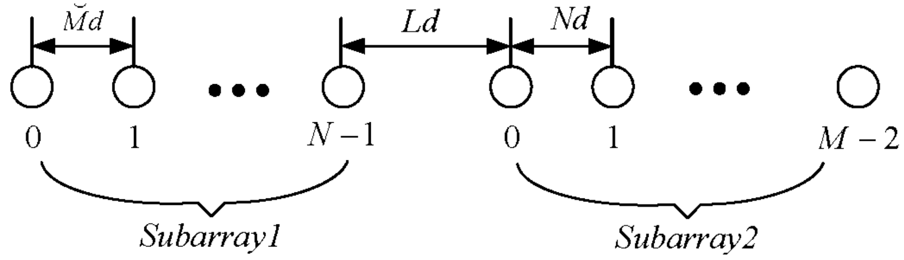

$\breve{M} = M/p$ with $2 \le p \le M$

S. Qin, Y. D. Zhang, and M. G. Amin, "Generalized coprime array configurations for direction-of-arrival estimation," *IEEE Trans. Signal Processing*, 2015.

Sparse array: CADiS

In CADiS configurations, the self-lags are less likely to coincide with the cross-lags:

(a) $L > (M-2)N$ achieves the maximum number of unique lags

(b) $L = \breve{M} + N$ yields the largest number of consecutive lags

η_c: consecutive lags; η_u: unique lags

$\breve{M} = 3, p = 2, N = 7, L = \breve{M} + N, \eta_c = 33, \eta_u = 89$

$\breve{M} = 2, p = 3, N = 7, L = \breve{M} + N, \eta_c = 38, \eta_u = 87$

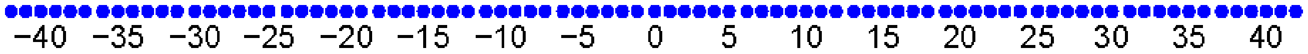

$\breve{M} = 1, p = 6, N = 7, L = \breve{M} + N, \eta_c = 85, \eta_u = 85$

- A smaller value of $\breve{M}$ reduces the unique lags and reduces the number of holes
- The lags become consecutive when $\breve{M} = 1$ (nested array)

S. Qin, Y. D. Zhang, and M. G. Amin, "Generalized coprime array configurations for direction-of-arrival estimation," *IEEE Trans. Signal Processing*, 2015.

Sparse arrays: Comparison

Consider $M = 6$ and $N = 7$ with $M + N - 1 = 12$ physical sensors

- LASSO-based method achieves better DOA estimation performance
- When LASSO is used, CADiS generally outperforms CACIS

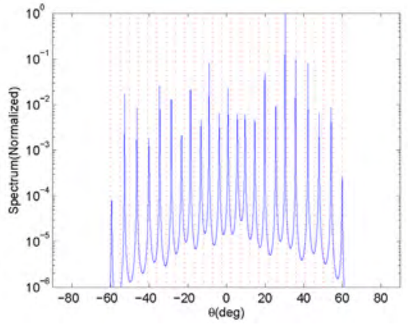

(a) CACIS with $\breve{M} = 3$ $(\eta_c = 47)$

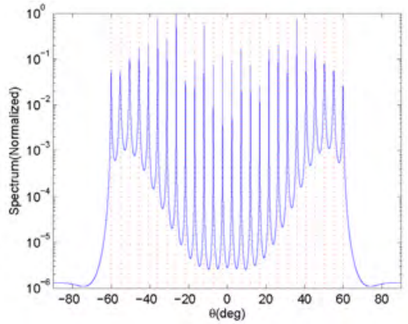

(b) CACIS with $\breve{M} = 2$ $(\eta_c = 59)$

MUSIC (26 signals)

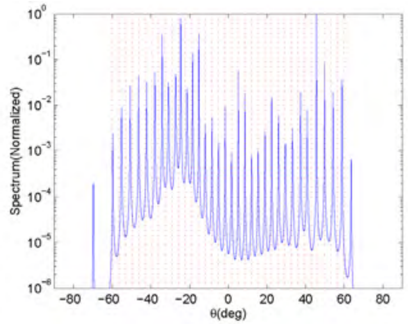

(a) CACIS with $\breve{M}$ =1 $(\eta_c = 71)$

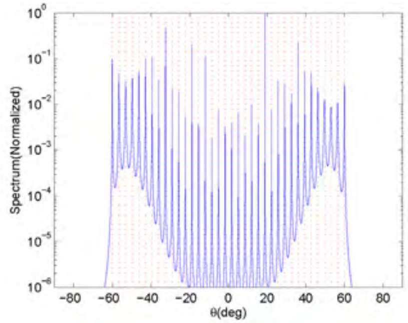

(b) CADiS with $\breve{M} = 1$ $(\eta_c = 85)$

MUSIC (36 signals)

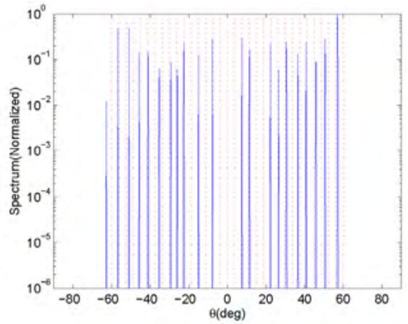

(a) CACIS with $\breve{M} = 2$ $(\eta_u = 65)$

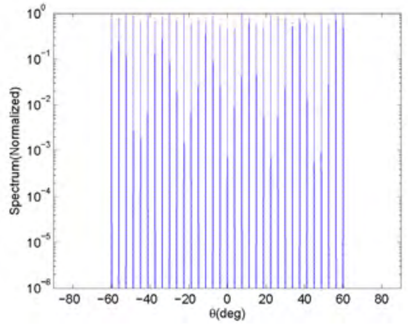

(b) CADiS with $\breve{M} = 2$ $(\eta_u = 87)$

LASSO (33 signals)

Off-grid problem

A major problem with the compressive sensing-based DOA estimation approach is that the DOAs must be on the defined grid, e.g., $[-90^{o} : 1^{o} : 90^{o}]$.

Signals arriving from other DOAs will suffer the **off-grid problem**, e.g., signal from 43.6^{o}.

- Less sparse solution
- Difficult to converge

Solutions in the context of compressive sensing:

- Finer grid resolution
- Grid refining
- Off-grid estimation

1^{o} grid DOA estimation

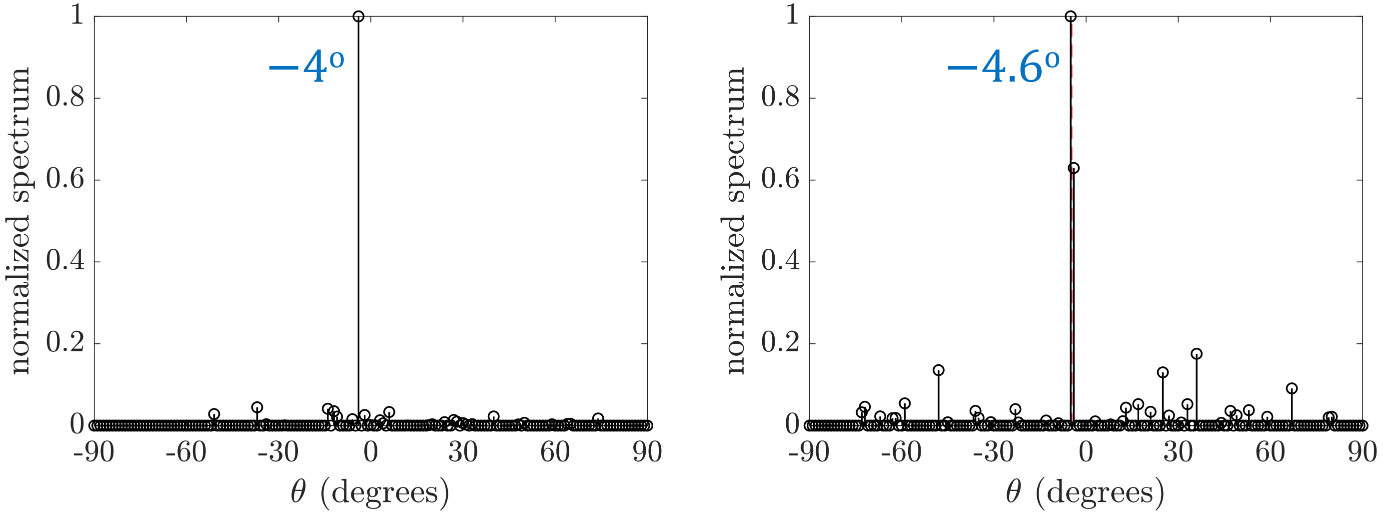

An attractive method is to **complete the covariance matrix** (matrix completion) so that conventional subspace-based methods (e.g., MUSIC) can be applied.

ASP Lab

Part III: Sparsity-based processing and array design

III-A. Sparsity-based DOA estimation

III-B. Structured matrix completion for DOA estimation

- Structured matrix completion methods
- Non-redundant sparse arrays
- 4D automotive radar sensing

III-C. Group sparsity-based DOA estimation

A
S
P
Lab

Matrix completion

Netflix problem: Predict unknown scores.

The data is **low-rank**, but the dictionary is unknown (unlike CS).

Let Ω be the region where the elements of matrix $\boldsymbol{M}$ are observed (i.e., $\{M_{ij} | (i,j) \in \Omega\}$), matrix completion finds a low-rank full matrix $\boldsymbol{X}$ which matches $\boldsymbol{M}$:

$$\min_{\boldsymbol{X}} \quad \mathrm{rank}(\boldsymbol{X}) \quad \text{subject to} \quad X_{ij} = M_{ij} \quad \forall\, (i,j) \in \Omega$$

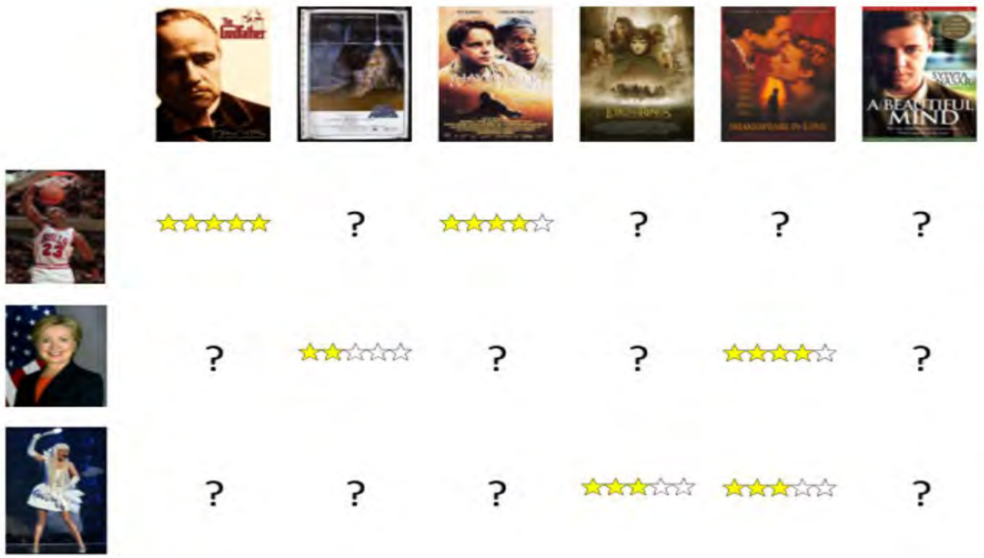

Because the problem involves matrix rank, it is non-convex and NP-hard.

Therefore, the matrix rank is often relaxed, e.g., to its **nuclear norm**:

$$\min_{\boldsymbol{X}} \quad ||\boldsymbol{X}||_* \quad \text{s.t.} \quad X_{ij} = M_{ij} \quad \forall\, (i,j) \in \Omega$$

where $||\boldsymbol{X}||_* = \mathrm{tr}(\sqrt{\boldsymbol{X}^H \boldsymbol{X}})$: nuclear norm of matrix $\boldsymbol{X}$

ASP Lab

Structured matrix completion of covariance matrix

A matrix cannot be completed when an entire row or column is missing in the observed matrix.

- Cannot complete covariance matrix of physical array
- However, for ULA, we can recover the covariance matrix utilizing its Toeplitz and Hermitian structure
- The completed covariance matrix can be defined by only a single column vector $\boldsymbol{w}$ as $\mathcal{T}(\boldsymbol{w})$, and obtained from the nuclear norm minimization

$$\min_{\mathbf{z}} \quad \left\| \left[\mathcal{T}(\boldsymbol{w}) - \boldsymbol{R}_{\boldsymbol{y}}\right] \circ \boldsymbol{B}_{\Omega} \right\|_F^2 + \xi \|\mathcal{T}(\boldsymbol{w})\|_*$$
$$\text{subject to} \quad \mathcal{T}(\boldsymbol{w}) \succcurlyeq \mathbf{0}$$

where

$\boldsymbol{B}_{\Omega}$: mask matrix with $[\boldsymbol{B}_{\Omega}]_{ij} = \begin{cases} 1, & \text{if } (i,j) \in \Omega \\ 0, & \text{otherwise} \end{cases}$

$\boldsymbol{R}_{\boldsymbol{y}}$: observed sparse covariance matrix (nonzero only in $\boldsymbol{B}_{\Omega}$)

ξ: regularization parameter

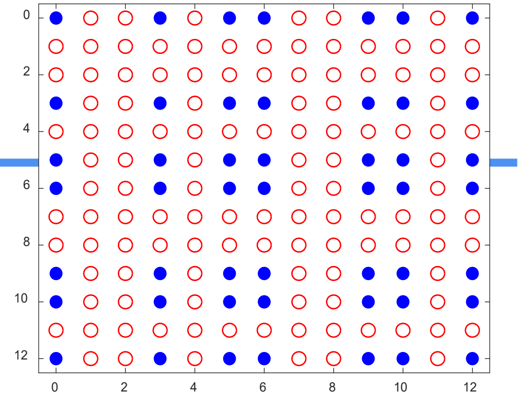

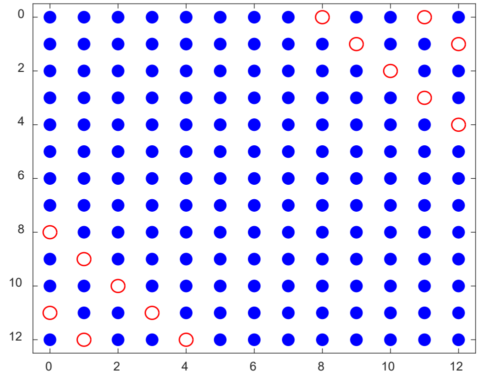

In a Hermitian Toeplitz matrix, a single column w uniquely specifies all the elements of the matrix.

$$\mathcal{T}(\boldsymbol{w}) = \begin{bmatrix} w_1 & w_2^* & w_3^* & w_4^* \\ w_2 & w_1 & w_2^* & w_3^* \\ w_3 & w_2 & w_1 & w_2^* \\ w_4 & w_3 & w_2 & w_1 \end{bmatrix}$$

$\boldsymbol{w}$

H. Qiao and P. Pal, "Unified analysis of co-array interpolation for direction-of-arrival estimation," IEEE ICASSP, 2017.

C. Zhou, Y. Gu, Z. Shi, and Y. D. Zhang, "Off-grid direction-of-arrival estimation using coprime array interpolation," *IEEE Signal Processing Letters*, 2018.

Structured matrix completion of covariance matrix

Atomic norm

- A more general alternative is based on the minimization of the atomic norm.
- Using **atomic set** $\mathcal{A} = \{\boldsymbol{a}_i\}$, an observation vector can be expressed as

$$\boldsymbol{x} = \sum_i c_i \boldsymbol{a}_i, \qquad \boldsymbol{a}_i \in \mathcal{A}$$

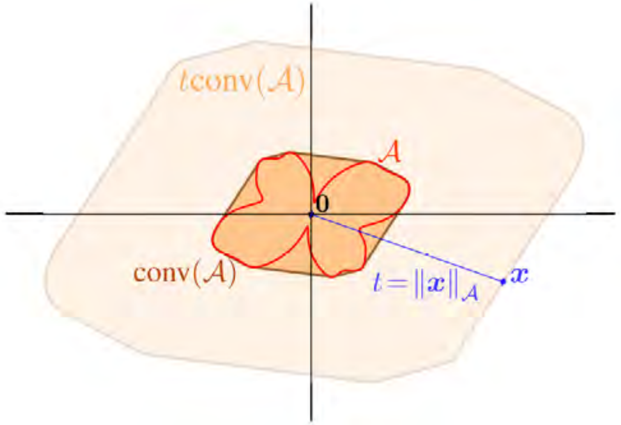

- The atomic norm of $\boldsymbol{x}$ is defined as

$$\|\boldsymbol{x}\|_{\mathcal{A}} = \inf\{t \geq 0 : x \in t \cdot \mathrm{conv}(\mathcal{A})\}$$

where $\mathrm{conv}(\mathcal{A})$ is the convex hull of $\mathrm{conv}(\boldsymbol{\mathcal{A}})\}$

Rank minimization-based structure matrix reconstruction

- Both nuclear and atomic norm minimization problems approximate rank minimization.
- To prevent the approximation loss, the rank function can be reformulated a multi-convex form.

C. Zhou, Y. Gu, X. Fan, Z. Shi, G. Mao, and Y. D. Zhang, "Direction-of-arrival estimation for coprime array via virtual array interpolation," *IEEE Trans. Signal Processing*, 2018.
Y. Chi and M. Ferreira Da Costa, "Harnessing sparsity over the continuum: Atomic norm minimization for superresolution," *IEEE Signal Processing Magazine*, 2020.
S. Liu, Z. Mao, Y. D. Zhang, and Y. Huang, "Rank minimization-based Toeplitz reconstruction for DoA estimation using coprime array," *IEEE Communications Letters*, July 2021.

Matrix completion-aware sparse array design

Matrix completion

- Fills in information in missing lags
- Converts missing holes in the lag from obstacles in consecutive-lag construction into a resource for aperture extension
- Enabling off-grid DOA estimation with larger array apertures

Direct MUSIC

MUSIC with matrix completion

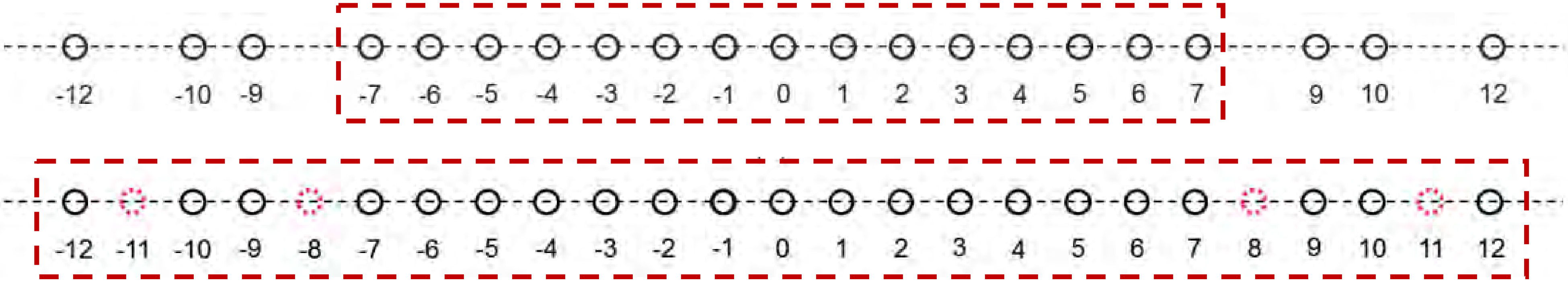

With such capability, how shall we consider the “optimality” of a sparse array?

We introduce **optimized non-redundant array (ONRA)**:

- Redundancy-free: Each lag only appears once (except lag-0)
- Introduce holes in the lag for reducing mutual coupling and enlarging array aperture
- Optimized using mixed-integer linear programming approach (not systematical)

A. Ahmed and Y. D. Zhang, "Generalized non-redundant sparse array designs," *IEEE Trans. Signal Processing*, 2021.

Non-redundant sparse array: Comparison

- Comparison for 6-sensor arrays (DOA estimation for 13 sources; LASSO)
- ONRA has very low mutual coupling effect as the minimum interelement spacing is 2 units

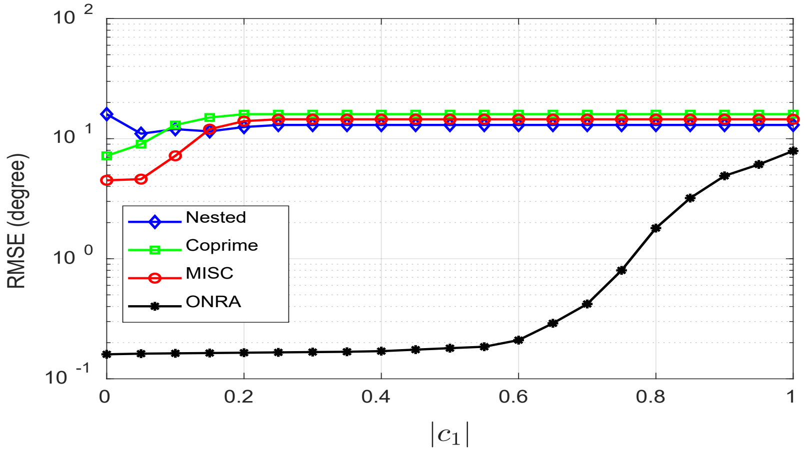

RMSE for two closely spaced source case

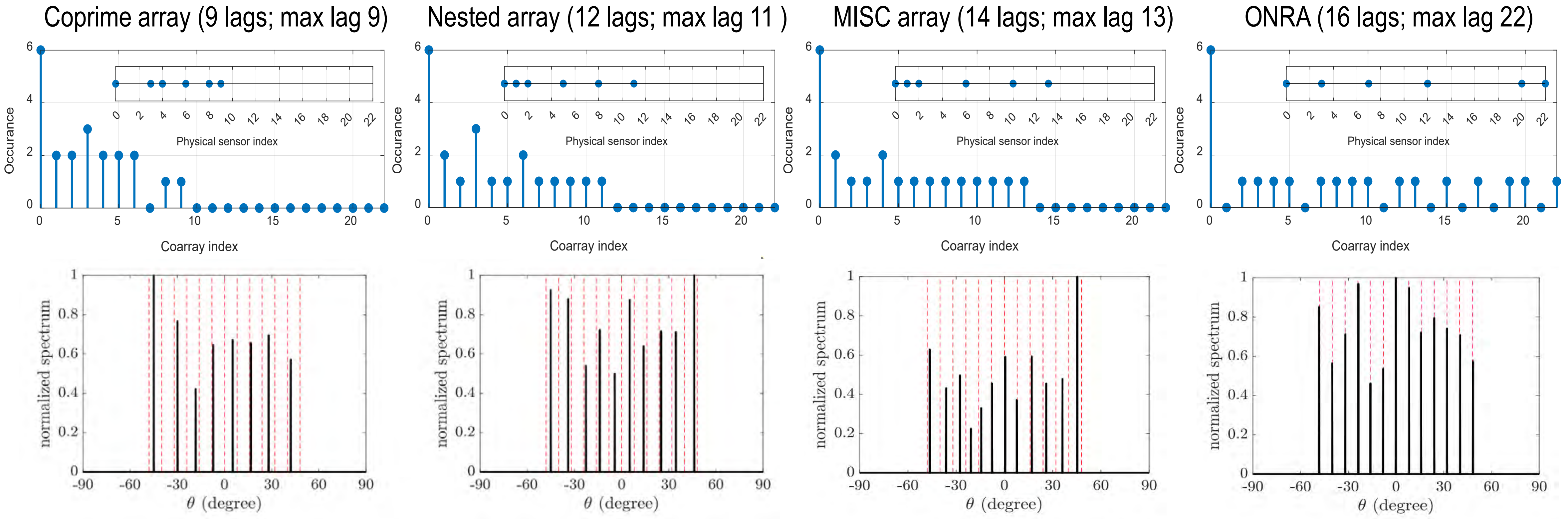

A. Ahmed and Y. D. Zhang, "Generalized non-redundant sparse array designs," *IEEE Trans. Signal Processing*, 2021.

ASP Lab

Automotive radar application

- Radar has emerged as one of the key technologies in autonomous driving systems.
  - Low-cost implementation
  - Resilient sensing in all weather/lighting conditions
- Automotive radar first performs range Doppler mapping, and the result data may only provide few (even one) data samples.
- A large aperture in both azimuth and elevation is important to identify objects and enable drive-over and drive-under.
- To achieve a $\Delta\theta = 1^{\text{o}}$ resolution, a 2D array with an aperture of $D = 1.4/(\pi \sin(\Delta\theta/2)) \approx 51$ wavelengths is needed in each dimension.
- Very few antennas can be used to keep a low cost.

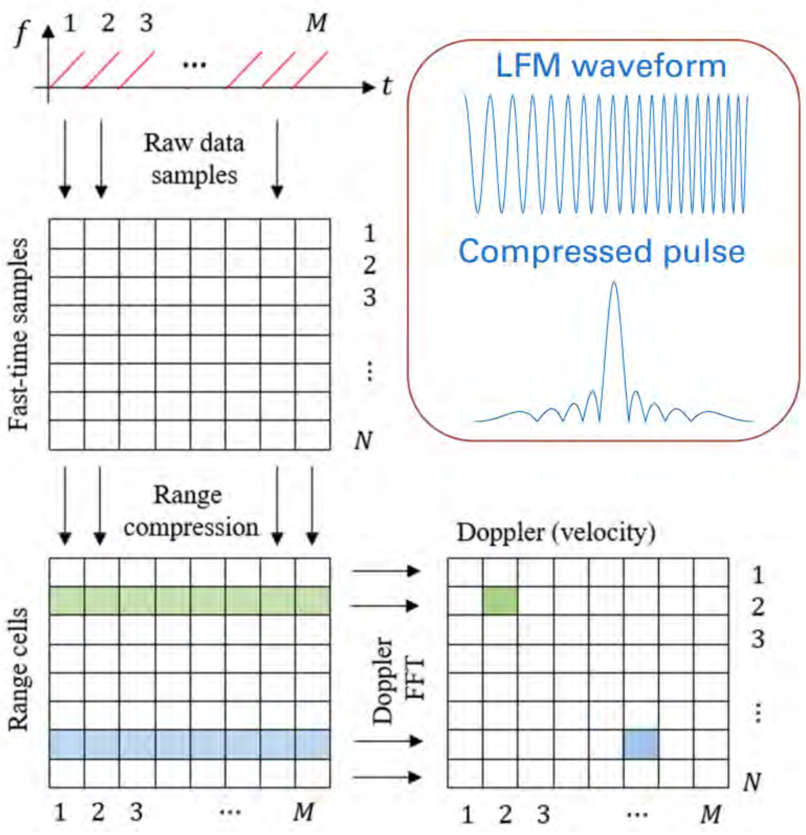

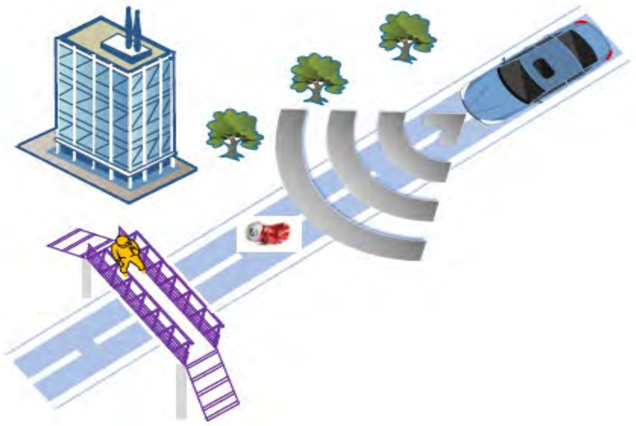

S. Sun and Y. D. Zhang, "4D automotive radar sensing for autonomous vehicles: A sparsity-oriented approach," *IEEE Journal of Selected Topics in Signal Processing*, 2021.

S. Sun and Y. D. Zhang, "Redefining radar perception for autonomous driving: The role of sparse array and waveform design in 4D automotive radar," IEEE Signal Processing Society Webinar Series, Sept. 2023.

ASP Lab

MIMO radar and sum coarray

- Sparse 2-D MIMO radar is commonly used to achieve sum coarray.
- The sum coarray in a MIMO radar is synthesized as $S = \{x + y \,|x \in \mathbb{S}_T, y \in \mathbb{S}_R\}$, where $\mathbb{S}_T$ and $\mathbb{S}_R$ are Tx and Rx antenna positions.
- Texas Instruments (TI) AWRx Cascaded Radar RF Evaluation Module (MMWCAS-RF-EVM) use 12 Tx 16 Rx configuration to provide a large horizontal sum coarray and small vertical aperture.

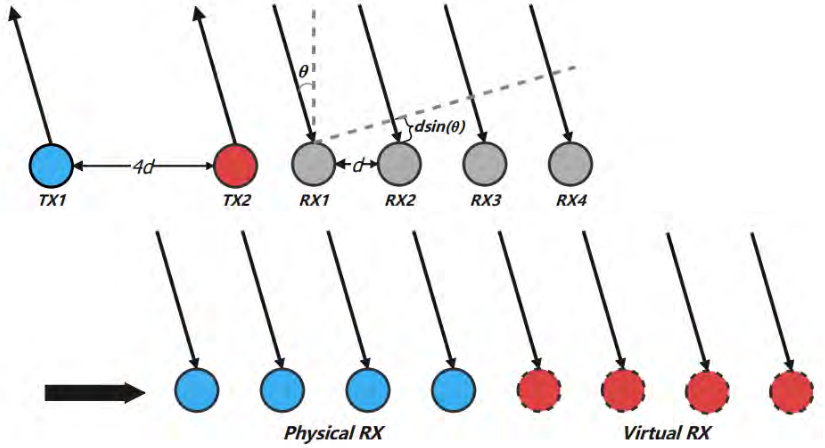

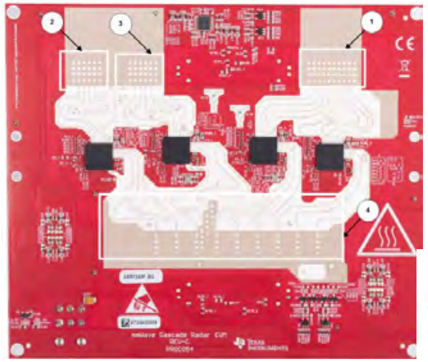

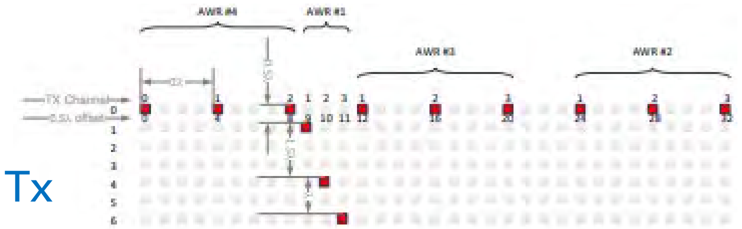

Tx

Rx

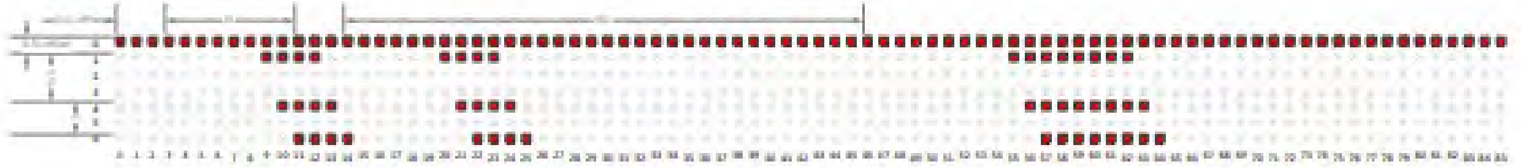

Sum coarray

S. Sun and Y. D. Zhang, “4D automotive radar sensing for autonomous vehicles: A sparsity-oriented approach,” *IEEE Journal of Selected Topics in Signal Processing*, 2021.

A
S
P
Lab

Automotive radar application

Simulation example:

- Consider randomly placing 12 Tx and 16 Rx antennas in about 100 half-wavelength 2D range with 196 virtual antennas: Very sparse antenna placement
- Direct 2-D imaging renders high sidelobes due to missing elements in the sum coarray
- Data completion is important to recover a uniform rectangular array (URA) and reduce the sidelobes
- How to perform data completion when there is a single snapshot?

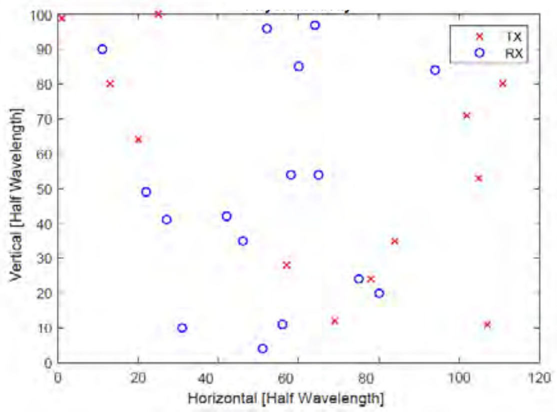

Physical antennas

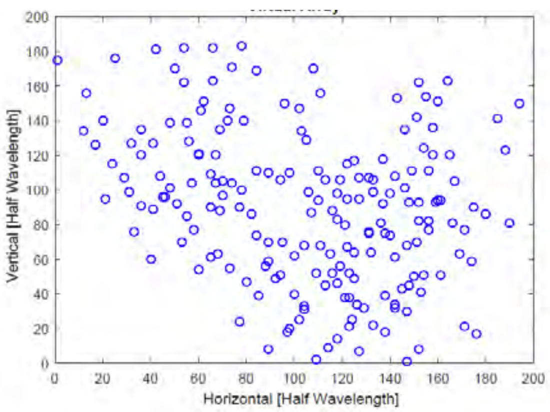

virtual sensors of sum coarray

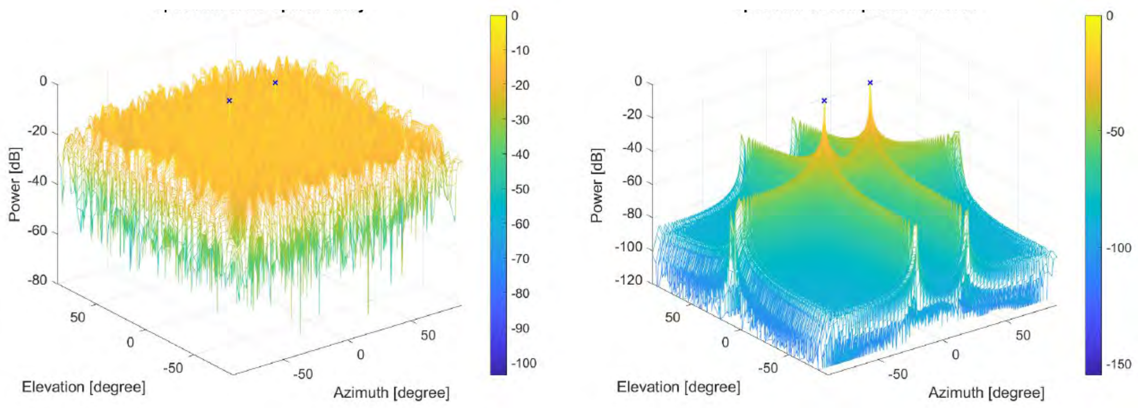

Azimuth & elevation imaging without completion and with completion

S. Sun and Y. D. Zhang, "4D automotive radar sensing for autonomous vehicles: A sparsity-oriented approach," *IEEE Journal of Selected Topics in Signal Processing*, 2021.

Automotive radar application

Hankel matrix construction for M-element ULA:

- Assume noiseless array response $\boldsymbol{y} = [y_1, y_2, \dots, y_M]^T$, we construct a Hankel matrix as

$$\mathcal{H}(\boldsymbol{y}) = \begin{bmatrix} y_1 & y_2 & \cdots & y_L \\ y_2 & y_3 & \cdots & y_{L+1} \\ y_3 & y_4 & \cdots & y_{L+2} \\ \vdots & \vdots & \ddots & \vdots \\ y_{M_1} & y_{M_1+1} & \cdots & y_M \end{bmatrix}$$

  where L is the pencil parameter and $M_1 = M - L + 1$

- When K ($K < M_1$ and $K < L$) sources imping to the array, the Hankel matrix $\mathcal{H}(\boldsymbol{y})$ has a Vandermonde decomposition structure $\mathcal{H}(\boldsymbol{y}) = \boldsymbol{A}\,\boldsymbol{\Sigma}_s\boldsymbol{B}^T$ with rank K, where

$$\boldsymbol{A} = [\boldsymbol{a}(\theta_1), \cdots, \boldsymbol{a}(\theta_K)] \text{ with } \boldsymbol{a}(\theta_k) = \left[1, e^{\frac{j2\pi d \sin(\theta_k)}{\lambda}}, \cdots, e^{\frac{j2\pi (M_1-1) d \sin(\theta_k)}{\lambda}}\right]^T$$

$$\boldsymbol{B} = [\boldsymbol{b}(\theta_1), \cdots, \boldsymbol{b}(\theta_K)] \text{ with } \boldsymbol{b}(\theta_k) = \left[1, e^{\frac{j2\pi d \sin(\theta_k)}{\lambda}}, \cdots, e^{\frac{j2\pi (L-1) d \sin(\theta_k)}{\lambda}}\right]^T$$

$$\boldsymbol{\Sigma}_s = \mathrm{diag}([\beta_1, \cdots, \beta_K])$$

S. Sun and Y. D. Zhang, "4D automotive radar sensing for autonomous vehicles: A sparsity-oriented approach," *IEEE Journal of Selected Topics in Signal Processing*, 2021.

S. Sun and Y. D. Zhang, "Redefining radar perception for autonomous driving: The role of sparse array and waveform design in 4D automotive radar," IEEE Signal Processing Society Webinar Series, Sept. 2023.

Automotive radar application

Hankel matrix completion for sparse linear array:

- Missing sum coarray elements render a Hankel matrix with missing elements:

$$\mathcal{H}(\boldsymbol{y}) = \begin{bmatrix} y_1 & y_2 & \cdots & y_L \\ y_2 & y_3 & \cdots & y_{L+1} \\ y_3 & y_4 & \cdots & y_{L+2} \\ \vdots & \vdots & \ddots & \vdots \\ y_{M_1} & y_{M_1+1} & \cdots & y_M \end{bmatrix}$$

- The forward-only Hankel matrix completion problem is to find a Hankel matrix $\mathcal{H}(\boldsymbol{y})$ that has a minimum rank and its distance to the original data matrix at the observed positions meets the required error bound δ:

$$\min_{\boldsymbol{x}} \ \operatorname{rank}\big(\mathcal{H}(\boldsymbol{x})\big)$$
$$\text{s.t.} \ \|\mathcal{H}(\boldsymbol{x}) \circ \boldsymbol{M} - \mathcal{H}(\boldsymbol{y})\|_F \le \delta$$

where $\boldsymbol{M}$ is a mark matrix.

S. Sun and Y. D. Zhang, "4D automotive radar sensing for autonomous vehicles: A sparsity-oriented approach," *IEEE Journal of Selected Topics in Signal Processing*, 2021.

S. Sun and Y. D. Zhang, "Redefining radar perception for autonomous driving: The role of sparse array and waveform design in 4D automotive radar," IEEE Signal Processing Society Webinar Series, Sept. 2023.

Automotive radar application

2-D sparse array completion:

- We can construct an $N_1 \times (M_1 - N_1 + 1)$ block Hankel matrix as :

$$\boldsymbol{Y}_E = \begin{bmatrix} \boldsymbol{Y}_0 & \boldsymbol{Y}_1 & \cdots & \boldsymbol{Y}_{M_1-N_1} \\ \boldsymbol{Y}_1 & \boldsymbol{Y}_2 & \cdots & \boldsymbol{Y}_{M_1-N_1+1} \\ \boldsymbol{Y}_2 & \boldsymbol{Y}_3 & \cdots & \boldsymbol{Y}_{M_1-N_1+2} \\ \vdots & \vdots & \ddots & \vdots \\ \boldsymbol{Y}_{N_1-1} & \boldsymbol{Y}_{N_1} & \cdots & \boldsymbol{Y}_{M_1-1} \end{bmatrix} \text{ with } \boldsymbol{Y}_m = \begin{bmatrix} x_{m,0} & x_{m,1} & \cdots & x_{m,M_2-L} \\ x_{m,1} & x_{m,2} & \cdots & x_{m,M_2-L+1} \\ x_{m,2} & x_{m,3} & \cdots & x_{m,M_2-L+2} \\ \vdots & \vdots & \ddots & \vdots \\ x_{m,L-1} & x_{m,L} & \cdots & x_{m,M_2-1} \end{bmatrix}$$

- The array response of the URA can be obtained via completing the block Hankel matrix $\boldsymbol{Y}_E$ based on the array response of sparse arrays.

Decoupled atomic norm minimization

- The high-dimensional problem can be decoupled Toeplitz matrices in one dimension, followed by 1D angle estimation with automatic angle pairing.
- The computational complexity is reduced by several orders of magnitude.

S. Sun and Y. D. Zhang, “4D automotive radar sensing for autonomous vehicles: A sparsity-oriented approach,” *IEEE Journal of Selected Topics in Signal Processing*, 2021.

Z. Tian, Z. Zhang and Y. Wang, "Low-complexity optimization for two-dimensional direction-of-arrival estimation via decoupled atomic norm minimization," IEEE ICASSP, 2017.

Part III: Sparsity-based processing and array design

III-A. Sparsity-based DOA estimation

III-B. Structured matrix completion for DOA estimation

III-C. Group sparsity-based DOA estimation

- Multi-frequency array
- Frequency-switching array

Multi-frequency sparse array

- Difference coarray is obtained from array data covariance matrix, which requires (time-domain) snapshots.
- Can we further utilize resources in other domains, such as frequency?
- Multi-frequency sparse array exploits two or more frequencies to obtain virtual arrays.

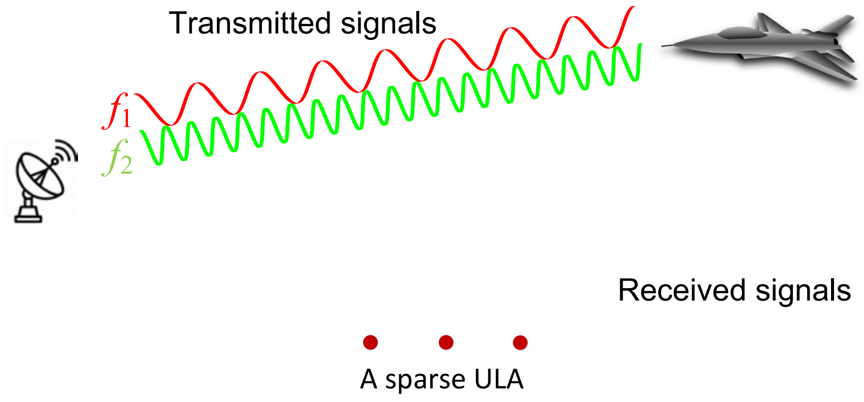

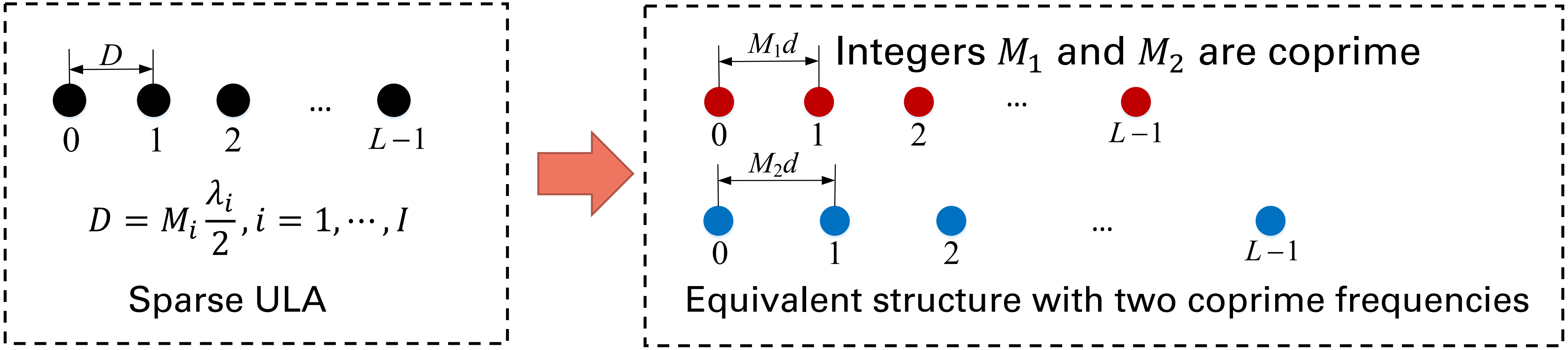

S. Qin, Y. D. Zhang, M. G. Amin, and B. Himed, "DOA estimation exploiting a uniform linear array with multiple co-prime frequencies," *Signal Processing*, 2017.

Multi-frequency sparse array

Maximize the number of virtual sensors: choosing the array configuration and frequencies such that the virtual sensors corresponding to different frequencies do not overlap.

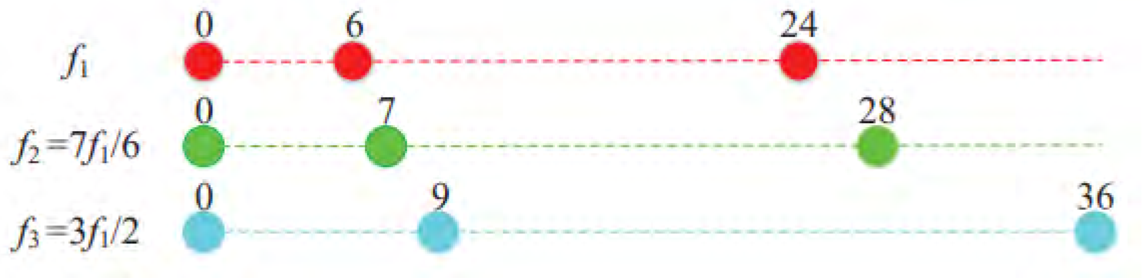

Example: 3 antennas, 3 frequencies

- 7 virtual sensors at $\{0, 6, 7, 9, 24, 28, 36\}\bar{d}$, where $\bar{d}$ denotes half-wavelength without referring to a specific frequency
- 10 non-negative self-lags: $\{0, 6, 7, 9, 18, 21, 24, 27, 28, 36\}\bar{d}$
- 12 non-negative cross-lags: $\{1, 2, 3, 4, 8, 12, 15, 17, 19, 22, 29, 30\}\bar{d}$
- All lags appear only once (redundancy-free)

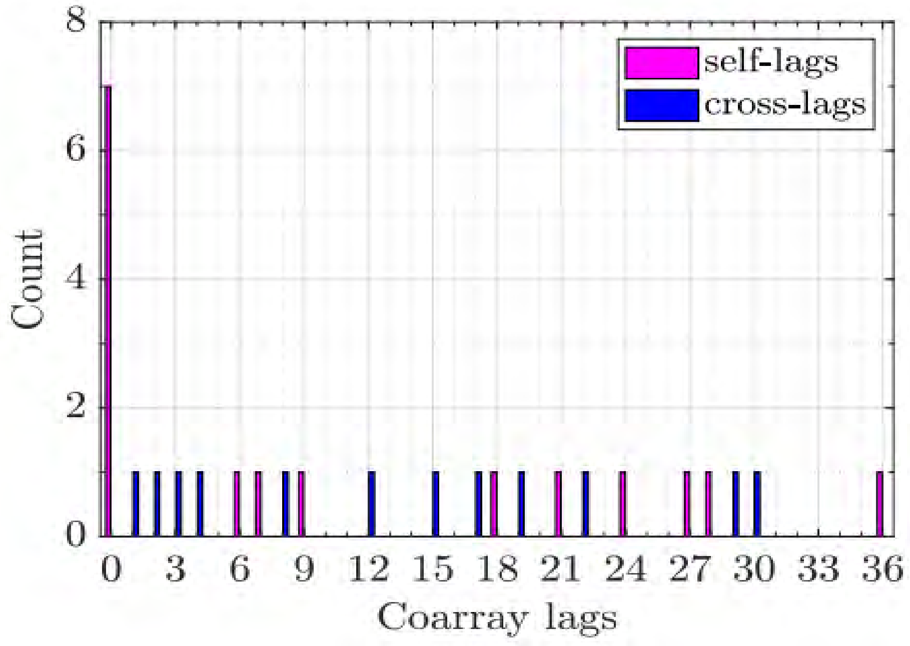

S. Zhang, A. Ahmed, Y. D. Zhang, and S. Sun, "Enhanced DOA estimation exploiting multi-frequency sparse array," *IEEE Trans. Signal Processing*, 2021.

A
S
P
Lab

Multi-frequency sparse array

- Received signal vector for frequency i from K sources

$$\boldsymbol{x}_{\mathbb{S}_i}(t) = \sum_{k=1}^{K} \rho_k^i(t)\boldsymbol{a}_{\mathbb{S}_i}(\theta_k) + \boldsymbol{n}_{\mathbb{S}_i}(t)$$

- We obtain I^2 covariance matrices

$$\boldsymbol{R}_{\boldsymbol{x}_{\mathbb{S}_i}\boldsymbol{x}_{\mathbb{S}_j}} = \mathrm{E}\left\{\boldsymbol{x}_{\mathbb{S}_i}(t)\boldsymbol{x}_{\mathbb{S}_j}^H(t)\right\} = \begin{cases} \boldsymbol{A}_{\mathbb{S}_i}\boldsymbol{R}_{\mathbb{S}_i\mathbb{S}_i}\boldsymbol{A}_{\mathbb{S}_i}^H + \sigma_n^2\boldsymbol{I}_L, & i = j \\ \boldsymbol{A}_{\mathbb{S}_i}\boldsymbol{R}_{\mathbb{S}_i\mathbb{S}_j}\boldsymbol{A}_{\mathbb{S}_j}^H, & i \neq j \end{cases}$$

- Important to note that $\rho_k^i(t) \neq \rho_k^j(t)$
  - $\boldsymbol{R}_{\mathbb{S}_i\mathbb{S}_i}$ is real diagonal, but $\boldsymbol{R}_{\mathbb{S}_i\mathbb{S}_j}$ is generally complex and differs for different frequency pairs
  - The signals observed at different frequencies cannot be directly combined or stacked together
  - However, because they share the same signal DOAs, group sparsity-based approaches are effective to perform DOA estimation

S. Zhang, A. Ahmed, Y. D. Zhang, and S. Sun, "Enhanced DOA estimation exploiting multi-frequency sparse array," *IEEE Trans. Signal Processing*, 2021.

Multi-frequency sparse array

Array interpolation using self-lags only

- Construct $\boldsymbol{R}^{i}_{\boldsymbol{x}_{\mathbb{U}}\boldsymbol{x}_{\mathbb{U}}}$ corresponding to the ULA for frequency i from $\boldsymbol{R}_{\boldsymbol{x}_{\mathbb{S}_i}\boldsymbol{x}_{\mathbb{S}_i}}$, and estimate $\boldsymbol{R}_{\boldsymbol{y}_{\mathbb{U}}\boldsymbol{y}_{\mathbb{U}}}$ as

$$\boldsymbol{R}_{\boldsymbol{y}_{\mathbb{U}}\boldsymbol{y}_{\mathbb{U}}} = \left(\sum_{i=1}^{I} \boldsymbol{R}^{i}_{\boldsymbol{x}_{\mathbb{U}}\boldsymbol{x}_{\mathbb{U}}} \circ \boldsymbol{B}_i\right) \circ \boldsymbol{D}$$

  where $B_i(m,n)$ denotes binary mask,

$$D(m,n) = \frac{1}{\sum_{i=1}^{I} B_i(m,n) + \epsilon}$$

  and $\epsilon > 0$ is a small positive value

- Sparsity-based optimization

$$\min_{\boldsymbol{w},\boldsymbol{R}} \ \left\|\boldsymbol{\mathcal{T}}(\boldsymbol{w}) \circ \boldsymbol{B} - \boldsymbol{R}_{\boldsymbol{y}_{\mathbb{U}}\boldsymbol{y}_{\mathbb{U}}}\right\|_F^2 + \zeta \,\mathrm{Tr}\,(\boldsymbol{\mathcal{T}}(\boldsymbol{w}))$$

$$\text{s.t.} \quad \boldsymbol{\mathcal{T}}(\boldsymbol{w}) \succcurlyeq 0$$

  $\mathcal{T}(\boldsymbol{w})$: Hermitian Toeplitz matrix with $\boldsymbol{w}$ as the first column

  ζ: regularization parameter

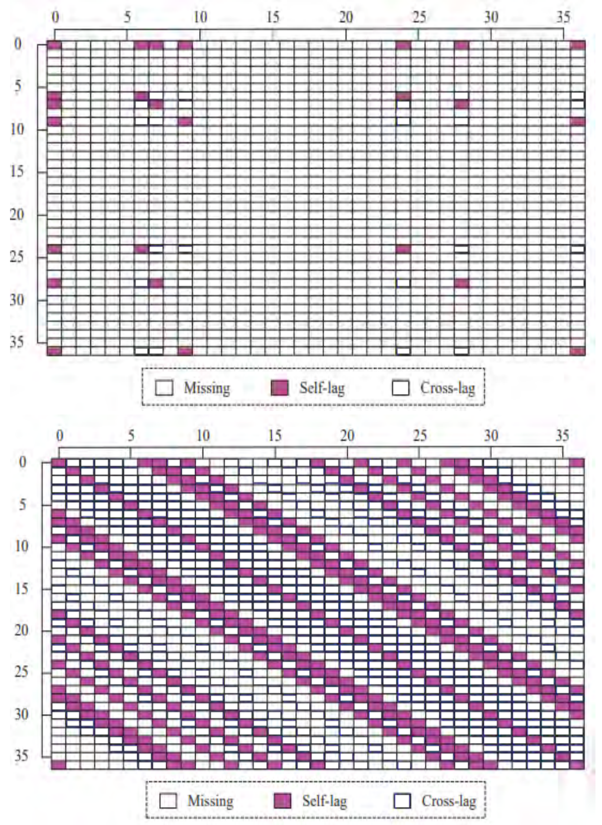

In a Hermitian Toeplitz matrix, a single column w uniquely specifies all the elements of the matrix.

$$\boldsymbol{\mathcal{T}}(\boldsymbol{w}) = \begin{bmatrix} w_1 & w_2^* & w_3^* & w_4^* \\ w_2 & w_1 & w_2^* & w_3^* \\ w_3 & w_2 & w_1 & w_2^* \\ w_4 & w_3 & w_2 & w_1 \end{bmatrix}$$

$\boldsymbol{w}$

S. Zhang, A. Ahmed, Y. D. Zhang, and S. Sun, "Enhanced DOA estimation exploiting multi-frequency sparse array," *IEEE Trans. Signal Processing*, 2021.

Multi-frequency sparse array

Array interpolation using both self- and cross-lags

- Exploiting both self- and cross-lags more effective utilization of the observed information.
- Vectorizing $\boldsymbol{R}_{\boldsymbol{x}_{\mathbb{S}_i}\boldsymbol{x}_{\mathbb{S}_j}}$, $i \neq j$, renders

$$\boldsymbol{z}_{\mathbb{S}_i\mathbb{S}_j} = \mathrm{vec}\{\boldsymbol{R}_{\boldsymbol{x}_{\mathbb{S}_i}\boldsymbol{x}_{\mathbb{S}_j}}\} = \widetilde{\boldsymbol{A}}_{\mathbb{S}_i\mathbb{S}_j}\boldsymbol{r}_{i,j} = \boldsymbol{\Phi}_{\mathbb{S}_i\mathbb{S}_j}\tilde{\boldsymbol{r}}_{i,j}$$

  where $\boldsymbol{\Phi}_{\mathbb{S}_i\mathbb{S}_j} = [\widetilde{\boldsymbol{A}}_{\mathbb{S}_i\mathbb{S}_j} \ \ 0]$ is the dictionary counting for noise term
- Because $\boldsymbol{r}_{i,j}$ differs to each other, we need to solve them for all frequency pairs, rendering a high number of unknowns
- However, all these unknown vectors should have the same **support**, i.e., same nonzero positions indicating the same signal DOAs.
- Such property is referred to as **group sparsity,** and group compressive sensing methods can achieve near-coherent data fusion.

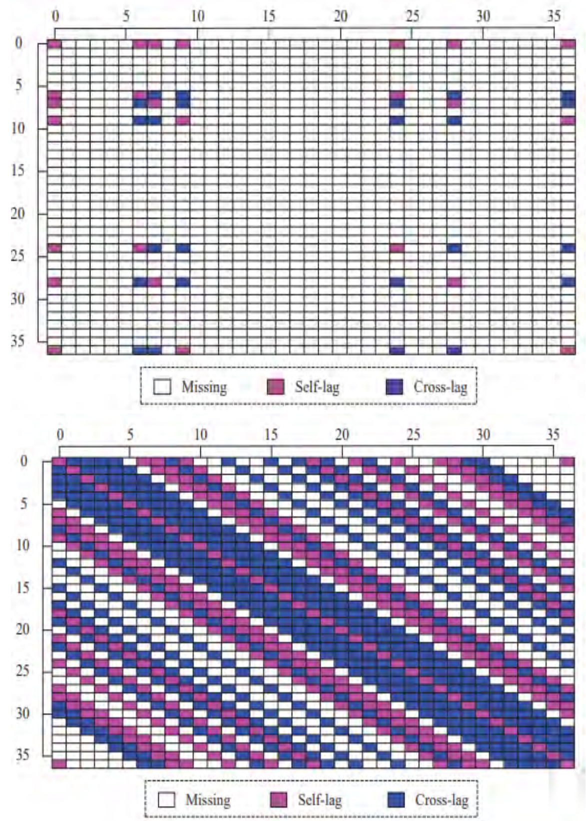

S. Zhang, A. Ahmed, Y. D. Zhang, and S. Sun, "Enhanced DOA estimation exploiting multi-frequency sparse array," *IEEE Trans. Signal Processing*, 2021.

Group sparsity

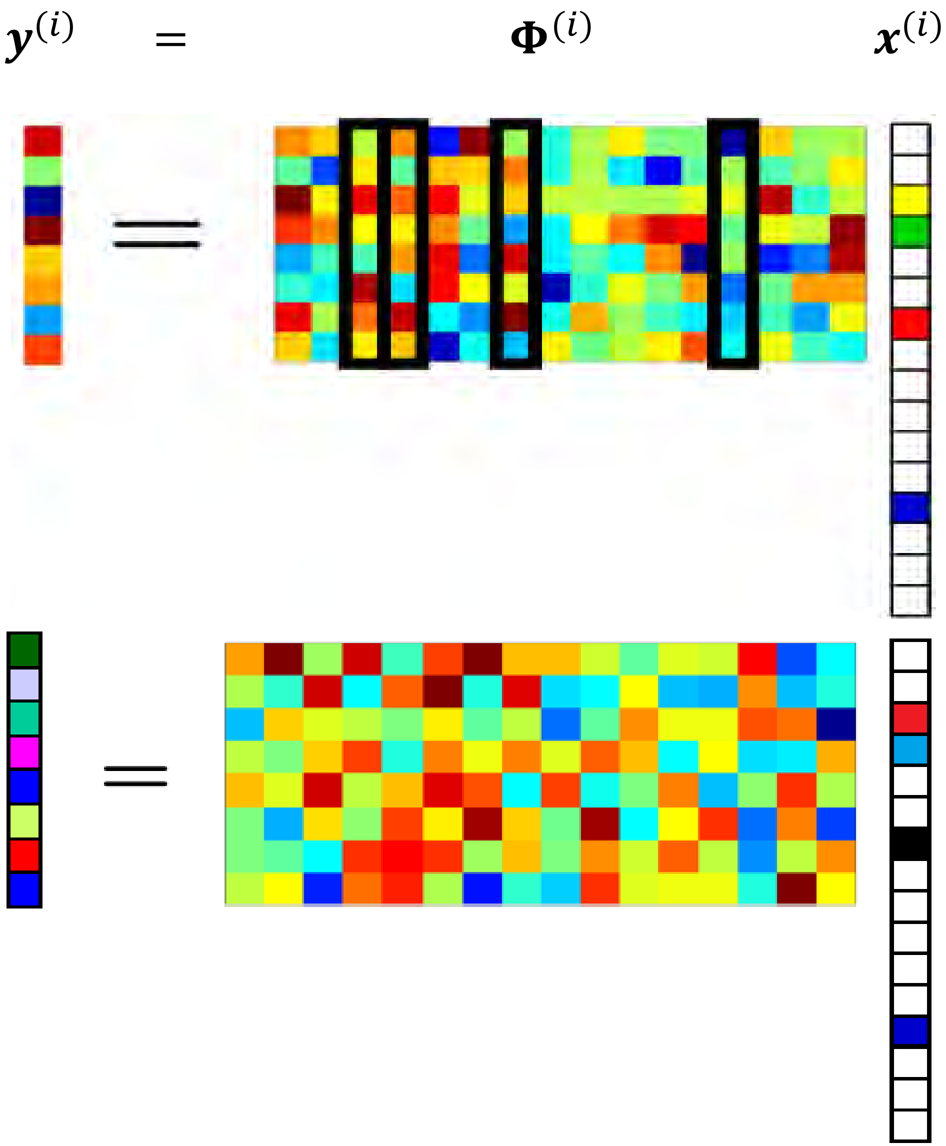

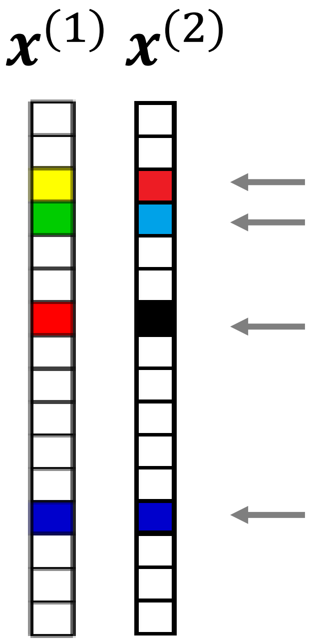

Same positions of nonzero values, but generally with different values

Group sparsity

- OMP and Lasso use mixed l_2/l_1-norm (l_2-norm of the absolute values; also called mixed l_{12}-norm) to handle signal group sparsity.
- l_1-norm relaxation ➔ mixed $l_{1,2}$-norm relaxation

$$\min \quad \|\boldsymbol{x}\|_{1,2} \quad \text{s.t.} \quad \|\boldsymbol{y}-\boldsymbol{\Phi}\boldsymbol{x}\|_2 \le \epsilon$$

where

$$\boldsymbol{y}=\begin{bmatrix}\boldsymbol{y}^{(1)}\\ \boldsymbol{y}^{(2)}\\ \vdots\\ \boldsymbol{y}^{(L)}\end{bmatrix} \qquad \boldsymbol{x}=\begin{bmatrix}\boldsymbol{x}^{(1)}\\ \boldsymbol{x}^{(2)}\\ \vdots\\ \boldsymbol{x}^{(L)}\end{bmatrix} \qquad \boldsymbol{\Phi}=\begin{bmatrix}\boldsymbol{\Phi}^{(1)} & & & \\ & \boldsymbol{\Phi}^{(2)} & & \\ & & \ddots & \\ & & & \boldsymbol{\Phi}^{(L)}\end{bmatrix}$$

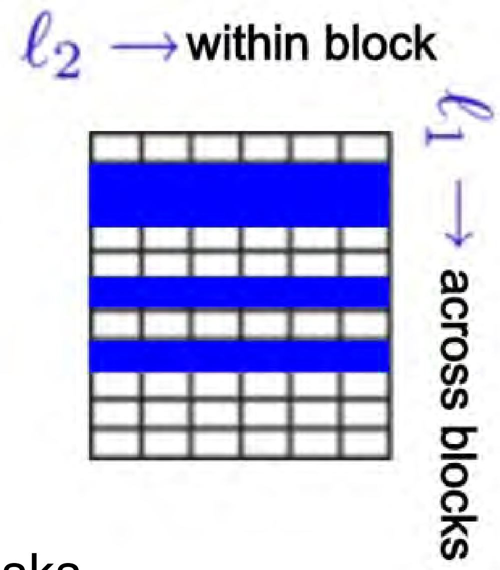

- Multitask sparse Bayesian learning uses the same prior for different tasks

$$\boldsymbol{y}_l=\boldsymbol{\Phi}_l\boldsymbol{x}_l+\boldsymbol{\varepsilon}_l, \quad \boldsymbol{\varepsilon}_l \sim \mathcal{N}(\boldsymbol{0},\beta_l\boldsymbol{I})$$

$$p(\boldsymbol{y}_l|\boldsymbol{\Phi}_l,\boldsymbol{x}_l)=\mathcal{N}(\boldsymbol{y}_l|\boldsymbol{\Phi}_l\boldsymbol{x}_l,\beta_l\boldsymbol{I})$$

$$p(\boldsymbol{x}_l|\boldsymbol{\gamma})=\prod_i \mathcal{N}(x_{l,i}|0,\gamma_i)$$

Same prior $\boldsymbol{\gamma}$ is used for all $\boldsymbol{x}_l$

L. Jacob, G. Obozinski, and J-P. Vert, "Group Lasso with overlap and graph Lasso," *International Conference on Machine Learning*, 2009.

Y. C. Eldar, P. Kuppinger, and H. Bölcskei, "Block-sparse signals: Uncertainty relations and efficient recovery," *IEEE Trans. Signal Processing*, 2010.

S. Ji, D. Dunson, and L. Carin, "Multi-task compressive sampling," *IEEE Trans. Signal Processing*, 2009. [MATLAB code available]

Z. Zhang and B. D. Rao, "Extension of SBL algorithms for the recovery of block sparse signals with intra-block correlation," *IEEE Trans. Signal Processing*, 2013 [MATLAB code available]

Q. Wu, Y. D. Zhang, M. G. Amin, and B. Himed, "Complex multitask Bayesian compressive sensing," IEEE ICASSP, 2014.

Multi-frequency sparse array

Group sparse reconstruction

- Achieve near-coherent data fusion
- Useful in DOA estimation when involving unknown phase

Array Interpolation Using Both Self- and Cross-lags (con't)

- Vectorizing $\boldsymbol{\mathcal{T}}(\boldsymbol{w})$ renders $z_{\mathbb{UU}} = \mathrm{vec}\big(\boldsymbol{\mathcal{T}}(\boldsymbol{w})\big) = \boldsymbol{\Phi}_{\mathbb{UU}}\,\boldsymbol{r}$
- Group sparsity-based optimization

$$\min_{\boldsymbol{w},\boldsymbol{\mathcal{R}}} \left\| \boldsymbol{\mathcal{T}}(\boldsymbol{w}) \circ \boldsymbol{B} - \boldsymbol{R}_{y_{\mathbb{U}} y_{\mathbb{U}}} \right\|_{\mathrm{F}}^{2} + \zeta\,\mathrm{Tr}\,\left(\boldsymbol{\mathcal{T}}(\boldsymbol{w})\right) + \beta_1 \sum_{1 \le i < j \le I} \left\| \boldsymbol{z}_{\mathbb{S}_i \mathbb{S}_j} - \boldsymbol{\Phi}_{\mathbb{S}_i \mathbb{S}_j}\,\boldsymbol{r}_{i,j} \right\|_2 + \beta_1 \| z_{\mathbb{UU}} - \boldsymbol{\Phi}_{\mathbb{UU}} \boldsymbol{r} \|_2 + \beta_2 \|\boldsymbol{\mathcal{R}}\|_{1,2}$$

$$\mathrm{s.t.}\ \boldsymbol{\mathcal{T}}(\boldsymbol{w}) \succcurlyeq 0$$

where $\boldsymbol{\mathcal{R}} = [\boldsymbol{r}_{1,2}, \boldsymbol{r}_{1,3}, \ldots, \boldsymbol{r}_{I-1,I}, \boldsymbol{r}]$, β_1 and β_2 are regularization parameters, and the $l_{1,2}$-norm of $\boldsymbol{\mathcal{R}}$ is

$$\|\boldsymbol{\mathcal{R}}\|_{1,2} = \sum_{m=1}^{G+1} \left(\sum_{n=1}^{\frac{I(I-1)}{2}+1} \boldsymbol{\mathcal{R}}(m,n)\boldsymbol{\mathcal{R}}^*(m,n) \right)^{1/2}$$

G: dimension of $\boldsymbol{r}$ (number of angular grid points)

S. Zhang, A. Ahmed, Y. D. Zhang, and S. Sun, "Enhanced DOA estimation exploiting multi-frequency sparse array," *IEEE Trans. Signal Processing*, 2021.

Multi-frequency sparse array

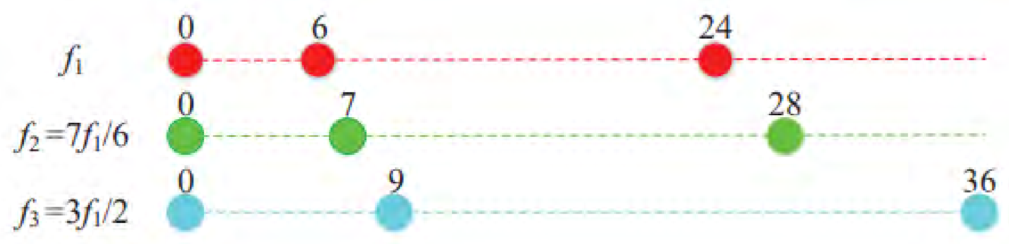

Simulation example:

- $K = 8$ targets are uniformly distributed in [−14°, 14°]
- Input SNR = 10 dB for all targets
- $T = 100$ snapshots

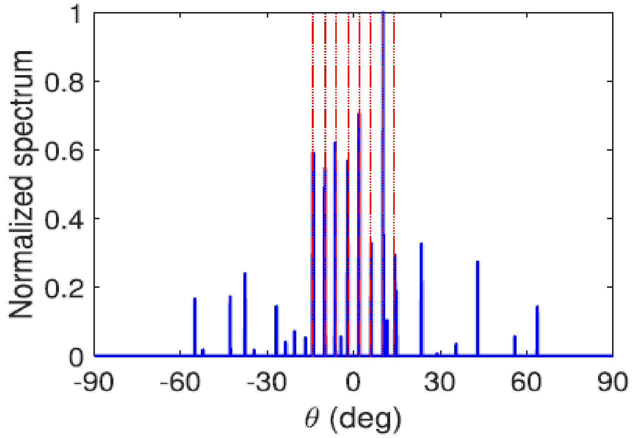

Group lasso without array interpolation [Ahmed 2020]

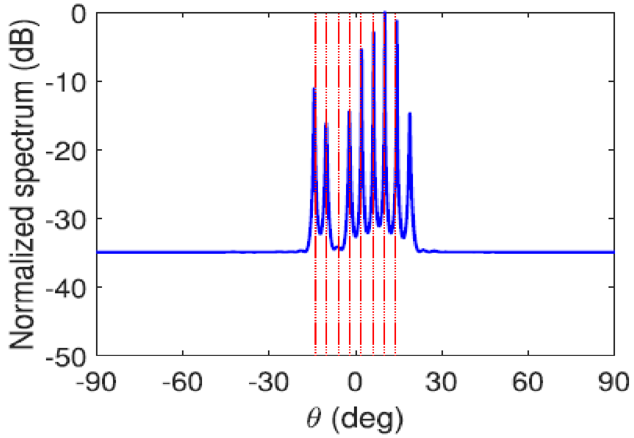

MUSIC after array interpolation with self-lags [Zhang 2020]

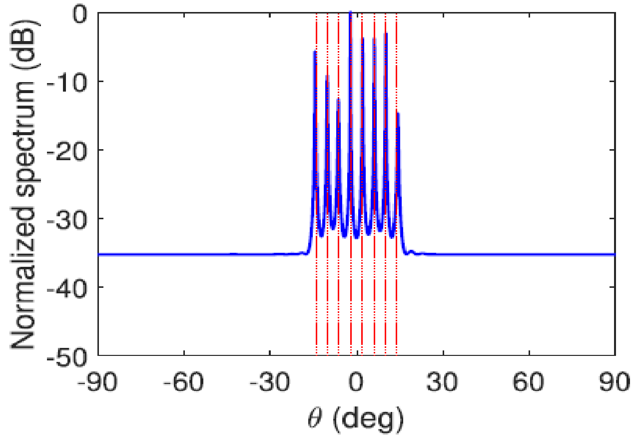

MUSIC using both self- and cross-lags [Zhang 2021]

A. Ahmed, D. Silage, and Y. D. Zhang, “High-resolution target sensing using multi-frequency sparse array,” *IEEE SAM Workshop*, 2020.
S. Zhang, A. Ahmed, Y. D. Zhang, and S. Sun, “DOA estimation exploiting interpolated multi-frequency sparse array,” *IEEE SAM Workshop*, 2020.
S. Zhang, A. Ahmed, Y. D. Zhang, and S. Sun, "Enhanced DOA estimation exploiting multi-frequency sparse array," *IEEE Trans. Signal Processing*, 2021.

Frequency-switching sparse array

- Multi-frequency sparse arrays require wideband processing of the received signal with a high complexity, making them infeasible for certain applications.
- Frequency-switching sparse arrays provide an effective alternative with similar performance.
- At any time, only a single-frequency component is processed.

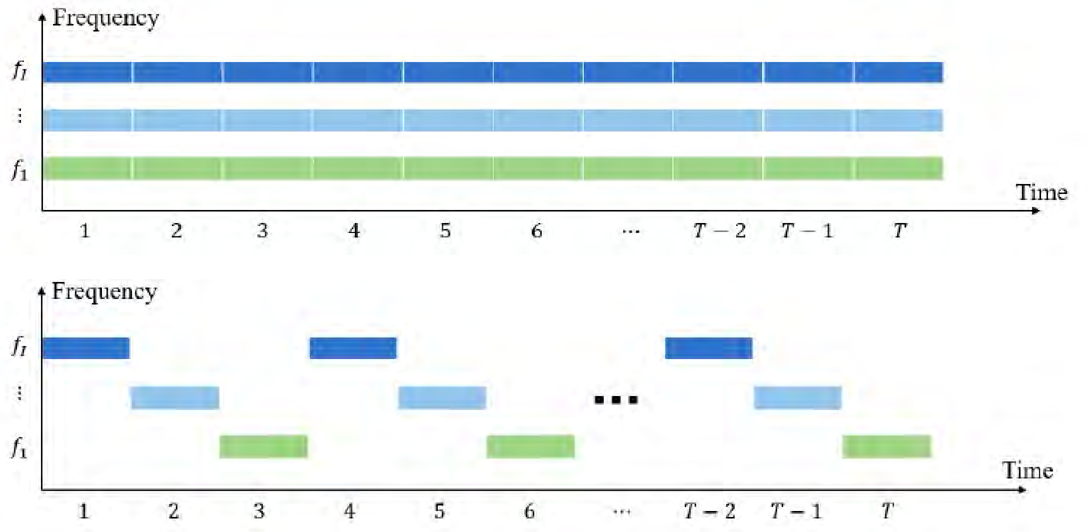

- Multi-frequency: Power divided by I; all time samples used
- Frequency-selective: full power used; time samples divided by I

Processing

- Similar processing methods to the multi-frequency sparse arrays can be used to perform array interpolation and DOA estimation

Y. D. Zhang and M. W. T. S. Chowdhury, "Frequency-switching sparse arrays," IEEE SAM Workshop, 2024.

A S P Lab

Frequency-switching sparse array

Cramer-Rao Bound (CRB) analysis

- Frequency-switches lowers the CRB at low SNR
- For over-determined DOA estimation, both sparse arrays achieve the same CRB at high SNR region
- For under-determined DOA estimation, multi-frequency sparse arrays achieve lower CRB at high SNR, due to the floor with the SNR

Example:

- 5 physical sensors; $I = 2$ frequencies
- $T = 5000$ snapshots
- 4 or 10 signals uniformly distributed in $[-60^o, 60^o]$

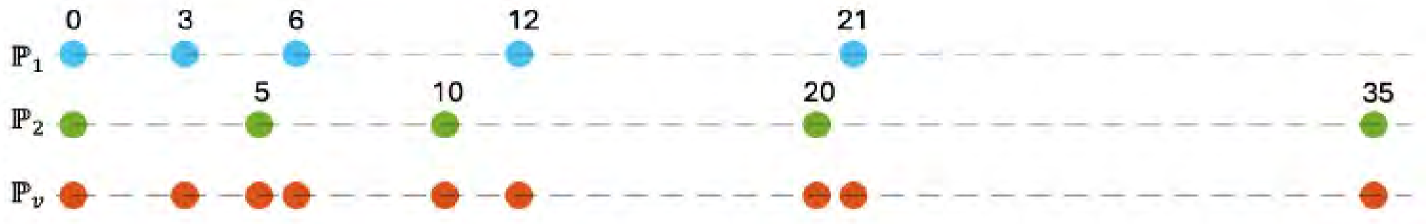

Y. D. Zhang and M. W. T. S. Chowdhury, "Frequency-switching sparse arrays," IEEE SAM Workshop, 2024.

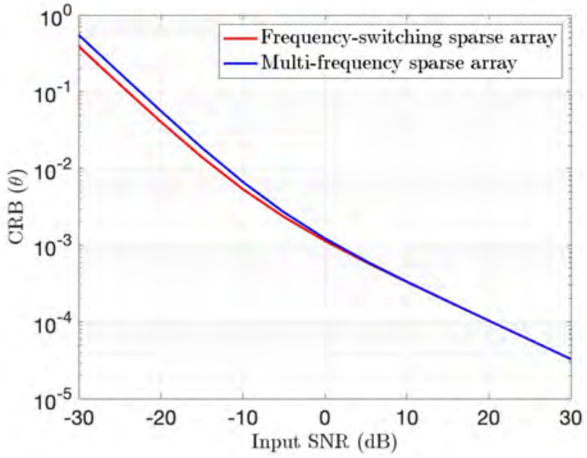

Overdetermined case (4 signals)

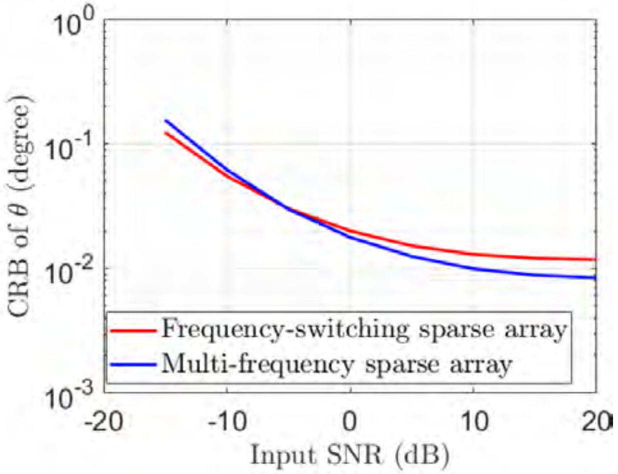

Underdetermined case (10 signals)

Part IV: Additional Topics

- DOA estimation exploiting high-order statistics
- Distributed array with mixed-precision covariance matrices
- Signal coherency consideration
- Machine learning for DOA estimation

Fourth-order difference coarray

- For zero-mean signals, fourth-order cumulant is defined as

$$\begin{aligned} c(l) &= \mathrm{cum}\{x_{q_1}, x_{q_2}^*, x_{q_3}, x_{q_4}^*\} \\ &= \mathrm{E}\{x_{q_1}x_{q_2}^*x_{q_3}x_{q_4}^*\} - \mathrm{E}\{x_{q_1}x_{q_2}^*\}\mathrm{E}\{x_{q_3}x_{q_4}^*\} - \mathrm{E}\{x_{q_1}x_{q_4}^*\}\mathrm{E}\{x_{q_2}^*x_{q_3}\} - \mathrm{E}\{x_{q_2}^*x_{q_4}^*\}\mathrm{E}\{x_{q_1}x_{q_3}\} \end{aligned}$$

- Compared to the difference coarray based on second-order statistics, fourth-order statistics offers more lags and solves more sources because it utilizes sum co-array of two difference co-arrays
- Typically, fourth-order difference coarrays require a much higher number of snapshots to obtain a good estimate of the statistics

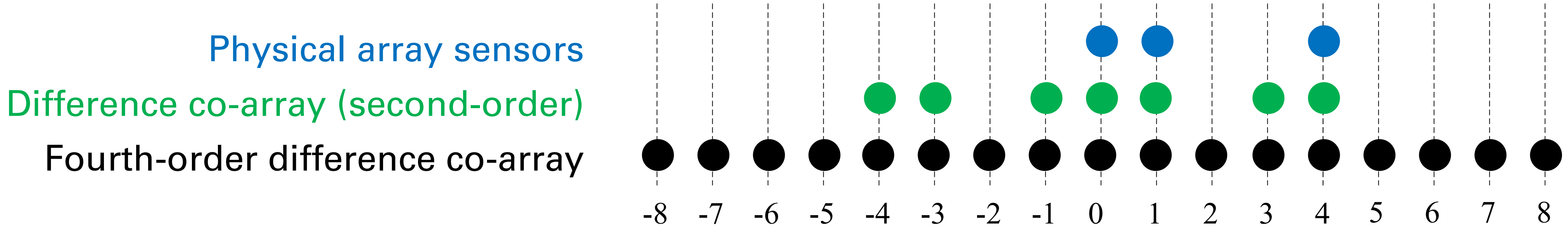

A. Ahmed, Y. D. Zhang, and B. Himed, "Effective nested array design for fourth-order cumulant-based DOA estimation," IEEE Radar Conference, 2017.

Fourth-order difference coarray

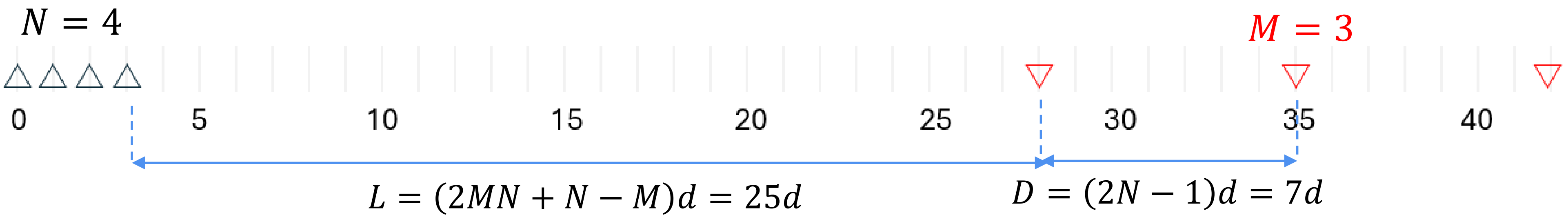

This “nested array” configuration achieves $16MN - 8M + 1 = 169$ consecutive lags.

Simulation example

- 7-element nested array ($M = 3, N = 4$)
- Four-order statistics provides consecutive lags between -84 and 84
- Number of uncorrelated sources = 40
- Uniformly distributed from -60^{o} to 60^{o}
- Number of snapshots = 500,000
- Additive white Gaussian noise with 0 dB input SNR
- MUSIC spectrum show all signals are resolved

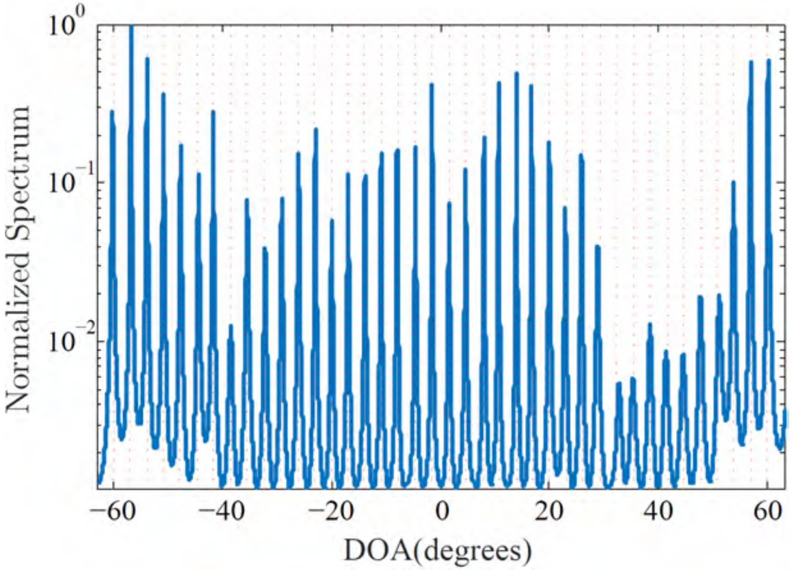

A. Ahmed, Y. D. Zhang, and B. Himed, "Effective nested array design for fourth-order cumulant-based DOA estimation," IEEE Radar Conference, 2017.

A S P Lab

Distributed array with mixed-precision data fusion

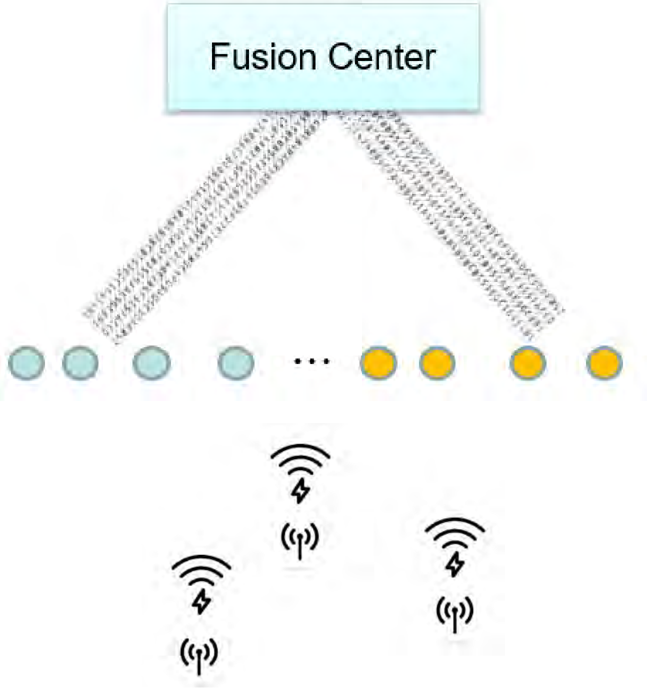

- A large array is required to achieve high resolution and high number of DOFs.
- Distributed array processing enables forming a large virtual array by exploiting multiple distributed subarrays.
- Signals received from distributed subarrays can be fused and processed coherently or non-coherently.
- Coherent signal fusion requires, among others, raw data from subarrays at the fusion center: High traffic overhead
- We consider a mixed-precision processing technique to achieve coherent processing with low traffic overhead.
  - Each subarray sends the full-precision self-covariance matrix and the one-bit data to the fusion center
  - Fusion center computes cross-subarray covariance matrices based on one-bit data

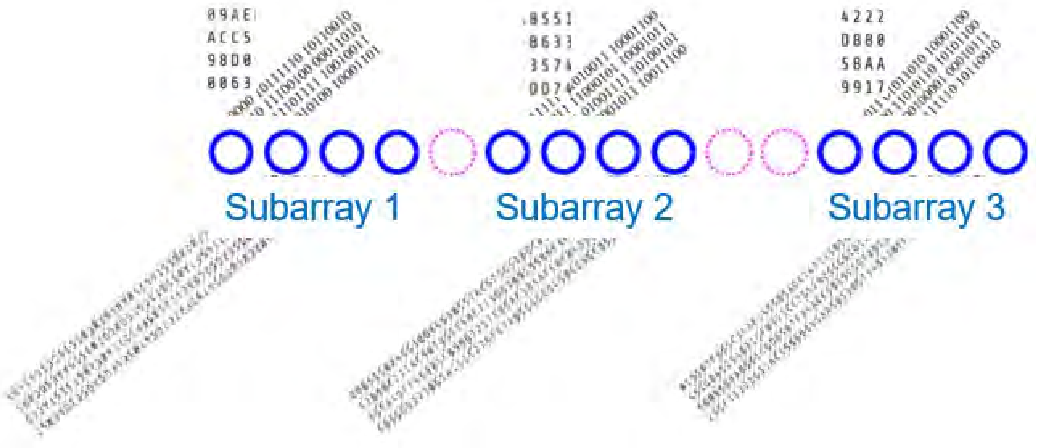

Y. D. Zhang and M. W. T. S. Chowdhury, "Direction-of-arrival estimation in closely distributed array exploiting mixed-precision covariance matrices," *Signal Processing*, 2024.

Distributed array with mixed-precision data fusion

Local processing at the k-th subarray

- Compute full-precision self-covariance matrix $\hat{\boldsymbol{R}}_k = \frac{1}{T}\sum_{t}^{T} \boldsymbol{x}_k(t)\boldsymbol{x}_k^H(t)$
- Compute one-bit complex array data $\boldsymbol{y}_k(t) = \frac{1}{\sqrt{2}}\{Q[\mathrm{Re}(\boldsymbol{x}_k(t))] + j \cdot Q[\mathrm{Im}(\boldsymbol{x}_k(t))]\}$

  where $Q[\cdot]$: one-bit quantization

$\hat{\boldsymbol{R}}_k$ and $\boldsymbol{y}_k(t)$ are sent to the fusion center for DOA estimation.

Processing at fusion center

- Compute one-bit cross-covariance matrix between subarrays as $\hat{\boldsymbol{R}}_{k_1k_2}^{[1\mathrm{B}]} = \frac{1}{T}\sum_{t=1}^{T} \boldsymbol{y}_{k_1}(t)\boldsymbol{y}_{k_2}^H(t)$
- Estimate normalized cross-covariance matrix as $\hat{\bar{\boldsymbol{R}}}_{k_1k_2} = \sin\left(\frac{\pi}{2}\mathrm{Re}[\hat{\boldsymbol{R}}_{k_1k_2}^{[1\mathrm{B}]}]\right) + j \cdot \sin\left(\frac{\pi}{2}\mathrm{Im}[\hat{\boldsymbol{R}}_{k_1k_2}^{[1\mathrm{B}]}]\right)$
- Estimate cross-covariance matrix as $\hat{\boldsymbol{R}}_{k_1k_2} = \boldsymbol{G}_{k_1}^{1/2}\hat{\bar{\boldsymbol{R}}}_{k_1k_2}\boldsymbol{G}_{k_2}^{1/2}$, $\quad [\boldsymbol{G}_k]_{m,m} = [\hat{\boldsymbol{R}}_k]_{m,m}$

Y. D. Zhang and M. W. T. S. Chowdhury, "Direction-of-arrival estimation in closely distributed array exploiting mixed-precision covariance matrices," *Signal Processing*, 2024.

Distributed array with mixed-precision data fusion

Assume all subarrays are precisely located on half-wavelength grid, we can apply structured matrix completion to obtain the full covariance matrix and perform MUSIC for DOA estimation.

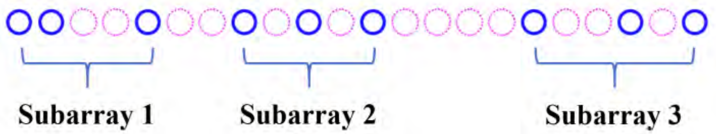

Errors due to subarray position errors can be iteratively estimated and compensated.

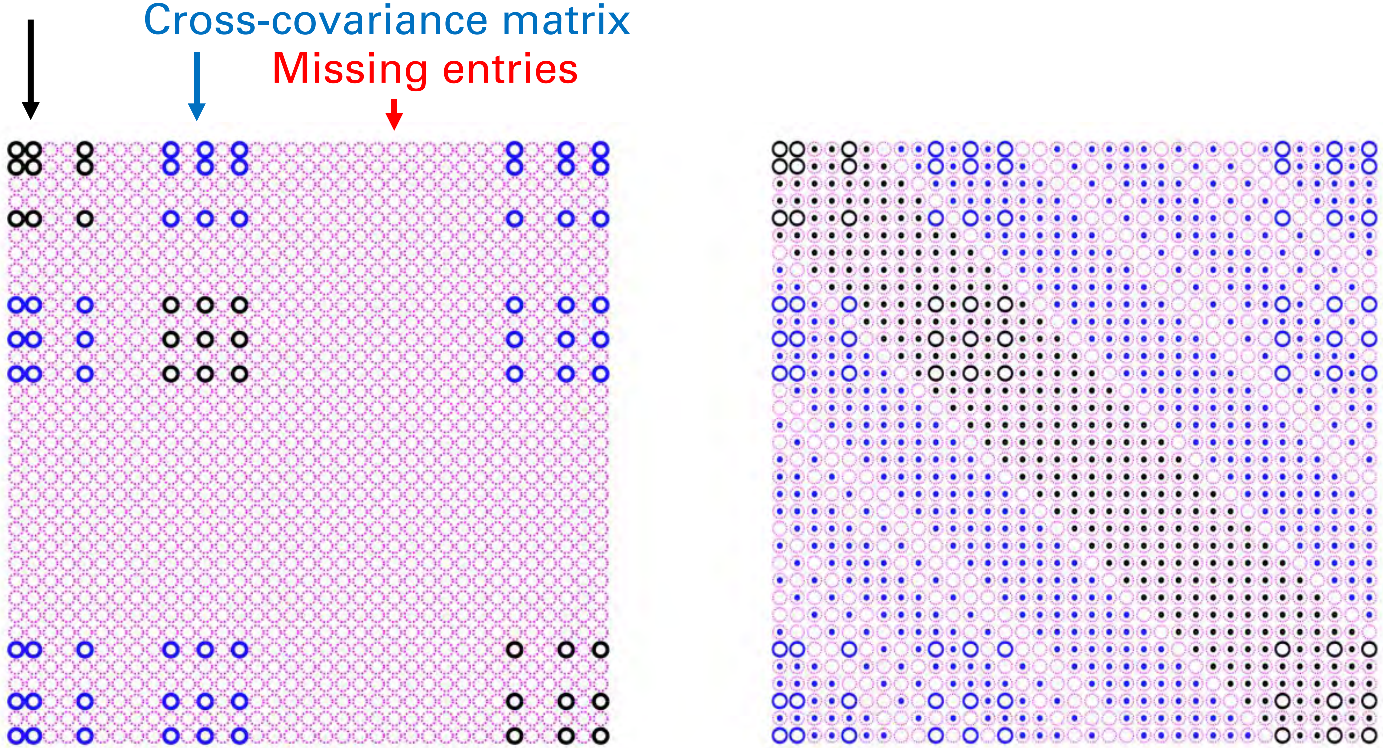

Y. D. Zhang and M. W. T. S. Chowdhury, "Direction-of-arrival estimation in closely distributed array exploiting mixed-precision covariance matrices," *Signal Processing*, 2024.

Distributed array with mixed-precision data fusion

Simulation results:

7 or 12 uncorrelated sources uniformly distributed between -50^{o} and 50^{o}.

$T = 200$ data snapshots at each subarray

Input SNR is 0 dB.

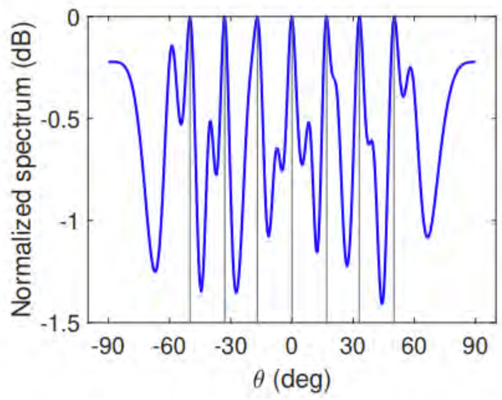

(a)

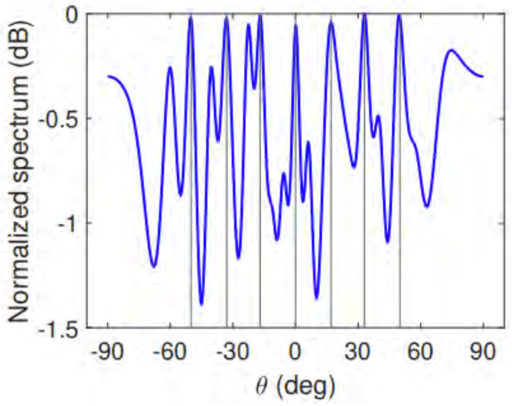

(b)

Comparison of MUSIC spectra

(a) No interpolation, full-precision data, 7 sources

(b) No interpolation, one-bit data, 7 sources

(c) With interpolation, self-covariance only, 12 sources

(d) with interpolation, mixed-precision data, 12 sources

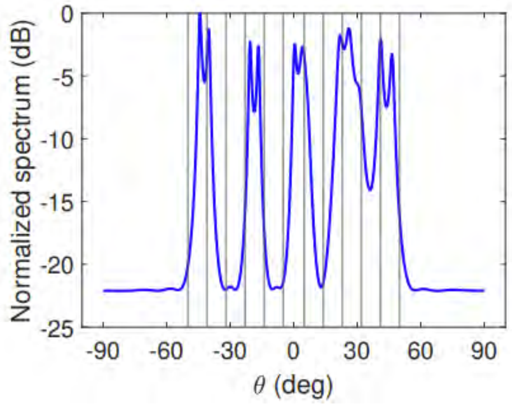

(c)

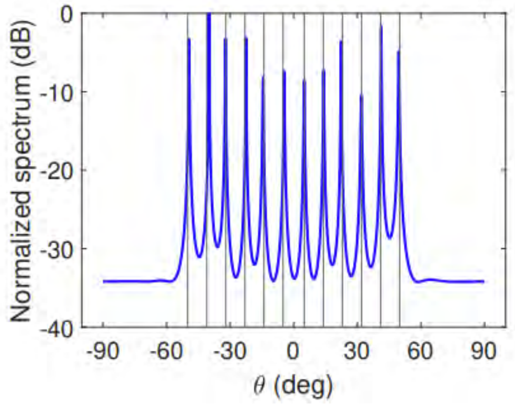

(d)

Y. D. Zhang and M. W. T. S. Chowdhury, "Direction-of-arrival estimation in closely distributed array exploiting mixed-precision covariance matrices," *Signal Processing*, 2024.

Distributed array with mixed-precision data fusion

Simulation results:

The full-precision subarray covariance matrices cost very low data traffic, but help improve the DOA estimation performance.

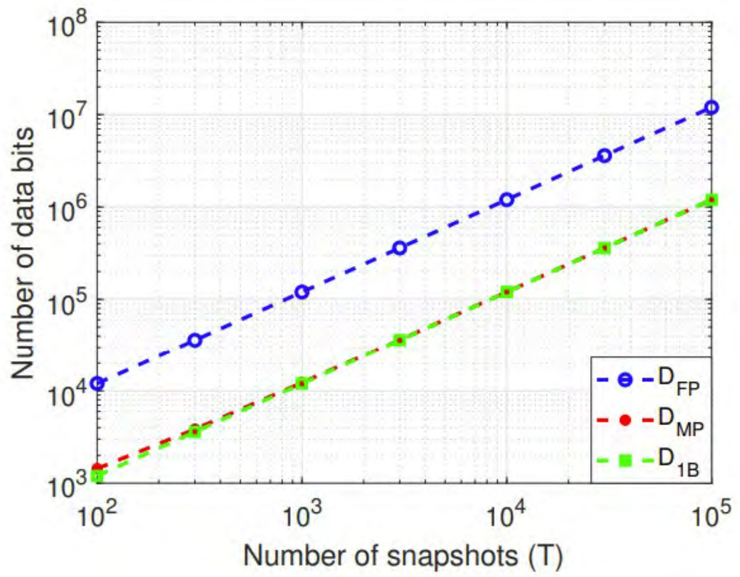

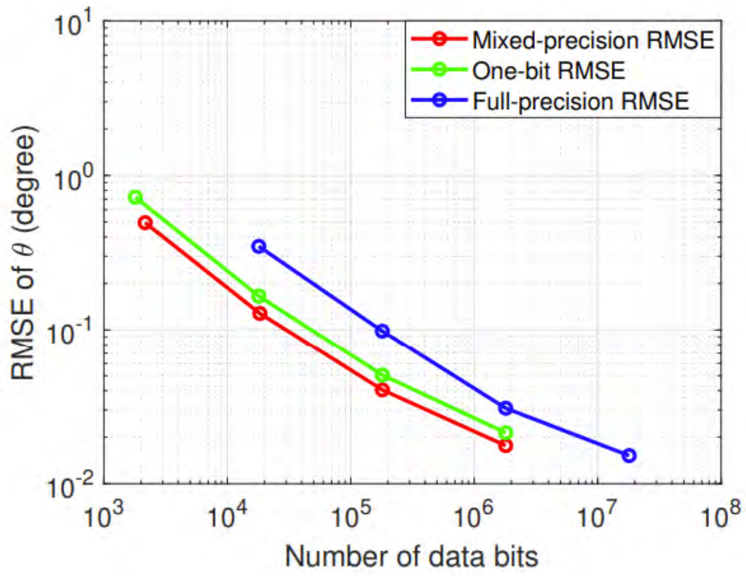

Y. D. Zhang and M. W. T. S. Chowdhury, "Direction-of-arrival estimation in closely distributed array exploiting mixed-precision covariance matrices," *Signal Processing*, 2024.

2-D sparse arrays

Extension to 2-D (planar) sparse arrays: Sparse array design and processing concepts apply for 2-D array but need additional considerations.

- Sparse arrays may have additional rooms for sensor reduction
- Covariance statistics becomes a tensor with high redundancies
- Multi-dimensional processing may require decoupling for reduced complexity

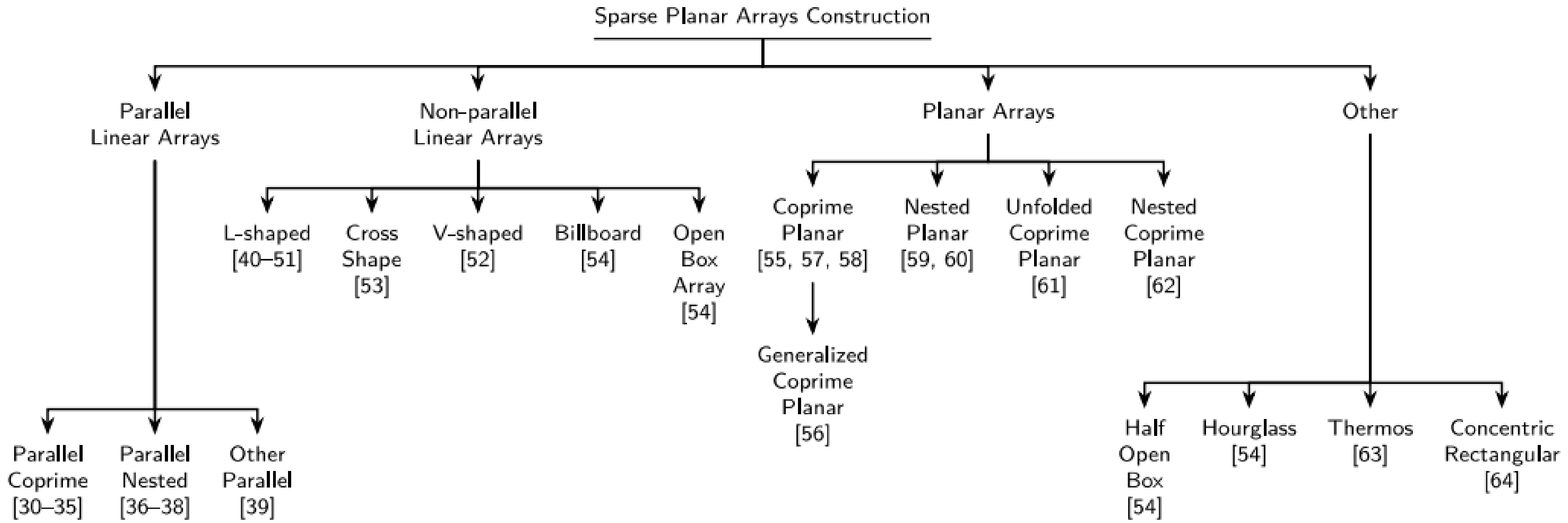

I. Aboumahmoud, A. Muqaibel, M. Alhassoun and S. Alawsh, "A Review of sparse sensor arrays for two-dimensional direction-of-arrival estimation," *IEEE Access*, 2021.

2-D sparse arrays: Semi-passive RIS channel estimation

Consider a planar reconfigurable intelligent surface (RIS) with $M = M_x \times M_z$ elements, where $\bar{M}$ elements are active elements in L-shape, and others can only reflect the impinging signals

- Consider L multipaths from mobile user to the RIS, the output signal vectors at the two RIS subarrays corresponding to the x-axis and z-axis are respectively given as:

$$\boldsymbol{x}(t) = \sum_{l=1}^{L} \beta_l \tilde{\boldsymbol{a}}_x(\varphi_l, \vartheta_l) s_u(t) + \boldsymbol{n}_x(t)$$

$$\boldsymbol{z}(t) = \sum_{l=1}^{L} \beta_l \tilde{\boldsymbol{a}}_z(\vartheta_l) s_u(t) + \boldsymbol{n}_z(t)$$

$\tilde{\boldsymbol{a}}_x(\varphi_l, \vartheta_l)$and $\tilde{\boldsymbol{a}}_z(\vartheta_l)$: sparse steering vectors of the RIS in x and z axes

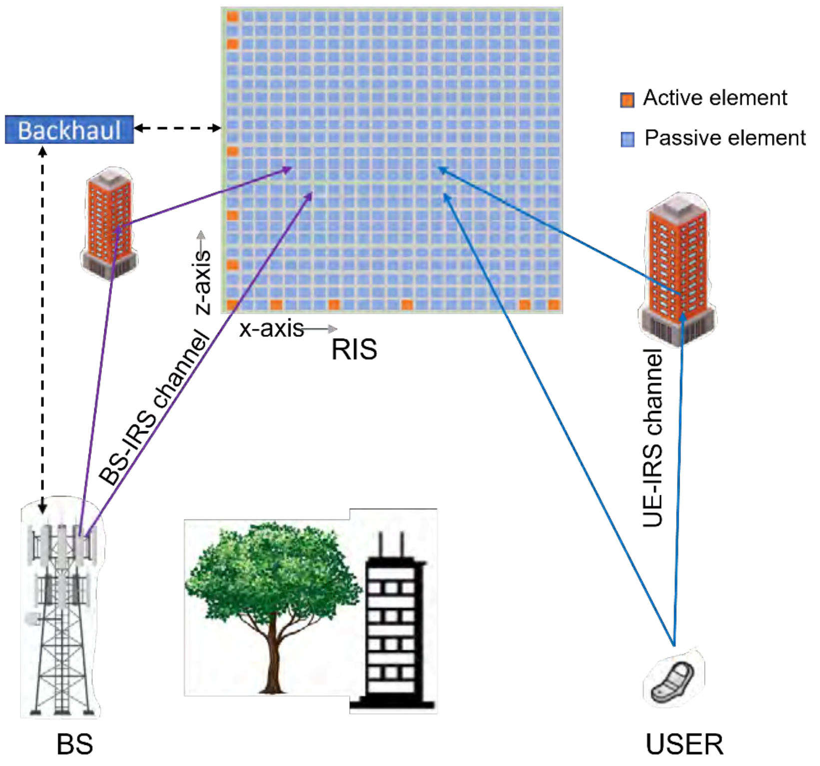

M. Asif Haider, Y. D. Zhang, and E. Aboutanios, "ISAC system assisted by RIS with sparse active elements," EURASIP Journal on Advances in Signal Processing, 2023.

2-D sparse arrays: Semi-passive RIS channel estimation

- The covariance matrices $\widetilde{\mathbf{R}}_{x_{IRS}}$ and $\widetilde{\mathbf{R}}_{z_{IRS}}$ become sparse with missing holes.
- $\widetilde{\mathbf{R}}_{x_{IRS}}$ and $\widetilde{\mathbf{R}}_{z_{IRS}}$ can be interpolated exploiting the Hermitian and Toeplitz structure of the covariance matrix of the fully interpolated uniform linear array.
- Interpolated covariance matrices contain all elements in the full uniform array.
- Subspace-based methods, such as MUSIC, can be applied to $\widehat{\boldsymbol{R}}_{\mathrm{z_{IRS}}}$ to estimate the z-axis DOAs $(\hat{\vartheta}_l \; \forall \; l = 1,2,\cdots,L)$ at the RIS for the user-RIS multipath signals.
- Source covariance matrix is estimated as:

$$\widehat{\boldsymbol{R}}_s = \boldsymbol{A}_z^{\dagger}(\hat{\theta})\boldsymbol{V}_{zs}\left(\widehat{\Gamma}_z - \sigma_n^2\boldsymbol{I}_L\right)\widehat{\boldsymbol{V}}_{zs}^H\left(\boldsymbol{A}_z^{\dagger}(\hat{\theta})\right)^{\mathrm{H}}$$

- The azimuth angles are then estimated from the following optimization problem:

$$\hat{\phi} = \arg \min_{\vartheta_l \in [-\frac{\pi}{2},\frac{\pi}{2}]} \left\| \left(\widehat{\boldsymbol{R}}_{x\,RIS} - \sigma_n^2\boldsymbol{I}_{W_x}\right) - \boldsymbol{A}_x(\hat{\phi},\hat{\theta})\widehat{\boldsymbol{R}}_s\boldsymbol{A}_x(\hat{\phi},\hat{\theta})^{\mathrm{H}} \right\|$$

- From the paired azimuth and elevation estimated angles, we generate the steering matrix of the RIS for the RIS-user channel as:

$$\widehat{\boldsymbol{A}}_{IRS} = [\widehat{\boldsymbol{a}}_{\mathrm{RIS}}(\vartheta_1, \varphi_1), \widehat{\boldsymbol{a}}_{\mathrm{RIS}}(\vartheta_2, \varphi_2) \cdots, \widehat{\boldsymbol{a}}_{\mathrm{RIS}}(\vartheta_L, \varphi_L)]$$

M. Asif Haider, Y. D. Zhang, and E. Aboutanios, "ISAC system assisted by RIS with sparse active elements," EURASIP Journal on Advances in Signal Processing, 2023.

ASP Lab

Coherent signals: Signal model

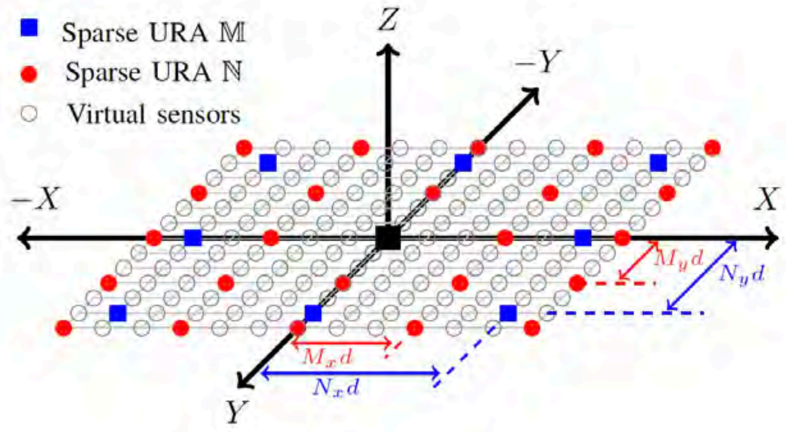

- $\mathbb{M}, \mathbb{N}$: two sparse uniform rectangular arrays (URAs) with $\mathbb{S} = \mathbb{M} \cup \mathbb{N}$ forming an origin-centric coprime planner array
- $M_x \times M_y$: Number of sensors in sparse subarray $\mathbb{M}$
- $N_x \times N_y$: Number of sensors in sparse subarray $\mathbb{N}$ with (M_x, N_x) and (M_y, N_y) being the coprime integer pairs
- The total number of sensors is $M_x M_y + N_x N_y - 1$
- L narrowband far-field coherent signals arrive from azimuth and elevation angle pairs (θ_l, ϕ_l) for $l = 1,2, \cdots, L$.
- The signals received at subarray $\mathbb{M}$ at time t is

$$\boldsymbol{X}_{\mathbb{M}}(t) = \sum_{l=1}^{L} \alpha_l s(t) \boldsymbol{a}_{\mathbb{M}}(\mu_l) \circ \boldsymbol{a}_{\mathbb{M}}(\nu_l) + \boldsymbol{W}_{\mathbb{M}} \in \mathbb{C}^{M_x \times M_y}$$

where α_l : complex scalar
$s(t)$: reference signal waveform
$\boldsymbol{W}_{\mathbb{M}}$: noise matrix

- The signals received at subarray $\mathbb{N}$ can be similarly defined.

M. S. R. Pavel, Y. D. Zhang, and B. Himed, "Tensor reconstruction-based sparse array interpolation for 2-D DOA estimation of coherent signals," *IEEE Radar Conference*, 2024.

Coherent signals: Signal model

- For L coherent signals, the signal matrix of the full URA is

$$\boldsymbol{X}_{\mathbb{U}}(t) = \sum_{l=1}^{L} \alpha_l s(t) \boldsymbol{a}_{\mathbb{U}}(\mu_l) \circ \boldsymbol{a}_{\mathbb{U}}(\nu_l) + \boldsymbol{W}_{\mathbb{U}}$$

- The augmented signal matrix $\boldsymbol{Y}(t)$ can be related to $\boldsymbol{X}_{\mathbb{U}}(t)$ as

$$\boldsymbol{Y}(t) = \boldsymbol{B} \circ \boldsymbol{X}_{\mathbb{U}}(t)$$

$\boldsymbol{B}$: masking matrix

- The covariance tensor of the augmented signal matrix $\boldsymbol{Y}(t)$:

$$\boldsymbol{\mathcal{R}} = \boldsymbol{\mathcal{B}} \circ \sigma_s^2 \sum_{l=1}^{L} \sum_{l'=1}^{L} \alpha_l^* \alpha_{l'} \boldsymbol{a}_{\mathbb{U}}(\mu_{l'}) \circ \boldsymbol{a}_{\mathbb{U}}(\nu_{l'}) \circ \boldsymbol{a}_{\mathbb{U}}^*(\mu_l) \circ \boldsymbol{a}_{\mathbb{U}}^*(\nu_l)$$

$$\in \mathbb{C}^{(2U_x+1)\times(2U_y+1)\times(2U_x+1)\times(2U_y+1)}$$

$\boldsymbol{\mathcal{B}}$: masking tensor

- Because of the signal coherency, the covariance tensor is rank-deficient.

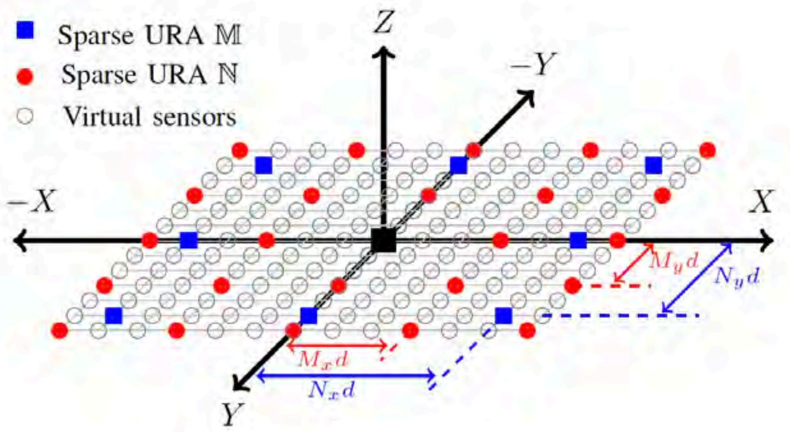

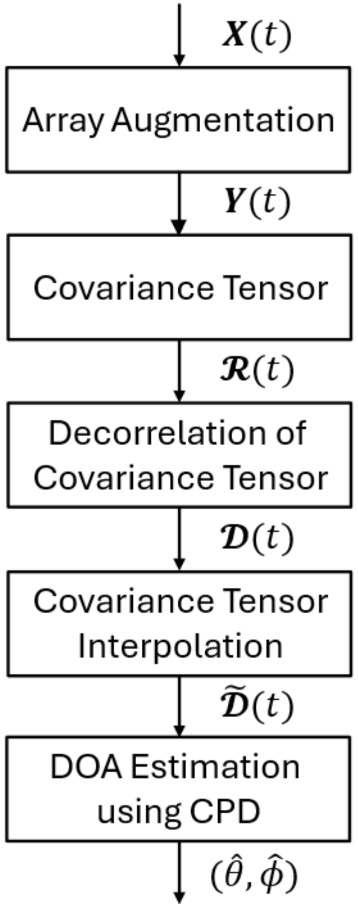

M. S. R. Pavel, Y. D. Zhang, and B. Himed, "Tensor reconstruction-based sparse array interpolation for 2-D DOA estimation of coherent signals," *IEEE Radar Conference*, 2024.

Coherent signals: Full rank recovery

- A structured Toeplitz tensor $\boldsymbol{\mathcal{D}}_{(u_x,u_y)} \in \mathbb{C}^{(U_x+1)\times(U_y+1)\times(U_x+1)\times(U_y+1)}$ is constructed from $\boldsymbol{\mathcal{R}}(u_x, u_y, :,)$ based on a particular pair of indices (u_x, u_y) for $\tilde{u}_x, \widetilde{u'}_x \in [0, U_x]$ and $\tilde{u}_y, \widetilde{u'}_y \in [0, U_y]$:

$$\boldsymbol{\mathcal{D}}_{(u_x,u_y)}(\tilde{u}_x, \tilde{u}_y, \tilde{u}'_x, \tilde{u}'_y) = \boldsymbol{\mathcal{R}}(u_x, u_y, -\tilde{u}_x + \tilde{u}'_x, -\tilde{u}_y + \tilde{u}'_y)$$

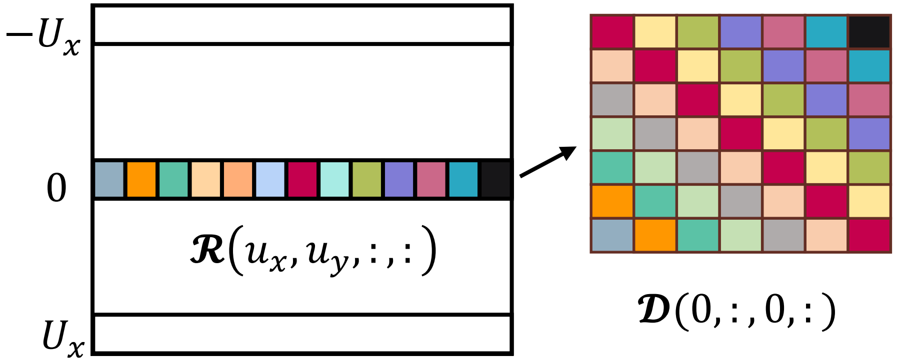

- The tensor $\boldsymbol{\mathcal{D}}_{(u_x,u_y)}$ exhibits a full-rank tensorial Toeplitz structure:

$$\boldsymbol{\mathcal{D}}_{(u_x,u_y)} = b_{(u_x,u_y)} \sum_{l=1}^{L} \boldsymbol{g}(\mu_l) \circ \boldsymbol{g}(\nu_l) \circ \boldsymbol{g}^*(\mu_l) \circ \boldsymbol{g}^*(\nu_l)$$

  where $\boldsymbol{g}(\mu_l) = \left[1, \cdots, e^{-j\pi U_x \mu_l}\right]^{\mathrm{T}} \in \mathbb{C}^{U_x+1}$ and $\boldsymbol{g}(\nu_l) = \left[1, \cdots, e^{-j\pi U_y \nu_l}\right]^{\mathrm{T}} \in \mathbb{C}^{U_y+1}$ act as the steering vectors for the lth coherent source in the X and Y directions.

- Due to the sparsity of 2-D coprime array $\mathbb{S}$, the covariance tensor $\boldsymbol{\mathcal{D}}$ contains holes.
- The unknown correlations associated with the missing sensors can be estimated through a gridless convex optimization problem through nuclear norm minimization.

H. Zheng, C. Zhou, Z. Shi, and Y. Gu, “Structured tensor reconstruction for coherent DOA estimation,” *IEEE Signal Processing Letters*, 2022.

M. S. R. Pavel, Y. D. Zhang, and B. Himed, "Tensor reconstruction-based sparse array interpolation for 2-D DOA estimation of coherent signals," *IEEE Radar Conference*, 2024.

ASP Lab

Coherent signals: Simulation results

- The subarray $\mathbb{M}$ consists of $M_x \times M_y = 3 \times 3 = 9$ sensors, and the subarray $\mathbb{N}$ consists of $N_x \times N_y = 5 \times 5 = 25$ sensors (total number of sensors: 33).
- The dimension of the interpolated URA $\mathbb{U}$ is $(2U_x + 1) \times (2U_y + 1) = 13 \times 13$.
- Therefore, the proposed approach can detect up to $U_x + U_y = 12$ coherent sources.
- The $(1,1)$ th slice of the covariance tensor, i.e., $\boldsymbol{\mathcal{R}}(1,1,:,:) \in \mathbb{C}^{1\times1\times13\times13}$, is used to obtain the decorrelated tensor $\boldsymbol{\mathcal{D}}_{(1,1)} \in \mathbb{C}^{7\times7\times7\times7}$.
- 9 coherent sources are considered with 20 dB input SNR and 1,000 snapshots.
- The azimuth and elevation angles are randomly sampled from uniform distributions with azimuth range $-60°$ to $60°$ and elevation range $0°$ to $60°$.
- All coherent sources are detected in this example.

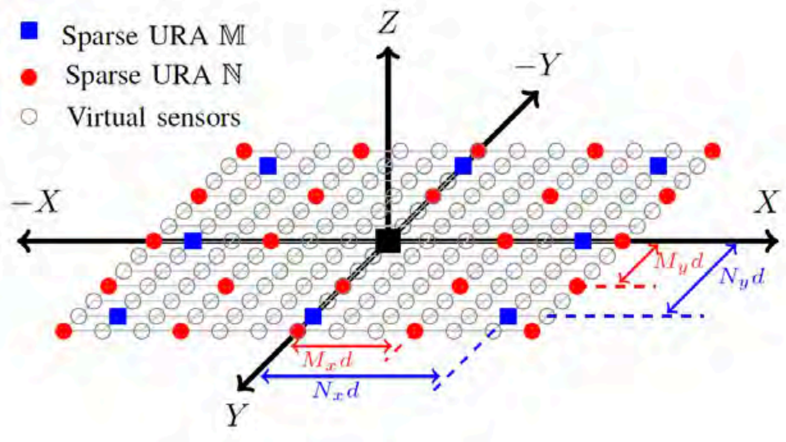

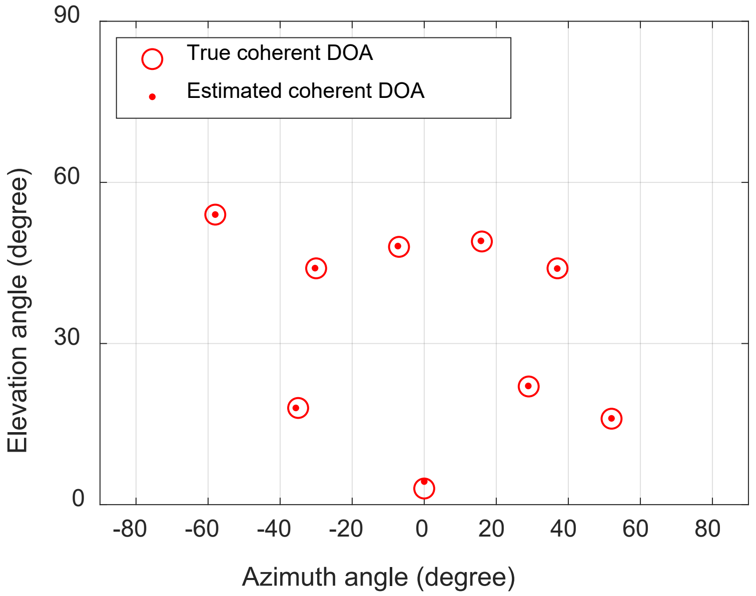

M. S. R. Pavel, Y. D. Zhang, and B. Himed, "Tensor reconstruction-based sparse array interpolation for 2-D DOA estimation of coherent signals," *IEEE Radar Conference*, 2024.

Machine learning for DOA estimation

Selected offerings

- Reduced complexity
- Robustness to imperfections
- Denoising
- Sequential Processing

[Reduced complexity]

M. Chen, Y. Gong, and X. Mao, "Deep neural network for estimation of direction of arrival with antenna array," IEEE Access, 2000.

R. Zheng, S. Sun, H. Liu, H. Chen and J. Li, "Interpretable and Efficient Beamforming-Based Deep Learning for Single Snapshot DOA Estimation," IEEE Sensors Journal, in press.

[Robustness to imperfections]

Z. M. Liu, C. Zhang, and S. Yu Philip. "Direction-of-arrival estimation based on deep neural networks with robustness to array imperfections." IEEE Trans. Antennas and Propagation, 2018.

H. Xiang, B. Chen, M. Yang, S. Xu, and Z. Li, Improved direction-of-arrival estimation method based on LSTM neural networks with robustness to array imperfections. Applied Intelligence, 2021.

M. S. R. Pavel, M. W. T. S. Chowdhury, Y. D. Zhang, D. Shen, and G. Chen, "Machine learning-based direction-of-arrival estimation exploiting distributed sparse arrays," Asi*lomar Conference on Signals, Systems, and Computers*, 2021.

[Denosing]

G. K. Papageorgiou and M. Sellathurai, "Direction-of-arrival estimation in the low-SNR regime via a denoising autoencoder," IEEE SPAWC, 2020.

[Sequential Processing]

F. Sohrabi, Z. Chen, and W. Yu, "Deep active learning approach to adaptive beamforming for mmWave initial alignment," IEEE Journal on Selected Areas in Communications, 2021.

S. R. Pavel and Y. D. Zhang, "Optimization of the compressive measurement matrix in a massive MIMO system exploiting LSTM networks," Algorithms, 2023.

Machine learning for DOA estimation

- Three sparse subarrays are colinear, forming a 31 × 31 augmented covariance matrix with missing entries.

- K = 15 sources arrive between -60º and 60º.
- The input SNR is set to 0 dB.
- The antenna gains follow a uniform distribution between 0.9 and 1.1, and the phase errors are uniformly distributed between −9º and 9º.

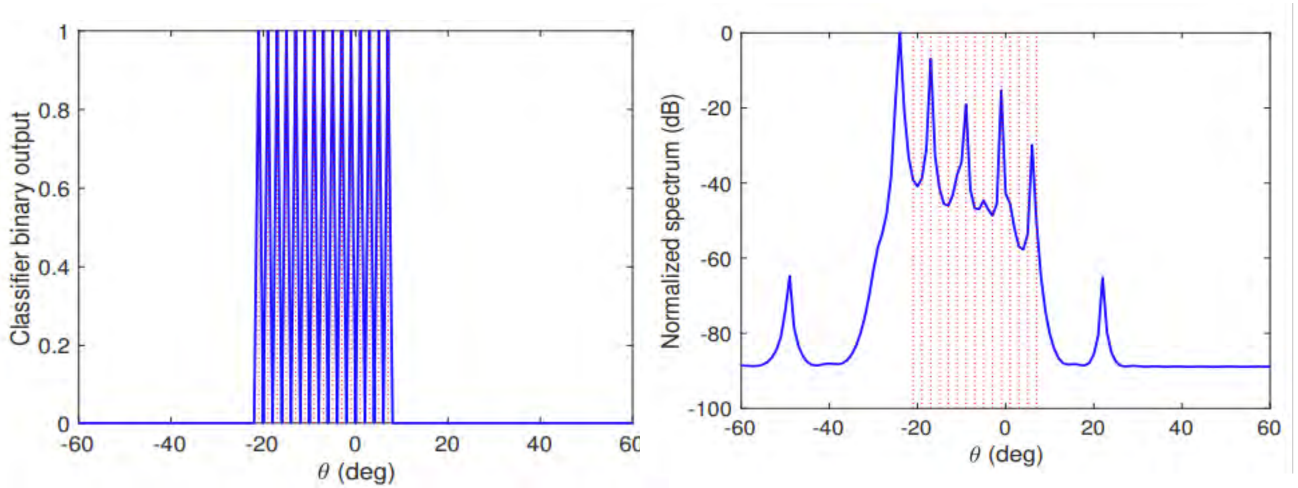

- By training the network with imperfect antenna model, it achieve robust DOA estimation performance. MUSIC assuming perfect antenna model fails.

M. S. R. Pavel, M. W. T. S. Chowdhury, Y. D. Zhang, D. Shen, and G. Chen, "Machine learning-based direction-of-arrival estimation exploiting distributed sparse arrays," *Asilomar Conference on Signals, Systems, and Computers*, 2021.

A S P Lab

Concluding remarks

Modern sensing applications require higher resolution (larger aperture), resolve more signals (more DOFs), low mutual coupling effect (avoid close placement).

The fundamental goals of sparse array design and processing are to answer these needs while keeping a low system complexity.

Sparse array designs are enabled by the signal processing techniques, such as compressive sensing, matrix completion, and tensor analysis.

While the last decade witnessed significant process in this area, many challenging issues remain to be explored.

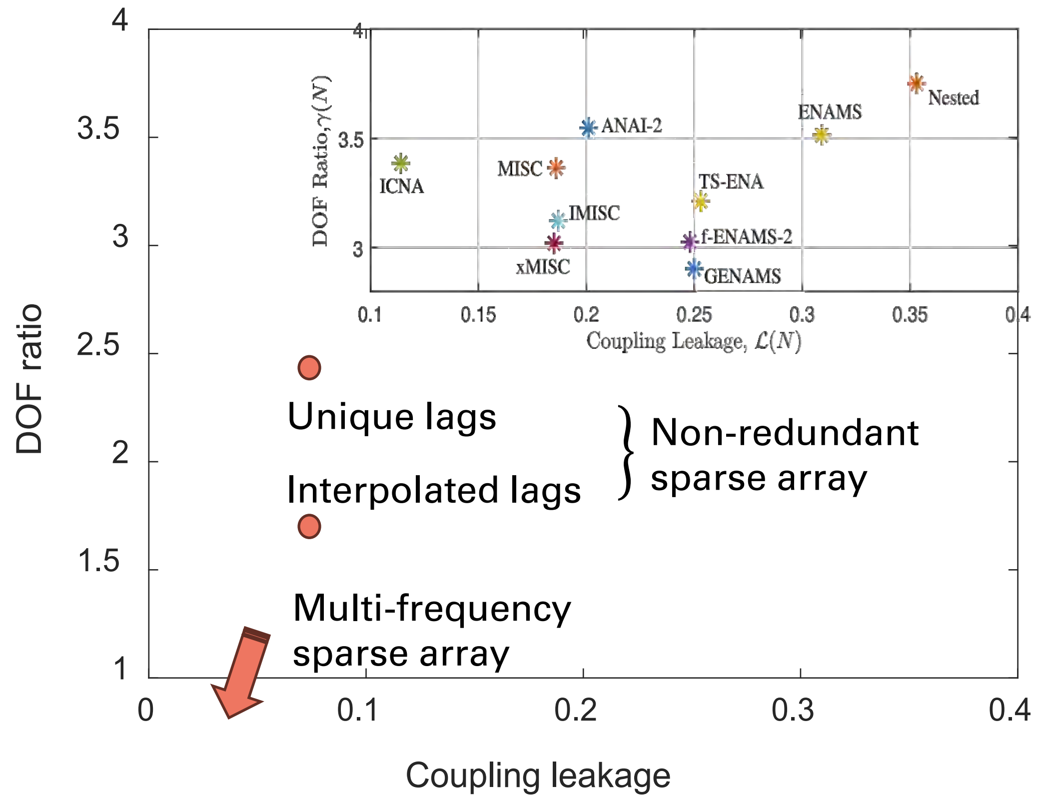

Sparse array design and processing: What is next?

Section II. More consecutive lags and lower coupling
- Coprime array with compressed inter-element spacing (CACIS)
- Maximum inter-element spacing constraint (MISC) array

Section III. Sparsity-based processing and array design

III-A. Sparsity-based DOA estimation
- Coprime array with displaced subarrays (CADiS)

III-B. Structured matrix completion for DOA estimation
- Non-redundant sparse arrays
- 4D automotive radar sensing

III-C. Group sparsity-based DOA estimation
- Multi-frequency array
- Frequency-switching array

Section IV. Additional topics
- DOA estimation exploiting high-order statistics
- Distributed array with mixed-precision covariance matrices
- 2-D sparse arrays
- Signal coherency consideration
- Machine learning for DOA estimation

General issues
- Low-complexity implementations
- Performance and bound analysis
- Robustness issues

Two/multi-dimensional arrays
- Array design
- Extreme sparse arrays
- Tensor-based processing

Bandwidth exploitation
- DOF analysis for wideband signals
- Low-complexity solutions
- Fractional sparse arrays

Signal coherency
- Coherent/correlated signals
- Mixed uncorrelated/coherent signals

References

- C. Zhou, Y. Gu, Y. D. Zhang, and Z. Shi, "Sparse array interpolation for direction-of-arrival estimation," in M. G. Amin (ed.), *Sparse Arrays for Radar, Sonar, and Communications*, Wiley-IEEE Press, 2024.

- S. Sun and Y. D. Zhang, "Redefining radar perception for autonomous driving: The role of sparse array and waveform design in 4D automotive radar," IEEE Signal Processing Society Webinar Series, Sept. 2023.
- https://yiminzhang.com/presentation/sps23_automotive.pdf
- https://rc.signalprocessingsociety.org/education/webinars/spsweb23024#

- Y. D. Zhang, "Signaling strategies and array processing for sensing and communications," IEEE ComSoc-SPS ISAC Webinar Series, Nov. 2021.
- https://yiminzhang.com/presentation/isac21.pdf
- https://www.youtube.com/watch?v=3fn8OPBNczI

A
S
P
Lab

References

- Q. Wu, Y. D. Zhang, M. G. Amin, and B. Himed, "Complex multitask Bayesian compressive sensing," *IEEE International Conference on Acoustics, Speech, and Signal Processing*, May 2014.
- S. Qin, Y. D. Zhang, and M. G. Amin, "Generalized coprime array configurations for direction-of-arrival estimation," *IEEE Trans. Signal Processing*, vol. 63, no. 6, pp. 1377-1390, March 2015. (2018 IEEE SPS Young Author Best Paper Award)
- S. Qin, Y. D. Zhang, M. G. Amin, and B. Himed, "DOA estimation exploiting a uniform linear array with multiple co-prime frequencies," *Signal Processing*, vol. 130, pp. 37-46, Jan. 2017. (2021 EURASIP Best Paper Award for Signal Processing)
- S. Qin, Y. D. Zhang, and M. G. Amin, "DOA estimation of mixed coherent and uncorrelated targets exploiting coprime MIMO radar," *Digital Signal Processing*, special issue on Co-prime array and sampling, vol. 61, pp. 26-34, Feb. 2017.
- A. Ahmed, Y. D. Zhang, and B. Himed, "Effective nested array design for fourth-order cumulant-based DOA estimation," *IEEE Radar Conference*, May 2017. (Student Paper Competition Award - Third Place)
- C. Zhou, Y. Gu, X. Fan, Z. Shi, G. Mao, and Y. D. Zhang, "Direction-of-arrival estimation for coprime array via virtual array interpolation," *IEEE Trans. Signal Processing*, vol. 66, no. 22, pp. 5956-5971, Nov. 2018. (2021 IEEE SPS Young Author Best Paper Award)
- C. Zhou, Y. Gu, Z. Shi, and Y. D. Zhang, "Off-grid direction-of-arrival estimation using coprime array interpolation," *IEEE Signal Processing Letters*, vol. 25, no. 11, pp. 1710-1714, Nov. 2018.
- Z. Zheng, W-Q. Wang, Y. Kong, and Y. D. Zhang, "MISC Array: A new sparse array design achieving increased degrees of freedom and reduced mutual coupling effect," *IEEE Trans. Signal Processing*, vol. 67, no. 7, pp. 1728-1741, April 2019.
- S. Zhang, A. Ahmed, Y. D. Zhang, and S. Sun, "DOA estimation exploiting interpolated multi-frequency sparse array," *IEEE Sensor Array and Multichannel Signal Processing Workshop*, June 2020. (Best Student Paper Award)
- A. Ahmed, D. Silage, and Y. D. Zhang, "High-resolution target sensing using multi-frequency sparse array," *IEEE Sensor Array and Multichannel Signal Processing Workshop*, June 2020.

A
S
P
Lab

References

- S. Sun and Y. D. Zhang, "4D automotive radar sensing for autonomous vehicles: A sparsity-oriented approach," *IEEE Selected Topics in Signal Processing*, vol. 15, no. 4, pp. 879-891, June 2021.
- S. Liu, Z. Mao, Y. D. Zhang, and Y. Huang, "Rank minimization-based Toeplitz reconstruction for DoA estimation using coprime array," *IEEE Communications Letters*, vol. 25, no. 7, pp. 2265-2269, July 2021.
- A. Ahmed and Y. D. Zhang, "Generalized non-redundant sparse array designs," *IEEE Trans. Signal Processing*, vol. 69, pp. 4580-4594, Aug. 2021.
- S. Zhang, A. Ahmed, Y. D. Zhang, and S. Sun, "Enhanced DOA estimation exploiting multi-frequency sparse array," *IEEE Trans. Signal Processing*, vol. 69, pp. 5935-5946, Oct. 2021.
- M. S. R. Pavel, M. W. T. S. Chowdhury, Y. D. Zhang, D. Shen, and G. Chen, "Machine learning-based direction-of-arrival estimation exploiting distributed sparse arrays," *Asilomar Conference on Signals, Systems, and Computers*, Oct. 2021.
- M. Asif Haider, Y. D. Zhang, and E. Aboutanios, "ISAC system assisted by RIS with sparse active elements," EURASIP *Journal on Advances in Signal Processing*, vol. 2023, no. 20, pp. 1-22, Feb. 2023.
- Y. D. Zhang and M. W. T. S. Chowdhury, "Direction-of-arrival estimation in closely distributed array exploiting mixed-precision covariance matrices," Signal Processing, vo. 240, no. 109463, pp. 1-12, March 2024.
- M. S. R. Pavel, Y. D. Zhang, and B. Himed, "Tensor reconstruction-based sparse array interpolation for 2-D DOA estimation of coherent signals," *IEEE Radar Conference*, May 2024.
- Y. D. Zhang and S. Sun, "Identical partitioning of consecutive integer set," *IEEE Sensor Array and Multichannel Signal Processing Workshop*, July 2024.
- Y. D. Zhang and M. W. T. S. Chowdhury, "Frequency-switching sparse arrays," *IEEE Sensor Array and Multichannel Signal Processing Workshop*, July 2024.

ASP Lab

Thank you

2024 IEEE Sensor Array and Multichannel Signal Processing Workshop Tutorial

Do More with Less: Revolutionize Direction Finding with Sparse Arrays

Yimin D. Zhang
Department of Electrical and Computer Engineering
Temple University

http://yiminzhang.com

http://asplab.net

Advanced Signal Processing Laboratory